Raman-spektroskopische Charakterisierung und Identifizierung von *Bacillus*-Endosporen

Dissertation

zur Erlangung des akademischen Grades

doctor rerum naturalium (*Dr. rer. nat.*)

vorgelegt dem Rat der Chemisch-Geowissenschaftlichen Fakultät

der Friedrich-Schiller-Universität Jena von

Diplom-Chemiker Stephan Stöckel

geboren am 25.12.1980 in Jena

Gutachter:

1. Prof. Dr. Jürgen Popp
   (Institut für Physikalische Chemie, Friedrich-Schiller-Universität Jena)
2. Prof. Dr. Erika Kothe
   (Institut für Mikrobiologie, Friedrich-Schiller-Universität Jena)

Tag der öffentlichen Verteidigung: 12. Dezember 2012

Danksagung

Zuerst sei Prof. Jürgen Popp dafür gedankt, mich erst als Diplomand, dann auch als Doktorand in seine Arbeitsgruppe aufgenommen zu haben. Ich weiß die Freiheit sehr zu schätzen, die mir zur Bearbeitung des spannenden Themas zugestanden wurde. Diese hätte ich allerdings nie effektiv zu nutzen gewusst, wenn mich Dr. Petra Rösch nicht während der ganzen Zeit angeleitet, beraten und unterstützt hätte. Auch Prof. Michael Schmitt leistete in diesem Sinne wertvolle Hilfestellung.

Eine Arbeit über Anthrax-Sporen ohne Anthrax-Sporen wäre ziemlich brotlos, insofern haben Frau Dr. Mandy Elschner und Frau Katja Fischer vom Friedrich-Loeffler-Institut einen großen Anteil an dieser Arbeit, da sie durch Bereitstellung hunderter Bakterienproben für reichlich Beschäftigung und durch umfängliche Beratung für ebenso viel Erkenntnis sorgten.

Auch die Raman-Spektroskopie bliebe ohne geeignete Spektrometer nur eine gut gemeinte Idee. Deshalb sei hier den Mitarbeitern der Firma rap.ID gedankt, welche zusammen mit uns den BioParticleExplorer so veredelt haben, dass oben genannte Mengen an Bakterien erst untersucht werden konnten.

Vor überraschenden Hürden oder gar Rückschlägen war man trotz dieser Hilfe natürlich nicht gefeit, weshalb ich weiterhin sehr froh und dankbar darüber bin, mit allen Kollegen der AG-Popp sowie den Mitarbeitern des IPCs in einem angenehmen und gedeihlichen Betriebsklima gearbeitet haben zu dürfen.

Dennoch wusste ich auch zu schätzen, ab und an von der Arbeit genügend Abstand und Ablenkung zu erhalten. Dies gewährleistete meine Familie über die gesamte Dauer der Dissertation, sodass auch ihr großer Dank gebührt.

Inhaltsverzeichnis

1 Zusammenfassung 1
1.1 Einleitung 1
1.2 Stand der Forschung 5
1.2.1 Bakteriologie *B. anthracis* 5
1.2.2 Nachweis von *B. anthracis* 8
1.2.3 Raman-Spektroskopie als alternative Detektionsmethode für *B. anthracis* 13
1.3 Eigene Forschungsergebnisse 20
1.3.1 Raman-spektroskopische Analyse des Einflusses von Mangan auf die Sporulation von *Bacillus*-Endosporen 20
1.3.2 Erarbeitung einer zur Raman-Spektroskopie kompatiblen Inaktivierungsmethode für *Bacillus*-Endosporen 22
1.3.3 Identifizierung von *Bacillus*-Endosporen mittels Raman-Spektroskopie und chemometrischer Methoden 25
1.3.4 Detektion von *B. anthracis* in Pulverproben 28
1.4 Resümee 31
Literaturverzeichnis 33

2 Publikationen und Konferenzbeiträge 47
2.1 Publikationen 47
2.1.1 Effect of supplementary manganese on the sporulation of *Bacillus* endospores analysed by Raman spectroscopy 47
2.1.2 Raman Spectroscopy-Compatible Inactivation Method for Pathogenic Endospores 59
2.1.3 Identification of *Bacillus anthracis* via Raman spectroscopy and chemometric approaches 75
2.1.4 Raman Spectroscopic Detection of Anthrax Endospores in Powder Samples 89
2.1.5 Weitere Publikationen 103
2.2 Konferenzbeiträge 105

Curriculum Vitae 107

Selbstständigkeitserklärung 109

1 Zusammenfassung

1.1 Einleitung

Erreger der Krankheit Milzbrand (Anthrax) ist das endosporenbildende Bakterium *Bacillus anthracis*. Dies postulierte Robert Koch bereits 1876 in einer seiner ersten Studien über Milzbrand, der zu damaliger Zeit eine verheerende Tierseuche darstellte und in einigen Fällen auch auf Menschen übertragen worden war [1]. Weltweit verursachte Milzbrand katastrophale Verluste in Beständen von Rindern, Schafen, Ziegen, Pferden und Schweinen, ehe 1939 der Veterinärmediziner Max Sterne einen wirksamen, bis heute regelmäßig eingesetzten Impfstoff entwickelte [2]. Zusammen mit dem verstärkten Einsatz von Antibiotika und nationaler Seuchenschutzprogramme konnte die Verbreitung der Tierseuche global zurückgedrängt werden, sodass Milzbrand in höheren Breitengraden Europas sowie Russland als getilgt gilt und dort allenfalls noch sporadisch auftritt. Dennoch zeigen aktuelle Berichte der *World Organization for Animal Health* (OIE), dass Milzbrand weiterhin enzootisch in den meisten Ländern Afrikas, Asiens sowie einigen Mittelmeeranrainerstaaten Europas (Albanien, Griechenland, Süditalien, Spanien, Türkei) und kleineren Arealen in Kanada und den USA ist [3].

Dieser natürlichen Verbreitung von Milzbrand steht die willentliche, durch Menschen verursachte Ausbreitung entgegen. Natürlich zustande kommende Kontaminationslevel betragen meistens weniger als 100 Anthraxsporen pro Gramm Probe, etwa in Kadavern von an Milzbrand erlegenen Tieren [4]. Unabsichtliche anthropogene Verseuchungen (Grundstücke von Gerbereien, Abdeckereien u. ä.) erzeugen höchstens Zehntausende Sporen pro Gramm Erde [5]. Für Milzbrand besonders empfängliche, pflanzenfressende Nutz- und Zuchttiere wie Rinder und Schafe sind von solchen Dosen gefährdet im Gegensatz zu mäßig anfälligen (Hunde, Schweine, auch Menschen) beziehungsweise nahezu unempfänglichen (Vögel) Spezies. Zudem gilt Milzbrand an sich als nicht invasiv, sodass die mittleren letalen Dosen (LD_{50}) nach einer Inhalation oder Aufnahme über den

Verdauungstrakt selbst bei als anfällig geltenden Spezies wie Schafen (LD_{50} parenteral 100 Sporen) einige zehn- bis hunderttausend Sporen betragen [5].

Millionen an infektionstüchtigen Endosporen pro Gramm Erde sind demnach nur durch willentliche Ausbringung der Erreger hervorzurufen, zum Beispiel in bioterroristisch motivierten Akten oder im Zuge biologischer Kriegsführung. Beispielsweise wurde während und nach dem 2. Weltkrieg in verschiedenen Ländern mit *B. anthracis* als Biowaffe experimentiert: So sorgten Experimente des britischen Militärs mit kontaminierten Leinsamenkuchen 1942 für eine jahrzehntelange Verseuchung von Gruinard-Island vor der Küste Schottlands [6]. Die USA und die Sowjetunion/Russische Föderation unterhielten bis 1967 beziehungsweise bis 1992 ein offensives B-Waffenprogramm mit Anthrax und 1995 hatte der Irak gegenüber den Vereinten Nationen bekundet, Bomben und SCUD-Raketen mit Anthrax-Sporen bestückt zu haben [7, 8]. Zu einer akzidentiellen Freisetzung von *B. anthracis*-Endosporen kam es 1979 in Swerdlowsk (Sowjetunion) aus einer Fabrik für biologische Kampfstoffe, die in der Abwindzone der Fabrik 66 Todesopfer bei 77 Infizierten forderte [6, 9]. Des Weiteren sei die Anschlagserie in den USA im Oktober 2001 erwähnt, als per Post verschickte Milzbrandsporen fünf Todesopfer nach insgesamt 22 Infektionen nach sich zogen [10]. Aktuell sind seit Dezember 2009 zuerst in Großbritannien, dann ebenfalls in weiteren europäischen Ländern mehrere Fälle von Infektionsmilzbrand unter i.v.-Drogenkonsumenten bekannt geworden [11, 12]. Allein zwischen Juni bis September 2012 wurden dem Robert Koch-Institut vier Fälle von Milzbrand bei Personen nach Drogenkonsum in Deutschland gemeldet [13]. Da es sich in allen Fällen um Heroinkonsumenten handelte, wird mit Milzbrandsporen kontaminiertes Heroin als die wahrscheinlichste Infektionsquelle angenommen.

Ein regulärer militärischer Einsatz biologischer Waffen wird zur Zeit als wenig wahrscheinlich erachtet, nicht zuletzt, da seit 1972 die *Biological and Toxin Weapons Convention*, der bis 2012 165 Staaten beigetreten sind, die Entwicklung, Herstellung sowie Lagerung biologischer Waffen verbietet und derzeit kein Staat offiziell ein B-Waffenprogramm unterhält. Viel eher sind absichtliche Freisetzungen hochpathogener Erreger durch bioterroristische Anschläge als Gefahr für die Gesellschaft einzustufen. Der 4. Bericht der Schutzkommission des Bundesministers des Inneren aus dem Jahre 2011 schätzt den Einsatz biologischer

Gefahrenstoffe im Vergleich mit anderen asymmetrischen CBRN-Bedrohungen (von chemisch, biologisch, radiologisch und nuklear) als besonders gefährlich ein [14]. Konkret haben die *Centers for Disease Control and Prevention* (CDC) in den USA *B. anthracis* in die Kategorie A der potentiell gefährlichsten Biowaffen katalogisiert, zu der obendrein das *Clostridium-botulinium*-Toxin (Botulismus) sowie *Yersinia pestis* (Pest), *Variola major* (Pocken), *Francisella tularensis* (Tularämie) und virales hämorrhagisches Fieber verursachende Viren gehören. *B. anthracis* (sowie weitere Erreger in den Kategorien B und C) werden durch die CDC als grundsätzlich geeignet angesehen, als biologische Waffen Verwendung zu finden. Auch das Robert Koch-Institut sieht in den Erregern der Pest, des Milzbrands und in Pockenviren die größte Gefahr hinsichtlich der vorsätzlichen Freisetzung biologischer Agenzien [15].

Für den Einsatz von *B. anthracis*-Endosporen als Biowaffe sprechen deren leichte Ausbringung sowie deren hohe Letalität: Aufgrund ihrer außergewöhnlichen Langlebigkeit und ausgesprochen hohen Resistenz gegenüber Umwelteinflüssen sind *B. anthracis*-Endosporen relativ leicht in großen Mengen zu generieren, zu lagern und auszubringen. Weiterhin wird angenommen, dass im Falle eines Lungenmilzbrandes (Einatmen von Sporen) eine Letalität von 95 % gegeben ist, wenn nicht eine entsprechende Antibiose innerhalb von 48 Stunden erfolgt [16]. Derartige Punkte überwiegen deutlich die relativ hohe mittlere Infektionsdosis (ID_{50} 8 000-10 000 Sporen) und mittlere letale Dosis (LD_{50} 2 500 bis 55 000 Sporen) von Lungenmilzbrand sowie die verschwindend geringe Wahrscheinlichkeit einer Mensch-zu-Mensch-Übertragung [17, 18]. Deshalb kommt dem Lungenmilzbrand eine besondere Bedeutung für B-Gefahrenlagen zu, obwohl 95 % der natürlichen Infektionen Hautmilzbrand (Sporenaufnahme über Hautwunden, LD_{50} bei 10-50 Sporen) ausmacht, der aber in 80-90 % der unbehandelten Fälle ausheilt [19].

Generell ist eine Früh- oder Echtzeiterkennung von Anschlägen mit Krankheitserregern kaum möglich. Im Gegensatz zu anderen Großschadenslagen ist die Ausbreitung der Erreger lautlos und unsichtbar. Weiterhin sind die Wirkungen auf den menschlichen Körper denen natürlicher Krankheiten nicht unähnlich; darüber hinaus kann sich der biologische Katastrophenfall ohne erkennbares initiales Ereignis schleichend entwickeln und für einige Tage bis Monate als Infektions-

geschehen überhaupt nicht wahrgenommen werden. Hinzu kommt die Unübersichtlichkeit der Vielfalt und Variabilität bioterroristischer Szenarien. So erfolgt das Erkennen der Gefahrenlage zum Teil erst mit deutlicher Latenz nach dem Freisetzungszeitpunkt und antiepidemische Maßnahmen können nicht rechtzeitig ergriffen werden. Zuletzt darf die psychosoziale Wirkung durch einen Einsatz von Biowaffen nicht unterschätzt werden, da insbesondere Infektionskrankheiten archaische Ängste, Panik oder Massenhysterien unter Menschen auslösen können [20]. Zur organisatorischen Vorbereitung auf bioterroristische Anschläge gehören neben der Erarbeitung von detaillierten Alarm- und Notfallplänen, der Beschaffung ausreichender Impfstoffvorräte (für Milzbrand in Deutschland nicht zur Verfügung stehend) auch die Bereitstellung von Überwachungs- und Laborkapazitäten, die eine schnelle und definitive Detektion und Diagnostik wichtiger bioterroristisch relevanter Erreger ermöglichen. Zurzeit existiert eine Vielzahl unterschiedlichster Nachweissysteme für *B. anthracis* zusammen mit einer großen Anzahl sich noch in der Entwicklung befindlicher Diagnosetechniken. Der nächste Abschnitt versucht, einen Abriss über etablierte Verfahren sowie über die neuesten Entwicklungen in diesem Feld zu geben.

1.2 Stand der Forschung

1.2.1 Bakteriologie *B. anthracis*

Folgende Punkte sind bei der Entwicklung eines geeigneten Detektionssystems für *B. anthracis* zu berücksichtigen: *B. anthracis* gehört zu den 200 Arten aerober Bakterien – aufgeteilt in mehr als 25 Gattungen –, die in der Lage sind, Endosporen auszubilden [21, 22]. Hierbei ist die Gattung *Bacillus* die größte und bildet ein weites Spektrum von Mikroorganismen ab, die sich verschiedenste, teils extreme Lebensräume zu eigen gemacht und sich eine Vielzahl organischer und anorganischer Stoffe als Nahrungsquellen erschlossen haben [23]. Die Endospore wird innerhalb der Mutterzelle als Reaktion auf Nähstoffmangel oder erhöhter Zelldichte gebildet und ist eine überaus widerstandsfähige, metabolisch weitestgehend inaktive und nicht vermehrungsfähige Überdauerungsform, welche dem Milzbranderreger im Boden und auf Oberflächen eine sehr hohe Tenazität von mehreren Jahrzehnten verleihen kann. Unter optimalen Laborbedingungen sind innerhalb von 7-8 Stunden nach Erreichen der Exponentialphase die ersten Endosporen zu beobachten. Unter suboptimalen Bedingungen indes treten diese auch sehr viel später auf, zum Beispiel bei einer Umgebungstemperatur von 12 °C erst nach zwei Wochen [24, 25]. Trotz metabolischer Inaktivität sind Endosporen in der Lage, sich bei Vorhandensein geringster Konzentrationen an Keimungsinduktoren (Aminosäuren, Zucker, Purinnukleoside, sublethale Hitzebehandlung mit 60 °C bis 100 °C) in eine stoffwechselaktive, vermehrungsfähige vegetative Zelle umzuwandeln. Der Prozess kann innerhalb von 10 bis 30 Minuten, im Falle sogenannter *superdormant spores* erst nach einigen Tagen erfolgen [26, 27]. Dies geht allerdings einher mit dem Verlust ihrer ausgeprägten Resistenzen. Endosporen können unter anderem (feuchte und trockene) Hitze, UV- und Gamma-Strahlung, hohe Drücke, extreme Trockenheit bis hin zum Vakuum sowie toxische Chemikalien in einem Maße überstehen, das vegetative Zellen sicher abtöteten würde [28].

Der Grund für diese außergewöhnliche Robustheit ist in dem Aufbau von Endosporen zu suchen, der sich wesentlich von denen vegetativer Zellen unterscheidet: (i) Endosporen besitzen einen Multischalenaufbau, bei dem der Sporenkern – das Analogon zum Protoplasten der vegetativen Zelle mit Zellwand, Membran, Zytoplasma und Nukleoid – umhüllt ist von einer Vielzahl weiterer Schichten (Sporenrinde/Cortex, innere Sporenhülle, äußere Sporenhülle, fallweise Exosporium), die die Durchlässigkeit für chemische Agenzien erniedrigen und eine Entgiftung herbeiführen können. (ii) Der Sporenkern liegt stark dehydratisiert vor (Wasser stellt bei Endosporen 27-55 % des Nassgewichts anstatt 75-80 % in vegetativen Zellen), weist aber einen hohen Grad an Mineralisierung auf. Besonders stark ist Ca^{2+} exprimiert und häufig durch Dipicolinsäure (Pyridin-2,6-dicarbonsäure, DPA) chelatisiert, sodass Calciumdipicolinat (CaDPA) circa 5-15 % des Trockengewichts einer Spore ausmacht. Eine starke Dehydratisierung des Sporenprotoplasten wirkt sich begünstigend auf die Hitzeresistenz von Sporen aus, ebenso ein hoher Gehalt an Ca^{2+}-Ionen [28]. (iii) Die Sporen-DNA ist gesättigt mit speziellen, DNA-bindenden Proteinen, den sogenannten kleinen säurelöslichen Sporenproteinen (*small acid-soluble protein,* SASP), welche 3-6 % des gesamten Proteinaufkommens in Endosporen ausmachen [29]. Dadurch erbringen sie einen wichtigen Beitrag zur UV-Strahlungs-, Hitze- und Chemikalienresistenz der Sporen und stehen ferner als Energie- und Kohlenstoffquelle bei der Sporenauskeimung zur vegetativen Zelle zur Verfügung. (iv) Ein Depot UV-Licht-absorbierender Pigmente in äußeren Sporenhüllen schirmt bei einigen *Bacillus*-Sporen photosensitive Komponenten (zum Beispiel DNA) vor UV-Strahlung ab [30].

Prinzipiell ist *B. anthracis* in der Umwelt als Endospore anzutreffen und repliziert sich fast ausschließlich innerhalb der kurzen Perioden einer Infektion, die entweder durch den Tod des Wirtsorganismus oder Abtötung des Keimes durch die Immunabwehr oder mithilfe therapeutischer Agenzien beendet werden. Deshalb ist die genetische Entwicklung von *B. anthracis* lediglich auf die kurze Phase zwischen Infektion und Tod des Wirtes beschränkt, was 20-40 Generationen ausmacht [31]. Dies ist der Grund, warum *B. anthracis* eine sehr homogene Spezies im Sinne genetischer und phänotypischer Eigenschaften ist (monomorph), was eine Differenzierung verschiedener *B. anthracis*-Stämme erschwert. Aber auch die Abgrenzung zu anderen *Bacillus*-Arten ist teilweise schwierig, insbesondere zu

den Spezies der so genannten *B. cereus*-Gruppe (BC-Gruppe) [32, 33]. Zu dieser gehören neben *B. anthracis* auch *B. cereus*, ein bekannter Lebensmittelkontaminat (insbesondere Milch und Milchprodukte) der Risikogruppe 2, dessen extrazelluläre Toxine Diarrhoe und Erbrechen auslösen können; *B. mycoides*, ein Risikogruppe-1-Keim mit auffällig rhizoider Kolonienmorphologie; *B. thuringiensis*, welcher kristalline Proteine (Bt-Toxine) bildet, die das Bakterium verbreitet zur biologischen Schädlingsbekämpfung Verwendung finden lässt; sowie *B. weihenstephanensis*, eine psychotrope Art der Risikogruppe 2, die sich bei Temperaturen unter 7 °C vermehrt und wie *B. cereus* in der Lage ist, ein emetisches Toxin, Cereulid, zu produzieren [34-38]. Diese Spezies sind taxonomisch sehr eng verwandt und weisen hoch konservierte chromosomale Gensequenzen auf, zum Beispiel sehr ähnliche 16S rRNA und 23S rRNA Sequenzen, anhand der die taxonomische Differenzierung von Bakterien üblicherweise erfolgt [39]. Die 16S rRNA Sequenzen (1 446 Nukleotide) von *B. anthracis*, *B. cereus*, *B. mycoides* und *B. thuringiensis* sind zu >99 % identisch und lediglich zwei Unterschiede (ein Nukleotid verändert, eine Baseninsertion) wurden in den 23S rDNA-Genen (2 889 Nukleotide) zwischen *B. anthracis* und *B. cereus* festgestellt [40, 41]. So vertreten einige Taxonomen die Ansicht, die Spezies der BC-Gruppe als eine Art zusammenzufassen [33]. Dennoch überwiegen phänotypische Charakteristika, unterschiedliche Pathogenitätslevel, klinische Symptome sowie ökologische Nischen die gängigen Kriterien bakterieller Taxonomie, sodass die bisherige Nomenklatur Bestand hat. Die Pathogenität wird durch Toxine hervorgerufen, die zumeist auf Plasmiden kodiert sind. Im Falle von vollvirulenten Stämmen von *B. anthracis* handelt es sich um zwei Megaplasmide: pXO1 (Toxinplasmid, 182 kbp) sowie pXO2 (Kapselplasmid, 96 kbp) [42, 43]. Dank pXO1 können die vegetativen Zellen drei für die Toxinbildung wichtige Proteinkomponenten exprimieren, wohingegen pXO2 die Aminosäuresequenzen von Enzymen enkodiert, die für die Synthese einer Antiphagozytosekapsel aus Poly-D-Glutaminsäure verantwortlich sind. Weniger virulent sind *B. anthracis*-Stämme, denen eines der beiden Plasmide fehlt und gänzlich avirulent jene ohne Plasmide. Der Verlust von pOX1 in der Umwelt geschieht wesentlich seltener als der von pOX2 [44].

1.2.2 Nachweis von *B. anthracis*

Eine ideale Identifizierungsmethode zur Detektion von *B. anthracis* aus Umweltproben müsste eine Reihe von Eigenschaften in sich vereinen: Sie sollte einfach anzuwenden sein, die Operatoren einem möglichst geringen Infektionsrisiko aussetzen und kosteneffizient sein. Wesentlich ist zudem eine schnelle Ergebnisausgabe nach Probennahme und mit Hinblick auf eine Anwendung am unmittelbaren Einsatzgebiet eine ausreichende Robustheit, um häufigen Ortswechseln sowie Änderungen klimatischer Bedingungen Rechnung tragen zu können. Die Methode sollte eine geringe Anzahl an Organismen detektieren können (Spezifität), ohne dass ungewollte Kreuzreaktionen mit eng verwandten biologischen Keimen, die ubiquitär in der Umwelt vorliegen, auftreten (Sensitivität). Letzteres ist vor allem durch das Vorhandensein von nicht-virulentem *B. cereus* in Gegenwart von *B. anthracis* in Umweltproben erschwert, da beide Arten eng verwandt sind und eine Vielzahl an phäno- und genotypischen Eigenschaften teilen [41, 45, 46].

Das Panel zur Verfügung stehender Identifizierungsmethoden für *B. anthracis* lässt sich im Wesentlichen einteilen in konventionell-mikrobiologische, nukleinsäure-basierte, affinitäts-basierte sowie biochemische Ansätze [47].

Über viele Jahre hinweg haben sich die traditionellen mikrobiologischen Methoden als Goldstandard etabliert. Sie beruhen auf der Beobachtung morphologischer Eigenschaften von Bakterien, nachdem sie in der Regel auf Selektivmedien kultiviert sowie optional gefärbt worden sind. So wird *B. anthracis* bakterioskopisch als Gram-positives, nicht-bewegliches Stäbchen (0,8-1,2 µm Durchmesser, 3-5 µm Länge) wahrgenommen, das in der Lage ist, ellipsoide Sporen (0,7-0,8 µm Durchmesser, 1,5 µm Länge) zu bilden. Auf Blutagarplatten wächst der Erreger ohne Beta-Hämolyse und ist sensitiv gegenüber Gamma-Phagen und Penicillin [48]. Chromogene und selektive Nährmedien dienen zusätzlich zur Abgrenzung von *B. anthracis* gegen die taxonomisch nächsten Verwandten *B. cereus*, *B. mycoides* und *B. thuringiensis* [49]. Weiterhin kann die durch das Bakterium ausgebildete Kapsel durch Anfärben gut visualisiert werden [50]. Außerdem ist mithilfe elektronenmikroskopischer Aufnahmen der Keime eine grobe primäre Diagnostik und eine erste Abschätzung der Erregerkonzentration möglich [51]. Weltweit am häufigsten wird indes der Schnelltest über Thermopräzipitation nach

Ascoli angewandt, obgleich dieser bei Umweltproben häufig falsch-positive Ergebnisse anzeigt [52]. Zuletzt ist die Virulenz des Keimes durch Tierversuche nachweisbar. Obwohl die Durchführung all dieser konventionellen Tests durch erfahrene Bakteriologen sicher möglich ist, eignen sich diese nur bedingt zur Analyse von Umweltproben durch Einsatzkräfte vor Ort. Unter den praktischen Gesichtspunkten ist der hohe Arbeits- und Zeitaufwand dieser Methoden zu erwähnen. Zum einen müssen die Arbeitsschritte in Laboren der Sicherheitsstufe 3 durch entsprechend geschultes Personal durchgeführt werden. Zum anderen ist eine Erregeranzucht von 1-2 Tagen stets obligatorisch aufgrund der geringen Sensitivität der Methode und muss durch zusätzliche Tests unter Umständen um ein ähnliches Zeitintervall erweitert werden [18]. Überdies musste festgestellt werden, dass einige *B. cereus*-Umweltisolate eigentlich *B. anthracis*-exklusive phänotypische Merkmale aufweisen [53]. Aufgrund dessen wird sowohl vom Robert Koch-Institut als auch vom Nationalen Referenzlabor für Milzbrand des Friedrich-Loeffler-Instituts empfohlen, mit molekulargenetischen Verfahren den mikrobiologischen Befund in jedem Fall abzusichern.

Daher werden Nachweissysteme basierend auf der Polymerasekettenreaktion (PCR) zunehmend für die schnelle und sensitive Erkennung des Erbmaterials von pathogenen Erregern eingesetzt. In einem plattformübergreifenden Vergleich unterschiedlichster *B. anthracis*-Nachweissysteme wurden mittels *real-time*-PCR bzw. *end-point*-PCR mit 430 Zellen/ml bzw. 440 Zellen/ml die geringsten Nachweisgrenzen aller untersuchten Verfahren erreicht [54]. Voraussetzung ist die Wahl geeigneter *B. anthracis*-spezifischer Nukleinsäuressequenzen (Probe und Primer), will man Kreuzreaktionen mit verwandten Spezies ausschließen. Sich allein auf Gensequenzen der Virulenzplasmide pXO1 (zum Beispiel *pag*) und pXO2 (*capC*) zu beschränken, kann zu Fehldiagnosen führen, da pXO1- und pXO2-ähnliche Plasmide in einigen nicht-virulenten *B. cereus*-Umweltisolaten gefunden worden sind [55]. Überdies wurden zwei, ebenfalls pXO1- und pXO2-ähnliche Plasmide tragende *B. cereus*-Stämme (als *B. cereus* var. anthracis deklariert) von Menschenaffen in Kamerun und der Elfenbeinküste isoliert, die an einer Anthrax-ähnlichen Krankheit gestorben sind [56, 57]. Ein horizontaler Gentransfer der Virulenzplasmide zwischen eng verwandten Spezies ist bekannt [58]. Zugunsten der Spezifität gegenüber *B. anthracis* werden deshalb weitere chromosomale

Zielsequenzen zur Charakterisierung von Isolaten des Milzbranderregers hinzugezogen. Die Auswahl geeigneter Genabschnitte erweist sich jedoch aufgrund der hohen genetischen Ähnlichkeit zwischen den Spezies der BC-Gruppe als diffizil. So wurden zeitweise bestimmte Einzelnukleotid-Polymorphismen (SNP, *single nucleotide polymorphism*) als *B. anthracis*-spezifisch deklariert, ehe sie ebenso in Isolaten anderer *Bacillus*-Arten detektiert worden sind. Ein Beispiel ist das *rpoB*-Gen: 2001 durch Qi *et al.* als *B. anthracis*-exklusiv beschrieben, bis 2006 identische Polymorphismen durch Zasada *et al.* im Genom von *B. thuringiensis* aufgezeigt worden sind [59, 60]. Zudem erzeugten einige *B. cereus*-Isolate verzögerte *rpoB*-Signale durch mutmaßliches *mispriming* der DNA-Polymerase [53]. Diese verzögerten positiven Signale machen es schwierig abzuschätzen, ob diese nun tatsächlich von *B. cereus*-Keimen in der Probe stammen oder aber durch eine sehr geringe Anzahl von *B. anthracis*-Sporen. Ebenso hinderlich für den Einsatz vor Ort ist die Anfälligkeit der PCR gegenüber Inhibitoren in der Probenmatrix, da etwa Erdbestandteile oder ungünstige pH-Werte hemmend wirken [61-63]. So ist nachvollziehbar, dass die anfangs dieses Abschnittes angegebenen Nachweisgrenzen im Falle von Bodenproben bei weitem nicht erreicht werden: Hier gelten gerade noch 100 Sporen/mg Boden eines PCR-*Enzyme Linked Immunosorbent Assay*s (PCR-ELISA) als niedrigster publizierter Grenzwert [54]. Neben der Direktisolation der DNA aus den Proben gilt nur die zeitintensive Vorkultivierung als Alternative. Ferner ist die Portabilität präzise arbeitender Thermocycler selten gegeben und zeitaufwändige Arbeitsschritte nach einer *end-point*-PCR obligatorisch. Hier spielt die im Jahre 2000 von Notomi *et al.* eingeführte *loop-mediated isothermal amplification* (LAMP) ihre Stärken aus: Diese arbeitet unter Einsatz einer zur Strangverdrängung befähigten DNA-Polymerase sowie einem spezifischen Primersatz (typischerweise vier) konstant bei Temperaturen von 60-65 °C bei einer Reaktionszeit von 1 h [64]. Da außerdem größere Mengen von Magnesiumhydrogenphosphat ausfallen, ist eine Verfolgung des Reaktionsablaufs durch turbidimetrische Messungen möglich [65]. So konnten 1 000 Genomkopien von *B. anthracis* durch LAMP unter Verwendung eines Taschenwärmers detektiert werden [66, 67]. Die Spezifitäten einer *real-time*-PCR sind durch LAMP noch nicht erreicht worden und eine sichere Differenzierung von Spezies der BC-Gruppe verbleibt weiterhin schwierig. Weitere molekulargenetische Methoden wie

multi locus sequence typing (MLST), *multi locus variable number tandem repeat analysis* (MLVA), *amplified fragment-length polymorphism* (AFLP) oder gar die vollständige Genom-Sequenzierung haben eine klare Diskriminierung von *B. anthracis* und zusätzlichen Spezies der BC-Gruppe ermöglicht [32, 68-70], allerdings sind diese Techniken nur zur Analyse von isolierten Kolonien im Labor ausgelegt und kaum für eine schnelle Vor-Ort-Diagnose geeignet.

Viel eher werden zurzeit affinitätsbasierte Assays zum schnellen *B. anthracis*-Nachweis eingesetzt, von denen einzig die antikörperbasierten Ansätze kommerziell erhältlich sind, obwohl sich als Liganden ebenfalls Peptide oder Aptamere als geeignet erwiesen haben [47]. Diese Plattformen liefern binnen Minuten nach einfachster Handhabung Ergebnisse, die allerdings sowohl eine ausreichende Spezifität wie Sensitivität vermissen lassen, was dem Einsatz als Diagnoseinstrument vor Ort zugegen läuft [71]. Viel eher sind sie von Wert in epidemiologischen Studien und der Medizindiagnostik, das heißt in Situationen, in denen eine Infektion bereits erfolgt ist.

Zumindest eine Vorkultivierung ist bei analytischen Methoden, die sich exklusiv auf den Nachweis des endosporen-spezifischen CaDPAs kapriziert haben, nicht unbedingt notwendig. Die höchste Sensitivität wird augenblicklich durch fluorometrische Messungen von Lanthanoid-DPA-Komplexen erreicht, für die aber im Hinblick auf Realproben eine möglichst effiziente Extraktion und Aufreinigung von DPA aus den Proben obligat ist, beispielsweise unter Zuhilfenahme chromatographischer Methoden [72]. Eine Nachweisgrenze von 0,5 nM DPA (dies entspricht unter der Annahme von circa 0,5 fM CaDPA/Spore 10^3 Sporen/ml) wurde durch einen Hochleistungsflüssigkeitschromatographie-Ansatz (HPLC) mit angeschlossener Terbium-Komplexierung und Lumineszenzmessung erreicht [73, 74]. Ein Einsatz Europium-basierter Nanopartikel verspricht sogar Nachweisgrenzen von 0,2 nM CaDPA [75]. Da DPA andererseits nur ein genereller Sporenindikator ist, sind Unterscheidungen zwischen verschiedenen Sporenarten nicht möglich.

Biochemische Identifikationsmethoden für *B. anthracis* fußen auf der Erkennung biochemischer Muster innerhalb von Signaturen der untersuchten Keime. Die Art der Signaturen ist dabei mannigfaltig: Zum einen werden die Bazillen nach metabolischen Eigenschaften und ihrer Resistenz gegenüber Antibiotika charakte-

risiert [76]. Weiterhin können Profile bakterieller Fettsäuren (*fatty acid methyl ester*, FAME) via gaschromatographischer Verfahren als Unterscheidungsmerkmal herangezogen werden [77]. Außerdem erlauben Kombinationen verschiedener Biomarkerklassen die Diskriminierung von *Bacillus*-Spezies, wie im Falle einer Analyse durch Gaschromatographie mit Massenspektrometrie-Kopplung (GC/MS-Analyse) der Signaturen von FAMEs, Dipicolinsäure und Kohlenhydraten [78]. Im Falle massenspektrometrischer Ansätze sind aber vorwiegend Proteine die Biomarker der Wahl, speziell bei *Bacillus*-Sporen die SASPs, entweder detektiert in intakter Form oder aber als durch chemische oder enzymatische Verdauung proteolysierte Peptide [79, 80]. Allen gemein ist, dass eine standardisierte Erregeranreicherung unumgänglich ist, was sich in einem hohen Zeitaufwand äußert, der einen Einsatz dieser Techniken am Ort des Geschehens durch Ersthelfer konterkariert. Zum einen ist es nur durch eine Vorkultivierung möglich, genügend Analysematerial zu generieren [81]. Zum anderen ist bekannt, dass Typ, Zusammensetzung und Menge der FAMEs eines Organismus in hohem Maße abhängig sind von den Bedingungen, unter denen die Bakterien zuvor kultiviert worden sind (Anzuchtmedium, -temperatur, -zeit) [82]. Beispielsweise üben komplexe Additive in den Nährmedien (Fleisch-, Hefeextrakt…) sowie Proteinquellen (Pepton, Trypton…) einen erheblichen Einfluss auf die Fettsäureausstattung von *Bacillus*-Kulturen aus [83]. Ähnlich abhängig von Kultivierungsparametern sind MS-Biomarker aus intakten Proteinen oder Peptiden, wie eine Studie über die Reproduzierbarkeit von MS-Spektren einer *E. coli*-Kultur, aufgenommen in drei Laboratorien, zeigt: Nur 25 % der diesem Bakterium zugeordneten Biomarker konnten in Spektren aller drei Labore detektiert werden [84]. Ein Anziehen der Bakterien vor der MS-Analyse unter rigider Einhaltung wohl definierter Kultivierungsbedingungen ist neben einer standardisierten Probenvorbereitung deshalb zwingend erforderlich [85, 86].

1.2.3 Raman-Spektroskopie als alternative Detektionsmethode für *B. anthracis*

Schwingungsspektroskopische Techniken wie die Raman-Spektroskopie lassen sich gleichermaßen zu den biochemischen Identifikationsmethoden zählen. Ihr großes Potential besteht darin, dass sie *In-situ*-und *In-vivo*-Informationen von Biomolekülen in schneller, aber ausreichend spezifischer, nicht-invasiver Art unter physiologischen Bedingungen liefern können [87]. Basis für die Raman-Spektroskopie ist die inelastische Streuung von Licht an Molekülen, die von den beiden indischen Wissenschaftlern C. V. Raman und K. S. Krishnan entdeckt wurde [88-90]. Inelastisch heißt, dass die Wellenlänge des gestreuten Lichts mit jener des einfallenden Lichts nicht identisch ist wie im Falle der Rayleigh-Streuung. Unter Ausnutzung dieses so genannten Raman-Effektes können Informationen über alle Moleküle innerhalb einer Probe abgefragt werden. Die Probe wird dazu monochromatisch bestrahlt und das inelastisch gestreute Licht als Raman-Spektrum registriert. Das Spektrum entsteht durch eine Ensemblemittelung über alle Probensubstanzen, das heißt, es entspricht einer Superposition von Raman-Spektren der probeninhärenten Substanzen. Anhand der Spektren lassen sich Rückschlüsse auf die biochemische Zusammensetzung und molekulare Struktur der Probe ziehen. Werden mittels der Raman-Spektroskopie Bakterien analysiert, so sind Proteine, DNA/RNA, Kohlehydrate sowie Lipide die Molekülklassen, die im Wesentlichen das Raman-Spektrum der Probe dominieren, da dies die Hauptkonstituenten von Bakterien sind [91]. Lediglich das in allen Bakterien vorhandene Wasser trägt aufgrund seines geringen Raman-Streuquerschnitts[1] kaum zum Raman-Spektrum einer Bakterie bei. Unter der Annahme, dass Bakterien unterschiedlicher taxonomischer Zugehörigkeit auch unterschiedliche biochemische Zusammensetzungen besitzen, die wiederum durch die Raman-Spektroskopie abgefragt werden können, ist eine Typisierung von Bakterien anhand ihrer spektroskopischen Signatur möglich [91, 92]. In der Regel sind diese Signaturen sehr komplex, weisen teils kaum wahrnehmbare Unterschiede auf und lassen sich

[1]Der Streuquerschnitt eines Moleküls spiegelt die Wahrscheinlichkeit aller möglichen Streuprozesse eines Moleküls wider und ist der Streuintensität proportional.

weiterhin nicht in ihre Einzelkomponenten entmischen. So werden die Spektren als solche – gleichsam eines Fingerabdruckes – einer Analyse zugeführt, ohne näher erklärt werden zu müssen. Auf Grund dessen sind datenbankbasierte statistische Auswerteroutinen unabdingbar, will man Raman-Spektroskopie zur Identifizierung von Bakterien anwenden (Chemometrik) [93]. Hierfür kommen überwachte Lernalgorithmen in Betracht, die Gruppenunterschiede modellieren können, beispielsweise die lineare Diskriminanzanalyse (LDA), die *Support Vector Machines* (SVM) oder die künstlichen neuronalen Netze (ANN). Mit Hilfe algorithmischer Schätzer wie der Kreuz- oder *Holdout*-Validierung versucht man dann, die Vorhersagequalität dieser Klassifikatoren zu evaluieren, indem ein Teil der Daten zum Aufbau des Modells herangezogen und mit dem Rest der Daten ausgetestet wird[2]. Auf diese Weise ist es möglich, das Diskriminierungsvermögen des Modells (Klassifizierung) einerseits, andererseits dessen Generalisierungspotential (Identifizierung) zu validieren.

Im Laufe der Jahrzehnte, in denen die Raman-Spektroskopie zur Analyse biologisch relevanter Sachverhalte herangezogen wurde, sind eine Reihe spezieller Raman-basierter Methoden entwickelt worden, um bestimmte Nachteile der konventionellen Raman-Spektroskopie zu minimieren. Insbesondere die geringe Quantenausbeute[3] des spontanen Raman-Effekts wirkt sich negativ auf die Sensitivität der Methode aus [94]. Die im Umfeld der Biospektroskopie am häufigsten angewandten Verstärkungstechniken sind die Resonanz-Raman-Spektroskopie (*resonance Raman spectroscopy*, RRS) sowie die oberflächenverstärkte Raman-Spektroskopie (*surface-enhanced Raman spectroscopy*, SERS). Bei der Resonanz-Raman-Spektroskopie wird die Raman-Anregungswellenlänge so gewählt, dass sie sich in der Nähe einer elektronischen Absorption eines in der Probe befindlichen Chromophores befindet. Dadurch werden jene Banden selektiv verstärkt, welche an den elektronischen Übergang gekoppelt sind und das ehemals komplexe

[2] Im Folgenden wird von einer Klassifizierung gesprochen, wenn das Modell mit Daten validiert wird, mit welchen es erstellt worden ist. Eine Identifizierung indes bedeutet ein Testen des Modells mit Daten, die völlig unabhängig von den Modelldaten generiert worden sind. Idealerweise stammen die Testdaten von anderen Präparaten als denen der Modelldaten und wurden nicht an denselben Tagen wie die Referenzspektren gemessen.

[3] Von 10^6 – 10^{10} gestreuten Photonen wird nur eines bei Raumtemperatur Stokes-Raman-gestreut.

Raman-Spektrum wird durch die Banden des Chromophores dominiert[4] [96]. Dies ist aber nur in Systemen beobachtbar, in denen die Stokes-Verschiebung zwischen Absorption und Fluoreszenz groß genug ist, andernfalls würden die Resonanz-Raman-Signaturen von der Fluoreszenz überdeckt werden. Durch die Resonanz-Raman-Spektroskopie sind somit sehr geringe Mengen eines Zielchromophores selbst in komplexen Matrices detektierbar. Bei sichtbarer Anregung sind dies bei Bakterien insbesondere Carotenoide und Hämoproteine wie Cyctochrome. Bei Verwendung von UV-Licht mit 218-231 nm werden besonders aromatische Proteine, bei 242-257 nm Nukleinsäuren in Bakterien adressiert, allerdings ist Photodegradation der Probe ein immanentes Problem der UV-Resonanz-Raman-Spektroskopie [97]. In UVRR-Spektren von Endosporen unter 242-244 nm Anregung stellte man fest, dass die Schwingungen von CaDPA resonant verstärkt werden [97, 98]. Mit derselben Anregung konnte eine Diskriminierung sechs verschiedener *Bacillus*-Arten anhand ihrer UVRR-Spektren gezeigt werden, der jedoch methodenbedingt eine Vorkultivierung vorausgehen musste [99].

Die oberflächenverstärkte Raman-Spektroskopie macht sich die Eigenschaft zu Nutze, dass in der Nähe nanostrukturierter Metalloberflächen (meist Silber, Kupfer oder Gold in Form von Kolloiden oder strukturierter Oberflächen) das eingestrahlte Feld verstärkt wird[5] [101]. Oberflächenplasmone koppeln mit dem externen elektrischen Feld und erzeugen so das verstärkte (evaneszente) Feld senkrecht zur Metalloberfläche, welches an Analytmolekülen in der Nähe der Metalloberfläche gestreut wird. Dieses Raman-gestreute Feld kann dann erneut an der Metalloberfläche verstärkt werden. Zusätzlich zu der eben beschriebenen elektromagnetischen Verstärkung kommt eine chemische Verstärkung hinzu, die auf einer Wechselwirkung zwischen dem Analytmolekül und der nanostrukturierten Metalloberfläche beruht. Mit Hilfe oberflächenverstärkter Raman-Spektroskopie wurden sensitive Verfahren entwickelt, mit welchen CaDPA von wenigstens 10 µg Sporen als Biomarker für Endosporen nachgewiesen werden konnte [102-104]. Selbst in Form eines portablen Raman-Spektrometers spürte man noch minimal 10^4 Sporen

[4] Im Vergleich zu nicht-resonanter Anregung sind Signalverstärkungen um bis zu sechs Größenordnungen möglich [95].

[5] Im Vergleich zu nicht-resonanter Anregung wird mit Signalverstärkungen von fünf bis sieben Größenordnungen gearbeitet [100].

auf [105]. Voraussetzung hierfür ist indes, dass CaDPA vor der Spektrenaufnahme aus den Endosporen extrahiert werden muss. Weiterhin kann eine Aussage, um welche Art von Endosporen es sich letztlich handelt, etwa pathogene oder harmlose, durch solche Ansätze natürlich nicht geliefert werden. Dass sich grundsätzlich SERS-Spektren intakter Endosporen von denen anderer möglicher Biowaffenagenzien sowie von Endosporen verschiedener *Bacillus*-Arten unterscheiden, wurde gezeigt, eine tatsächliche Identifizierung von Endosporen aus Realproben via SERS steht hingegen noch aus [106-108]. Allgemein ist bei SERS zu beachten, dass nur bestimmte Schwingungen des Analyten verstärkt werden. Lediglich die Moden mit Polarisierbarkeitskomponenten senkrecht zur Metalloberfläche werden intensiviert. Ein SERS-Spektrum kann folglich völlig anders aussehen als ein konventionelles Raman-Spektrum. Zudem ist eine identische Mikroumgebung relativ zur Metalloberfläche eines jeden Analystmoleküls nicht realisierbar, sodass die Vergleichbarkeit der SERS-Spektren häufig nicht ausreichend gegeben ist, wenn nicht eine sehr präzise Probenpräparation erarbeitet worden ist.

Genau Letzteres ist bei der Raman-Mikrospektroskopie weitaus weniger problematisch. Hier wird die hohe räumliche Auflösung eines konfokalen Mikroskops mit dem molekularen Kontrast der Raman-Spektroskopie zu einem Ansatz kombiniert, der gut zur Aufklärung biologischer Fragestellungen geeignet ist. Konfokale Mikroskope verwenden Aperturen, die die Auflösung in lateraler und axialer Richtung erhöhen. Durch das erste *Pinhole* wird die Anregungslichtquelle zu einer Punktquelle beschnitten, die zweite Apertur sorgt dafür, dass nur das Licht unmittelbar aus der Fokalebene passieren kann. So werden effektiv Beiträge aus Ebenen außerhalb des Fokus eliminiert. Durch den Einsatz von Objektiven hoher numerischer Aperturen (NA = 0,9-0,95) sind so fokale Volumina in geringen Breiten ($1{,}22\lambda/NA$) und Längen ($4n\lambda/NA^2$) realisierbar [109]. Mit einer Anregungswellenlänge von 532 nm sind daher Messvolumina von $<1\ \mu m^3$ möglich. Infolgedessen ist die Möglichkeit gegeben, einzelne Bakterienzellen zu messen – ganz im Gegensatz zu den zuvor beschriebenen Methoden, die nur große Haufen von Zellen (*bulk*-Messungen) analysieren können [110][6]. Eine teils sehr zeit-

[6] Zum Vergleich: Mit einem FT-IR-Mikroskop sind Messpunkte wellenlängenbegrenzt bis minimal 10 µm realisierbar, sodass etwa 10^2 Bakterien pro Messung beprobt werden [91].

aufwändige Kultivierung bis zu mehreren Tagen wird deshalb obsolet und Bakterien können direkt nach ihrer Isolierung aus der Probe untersucht werden [111-113].

Weiterhin erweist sich als vorteilhaft, dass zumindest Kokken und nicht allzu große Bazillen bei Verwendung von 532 nm Anregungswellenlänge durch das Messvolumen in Gänze erfasst werden. Überdies besitzen Bakterien im Gegensatz zu eukaryotischen Zellen keine Organellen und werden so innerhalb des Messvolumens als homogen wahrgenommen. Deshalb ist ein Spektrum zur Beschreibung einer Zelle hinreichend. Dies gilt umso mehr für Endosporen. Dementsprechend umfänglich ist das Ausmaß an Publikationen, die sich mit der Ramanspektroskopischen Charakterisierung von Endosporen auf Einzelzellebene beschäftigten. Hervorstechendes Merkmal in den Raman-Spektren von Einzelzellen sind die Banden des CaDPAs [111, 114]. Dessen Gehalt und die Gehaltsverteilung selbst nach variierten Kultivierungsbedingungen in Endosporenensembles konnte verfolgt werden. Ebenso wurde dessen Abnahme im Laufe der Endosporenkeimung registriert, um Aufschlüsse über die Kinetik der Keimung gewinnen zu können [115-118]. Außerdem wurde Raman-spektroskopisch versucht, Schlüsse auf den physikochemischen Zustand des CaDPAs in Endosporen abzuleiten, in denen es in Konzentrationen (>800 mM) weit über dessen eigentlicher Löslichkeit vorliegt [119]. Ähnliche Studien wurden an *superdormant spores* durchgeführt [27, 120]. Häufig wurden der Messlaser gleichzeitig als optische Pinzette angewandt, um Spektren isolierter Sporen ohne Einflüsse eines Substrates messen zu können [121]. Eine Detektion und Identifikation von *Bacillu*s-Endosporen mit Hilfe von konventioneller Raman-Spektroskopie und -Mikrospektroskopie wurde bisher nur sporadisch bearbeitet: Farquaharson *et al.* stellten ein faserbasiertes Raman-Spektrometer mit 785 nm Anregungswellenlänge vor, mit dem Briefe auf den Gehalt von Endosporen bis zu einer Menge von 4,5 mg Sporen automatisch geprüft werden konnten [122]. Eine Klassifizierung von *B. atrophaeus*- und *B. thuringiensis*-Sporen aus destilliertem Wasser anhand ihrer Raman-Einzelzellspektren bei 532 nm Anregung wurde auch realisiert, dies aber lediglich im Vergleich mit anderen Bakteriengattungen (wie *Escherichia* oder *Yersinia*) und biologischen Substanzen (wie Rinderserumalbumin oder Insulin) [123]. In einer

späteren Arbeit wurde dieser Datensatz um *B. anthracis* und *B. cereus* erweitert [124].

Zusammenfassend lässt sich konstatieren, dass weitreichende Studien zur Charakterisierung von Endosporen mithilfe Raman-spektroskopischer Methoden durchgeführt worden sind, ebenso wie Arbeiten, die das Diskriminierungspotential dieser Technik andeuten. Weiterführende Untersuchungen im Hinblick auf eine tatsächliche Identifizierung von Endosporen aus Umweltproben stehen indes noch aus. Als vielversprechendste Variante sticht hierfür die Raman-Mikrospektroskopie heraus, deren größter Vorteil die Möglichkeit ist, ohne vorherige Kultivierung einzelne Bakterienzellen schnell in physiologischer Umgebung *in situ* analysieren zu können. Der zeitliche, präparative und apparative Aufwand verbleibt gering, so dass ein Einsatz dieser Technik unmittelbar am Einsatzort (*point-of-care-testing*) plausibel erscheint. Als Anregungslaserwellenlängen eignen sich solche im sichtbaren Bereich, da sie einen guten Kompromiss zwischen der ν^4-Abhängigkeit[7] der Streueffizienz (UV wäre zu bevorzugen) und möglicher Fluoreszenz (Nah-IR wäre zu bevorzugen) darstellen.

Die hier vorgelegte Arbeit beschäftigt sich mit der Fortentwicklung und Anwendung der Raman-Mikrospektroskopie mit Anregung im sichtbaren Spektralbereich zur Identifikation von *Bacillus*-Endosporen, insbesondere *B. anthracis*, sowie der Detektion derselben in Umweltproben. Dies soll unmittelbar nach Isolation der Keime vor Ort im Sinne einer Schnelldiagnostik erfolgen; zur Spektrenanalytik soll sich chemometrischer Methoden bedient werden. Zuerst wurde untersucht, inwieweit divalentes Mangan als ein typischerweise als Sporulationsbeschleuniger eingesetzter Kultivierungsfaktor Einfluss auf Raman-Spektren von Einzelsporen und damit mutmaßlich auf das Diskriminierungspotential der gesamten Methodik hat. Dies ist ein nicht zu unterschätzender Faktor, da eine Analyse intakter Zellen hochgradig von den Umständen der Bakteriengenese beeinflusst wird, wozu mithin neben der Kultivierungstemperatur, -zeit oder -atmosphäre auch die zur Verfügung stehenden Nährstoffe und Supplemente zählen [86, 126, 127]. Um eine Isolierung und Analyse von möglicherweise hochpathogenen Endosporen durch

[7] Der Streuquerschnitt einer Schwingung ist zur 4. Potenz der Summe aus der Frequenz des einfallenden Lichtes und der Energiedifferenz zweier Schwingungszustände proportional [125].

Einsatzkräfte vor Ort zu ermöglichen, musste zudem eine effiziente und zur Raman-Spektroskopie kompatible Inaktivierungsmöglichkeit erarbeitet werden, sodass selbst außerhalb von BSL3-Laboratorien ein Umgang mit den Proben gefahrlos möglich ist. Mit derart vorbehandelten Endosporen wurden dann Datenbanken an Raman-Spektren von Endosporen aufgebaut und statistische Datenverarbeitungs- und Auswertealgorithmen erforscht, um eine Identifikation vieler verschiedener Arten an *Bacillus*-Endosporen selbst in Umweltproben zu ermöglichen.

1.3 Eigene Forschungsergebnisse

1.3.1 Raman-spektroskopische Analyse des Einflusses von Mangan auf die Sporulation von *Bacillus*-Endosporen

Wie bereits erwähnt, ist der Kern von Endosporen stark mineralisiert. Der Gehalt von Ca^{2+} ist besonders hoch und steht in direktem Zusammenhang mit der Hitzeresistenz der Sporen. Dies gilt in geringerem Maße auch für Mn^{2+}, welches darüber hinaus der Lage ist, die Sporulation von *Bacillus*-Endosporen einzuleiten [128]. Aktuelle genetische Studien haben gezeigt, dass die Mangan-Homöostasis in *B. subtilis* essentiell für eine effektive Sporulation ist und eine wichtige Rolle bei einigen Phasen der Sporulation spielt [129]. Aber selbst ohne präzise die biochemische Basis zu kennen, wird seit den 1950er Jahren in der Mikrobiologie divalentes Mangan als Supplement von Kulturmedien eingesetzt, um die Sporulation von *Bacillus*-Endosporen zu effektivieren. Da sich die Art und Zusammensetzung der Mineralien direkt in den Sporen je nach Zusammensetzung des Sporulationsmediums ändern kann, muss in Betracht gezogen werden, dass darüber hinaus die Raman-Spektren einzelner Sporen durch derartige Kultivierungszusätze verändert werden können [130]. Deshalb war ein Ziel dieser Arbeit zu untersuchen, inwieweit der Zusatz von divalentem Mangan als Sporulationsbeschleuniger Einfluss auf Endosporen-Raman-Spektren und damit auf das Diskriminierungspotential der Methode ausübt [SS1]. Dementsprechend wurden sechs verschiedene *Bacillus*-Stämme jeweils einmal mit Mangansupplement (10 mg $MnSO_4$ pro 1 Liter Kulturmedium) und ohne Manganzusatz unter ansonsten gleichen Bedingungen kultiviert, Raman-spektroskopisch vermessen und anhand chemometrischer Auswerteverfahren (hierarchische Clusteranalyse, kurz HCA und Hauptkomponentenanalyse, kurz PCA) analysiert. In der Tat konnten so spektrale Veränderungen in den Raman-Spektren von Endosporen gefunden werden, die mit der An-/Abwesenheit von Mn^{2+} im Medium während der Anzucht korreliert werden können: Insbesondere traten Veränderungen in Signallage und –intensität einiger Banden auf.

Dies ist deutlich bei den Signalen des CaDPAs bei 1400 cm^{-1} (symmetrische Streckschwingung der Carboxylatgruppe), 1450 cm^{-1} (Pyridin-Ringschwingung) sowie 1573 cm^{-1} (asymmetrische Streckschwingung der Carboxylatgruppe) zu beobachten, wie Abbildung 4 in [SS1] darstellt. Deutlicher tritt zudem die Bande bei 1030 cm^{-1} (u. a. CH-Deformationschwingung Phenylalanin) zu tage, wenn mit Mangan supplementiertem Medium angezogen wurde; weitere Veränderungen von Banden anderer Biomoleküle (zum Beispiel die Amid-I-Bande bei 1659 cm^{-1} oder die Signale der Ringatmungsschwingungen der Nukleinbasen Cytosin, Thymin, Uracil bei 785 cm^{-1}) sind nicht zu verzeichnen. Lediglich in den Raman-Spektren der Art *B. sphaericus* ist eine zusätzliche Bande bei 1485 cm^{-1} zu registrieren, aber nur, wenn die Bakterien zuvor ohne Sporulationsbeschleuniger kultiviert worden sind. Die Herkunft dieser Bande bleibt noch zu bestimmen.

In ihrer Gesamtheit erlaubten dieselben spektralen Änderungen eine Klassifizierung der Endosporen-Raman-Spektren nach An-/Abwesenheit des Manganzusatzes. Dies stand aber weniger in Konkurrenz mit der Kategorisierung der Sporen nach ihrer taxonomischen Zugehörigkeit, wie das Dendrogramm in Abbildung 1 in [SS1] darstellt. Hier ist zunächst eine eindeutige Clusterung der Daten in die vier *Bacillus* spp. zu sehen, ehe der Kultivierungsunterschied eine Klassifizierungshierarchie tiefer weitere Subcluster hervorbringt. Zu einem vergleichbaren Befund kommt man nach Analyse der PCA-Ergebnisse (Abbildungen 5-7 in [SS1]), in denen die *loadings*-Plots die bereits oben angesprochenen Bandenverschiebungen klar wiedergeben. Im Zuge dieser Ergebnisse und der Tatsache, dass die Mineralienzusammensetzung in den Sporen mit der Zusammensetzung des Sporulationsmediums korreliert, wurde die Hypothese aufgestellt, dass zumindest ein Teil der spektralen Veränderungen einhergeht mit einer intrasporalen Akkumulation von Mangandipicolinat (MnDPA), wenn der Sporulationsbeschleuniger eingesetzt worden ist. Zur Verifizierung dieser Hypothese wurden die beiden Salze CaDPA und MnDPA synthetisiert und deren Raman-Spektren aufgenommen. Desweiteren wurden mittels quantenmechanischer Rechnungen die theoretischen Raman-Spektren beider Salze kalkuliert. Beides wurde verglichen mit den Daten aus den Endosporen. Sowohl bei experimentell als auch berechneten Salzspektren lassen sich die Signalverschiebungen in den Endosporenspektren nachvollziehen. Insbesondere die Signale von Schwingungen der Carboxylat-Gruppen erfahren

Veränderungen beim Wechsel des Zentralmetalls von Ca^{2+} zu Mn^{2+}: Dies betrifft die symmetrische Streckschwingung der Carboxylatgruppe -COO^- bei 1400 cm^{-1} (Endosporen ohne Manganzusatz kultiviert) beziehungsweise 1390 cm^{-1} (Endosporen mit Manganzusatz kultiviert) sowie deren asymmetrisches Pendant bei 1573 beziehungsweise 1592 cm^{-1}. Theoretische und experimentelle Studien an Picolinaten bestätigen die Einflussnahme der Art des Zentralatoms auf die Bandenlage der Carboxylat-Valenzschwingungen [131, 132]. Die pyridinring-assoziierten Banden (1016 cm^{-1}, 1450 cm^{-1}) bewahrten indes ihre spektrale Lage. Diese Beobachtungen zusammen mit den spektralen Veränderungen in den Raman-Spektren der Endosporen untermauern die aufgestellte Hypothese, dass zumindest ein Teil des Mangans als MnDPA in den Sporen inkorporiert wurde. Dies ist sicher nur ein Effekt, den ein erhöhtes Angebot an divalentem Mangan während der Sporulation in den Endosporen hervorruft, nichtsdestotrotz lässt sich konstatieren, dass durch diesen Umstand messbare Veränderungen in den Raman-Spektren der Sporen zu tage treten. Entsprechendes muss bei der Anzucht von Endosporen berücksichtigt werden, will man sie Raman-spektroskopisch analysieren.

1.3.2 Erarbeitung einer zur Raman-Spektroskopie kompatiblen Inaktivierungsmethode für *Bacillus*-Endosporen

Beim Umgang mit Proben mit möglicherweise hochpathogenen Bakterien wie *B. anthracis* ist eine Inaktivierung der Keime vor jeglichen weiteren Arbeitsschritten obligatorisch. Praktisch stehen Myriaden an Desinfektionsmitteln und -verfahren zur Abtötung von Bakterien zur Verfügung, die allerdings stark eingeschränkt werden, gilt es, Endosporen abzutöten. Deren ausgesprochene Resistenz gegenüber einer Vielzahl physikalischer und chemischer Schadeinflüsse erfordert wesentlich stärkere Desinfektionsmaßnahmen, als es bei vegetativen Zellen der Fall ist. Einige Mechanismen, die Endosporen gegen Hitze, Strahlung oder Chemikalien schützen, sind aufgeklärt. So ist bekannt, dass der geringe Wasser- sowie hohe Mineraliengehalt im Sporenkern wesentlich zur Resistenz hinsichtlich feuchter Hitze beiträgt. Die SASPs verändern die Photochemie der Sporen-DNA und sind so der Hauptgrund für die UV-Resistenz – sie spielen

gegenüber Gamma-Strahlung aber keine Rolle. Die Effizienz chemischer Agenzien wird teils durch Hüllenproteine, die mit den Chemikalien reagieren, oder durch die innere Membran als Permeabilitätsbarriere herabgesetzt. Gelangen die Chemikalien in den Sporenkern und üben eine Schadwirkung auf die Sporen-DNA aus, so sind erneut die SASPs sowie DNA-Reparaturmechanismen Grund für eine herabgesetzte Wirkung der Agenzien [28, 29].

Daher ist eine Bewertung der Inaktivierungseffizienz unabdingbar, wenn wie in der vorliegenden Arbeit eine geeignete Inaktivierungsmethode erforscht werden soll. Gleichzeitig muss gewährleistet sein, dass die Inaktivierungsmethode sowohl zum nachfolgenden Isolierungsschritt der Sporen aus den Matrices als auch zur letztendlichen Raman-spektroskopischen Analyse kompatibel ist [SS2].

Zur Oberflächendesinfektion in Laboren existiert in Deutschland bisher kein zugelassenes, sporizides Desinfektionsmittel [133]. Die *World Health Organization* empfiehlt unter anderem die Verwendung von Formaldehyd und Peressigsäure [134]. Die Nachteile der Peressigsäure wie deren stechender Geruch und korrosive Eigenschaft lassen sich durch eine Alkalisierung weitestgehend eliminieren. Haushaltschemikalien wie Danklorix mit 1-4 % Natriumhypochlorid als aktivem Wirkstoff wurde ebenfalls sporizide Wirksamkeit bescheinigt [135]. Das in dieser Arbeit untersuchte Panel an chemischen Inaktivierungsmitteln bestand aus Formaldehyd, Danklorix, Wofasteril-Alcapur (ein Kombipräparat aus Peressigsäure und Natriumhydroxid), Peressigsäure sowie Autoklavieren bei 134 °C als physikalische Inaktivierungsmethode. Es wurde zuerst die Inaktivierungseffizienz jeder Methode eruiert, ehe durch Analysen einzelner Endosporen und mit einem Identifizierungsexperiment deren Einfluss auf die Raman-spektroskopischen Messungen ausgetestet wurde.

Zur Wirksamkeitsprüfung wurden die Präparate mit unterschiedlichen Behandlungszeiten (15 Minuten bis 4 Stunden) und Konzentrationen eingesetzt. Dabei wurde so vorgegangen, dass Inaktivierungsexperimente an jeweils zwei Stämmen von *B. thuringiensis* und *B. anthracis* in Ausgangskonzentrationen von 10^7 Sporen/ml durchgeführt wurden. Verlaufskontrollen gaben darüber Aufschluss, ob 2 Tage nach der Inaktivierung ein sichtbares Wachstum zu verzeichnen war. Lediglich bei Behandlungen mit 20%iger Formaldehydlösung, unverdünntem Danklorix, 2%iger Peressigsäure und dem Autoklavieren konnten bei allen Wirk-

zeiten keine gewachsenen Kolonien festgestellt werden (Tabelle 1 in [SS2]). Deshalb wurden für die darauf folgenden Analysen nur noch diese vier Inaktivierungsmethoden herangezogen.

Rasterelekronenmikroskopische Aufnahmen der Sporen zeigten deutliche morphologische Änderungen vor allem bei autoklavierten sowie in geringerem Maße bei peressigsäure-behandelten Sporen (Abbildung 1 in [SS2]). Formaldehyd-inaktivierte Zellen besaßen indes in Form und Oberflächentexturierung die größte Ähnlichkeit mit ihren unbehandelten Pendants. Zusätzlich konnten erhebliche Unterschiede in den Raman-Spektren einzelner autoklavierter Endosporen verglichen mit nicht behandelten Sporen festgestellt werden, da sämtliche CaDPA-korrelierte Banden gänzlich fehlten (Abbildung 3 in [SS2]). Abhängig von der Behandlungszeit konnte dies auch bei peressigsäure-inaktivierten Sporen wahrgenommen werden, wohingegen nach Applikation von Danklorix in allen untersuchten Proben die Endosporen vollständig zerstört vorlagen. Eine Ähnlichkeitsanalyse von 4x40 Endosporenspektren durch eine HCA bestätigte diese Befunde: Alle Spektren autoklavierter und ein Teil peressigsäure-behandelter Sporen formierten einen Hauptcluster, in dem ausschließlich Spektren ohne CaDPA-Signale arrangiert worden sind (Abbildung 6 in [SS2]). Der zweite Hauptcluster wurde durch den übrigen Teil der peressigsäure-inaktivierten Sporen konstituiert und bestand zudem aus einem Subcluster sämtlicher formaldehyd-behandelter und unbehandelter Sporen. Das heißt, selbst der Teil der Spektren von peressigsäure-behandelten Sporen, der die dominanten CaDPA-Signale enthielt, war unähnlicher zu den Spektren unbehandelter Sporen als die mit Formaldehyd behandelten. Aufgrund dessen wurde eine Inaktivierung mit einer 20 %igen Formaldehydlösung als Methode der Wahl auserkoren.

Ein Identifizierungsversuch sollte nun aufklären, inwieweit die Behandlung mit Formaldehyd die Diskriminierungskapazität der Raman-Mikrospektroskopie zwischen vier *Bacillus*-Arten (*B. mycoides*, *B. sphaericus*, *B. subtilis*, *B. thuringiensis*) beeinträchtigen würde. Dazu wurde jeweils ein Trainingsdatensatz unbehandelter und inaktivierter Endosporen erstellt. Anhand dessen wurden vier Klassifizierer (ANN, SVM, LDA und eine Kombination aller drei) berechnet, um einen Testdatensatz jeweils unbehandelter beziehungsweise inaktivierter Sporen auf Artebene zu identifizieren. Zur Erweiterung dieses an sich konventionellen Ansatzes

wurde in einer Konzeptstudie neben den vier *Bacillus*-Arten eine Klasse "unbekannt" eingeführt. Unter Ausnutzung des *one-against-the-rest*-Ansatzes, der im Prinzip die Lösung von Multiklassenproblemen durch binäre Klassifizierer erst ermöglicht, konnten nicht eindeutig zuordenbare Spektren in die "unbekannt"-Klasse überführt werden. Eine Mehrheitsentscheidung kam zum Tragen bei Verwendung mehrerer Klassifizierer. Die Identifizierungsraten bewegten sich bei den Datensätzen unbehandelter Sporen zwischen 81-83 %, bei den inaktivierten zwischen 80-83 % mit ähnlicher Verteilung falsch-positiver Einträge (Tabelle 4 und Tabelle 5 in [SS2]). Die insgesamt moderaten Identifizierungsraten kamen insbesondere dadurch zustande, dass bis zu 10 % der Spektren der Klasse "unbekannt" zugeordnet worden sind. Andererseits ist durch diesen Ansatz die Möglichkeit gegeben, auch Endosporen, deren Art nicht in der jeweiligen Referenzdatenbank registriert ist, in die Klasse "unbekannt" einzuordnen. Keiner der vier Klassifizierer ragte anhand seiner Identifizierungsleistung weder deutlich heraus noch fiel merklich ab und eine verminderte Identifizierungsrate bei den inaktivierten Proben war ebenso wenig beobachtbar.

Letztlich konnte eine Beeinträchtigung durch die Formaldehydbehandlung durch dieses Identifizierungsexperiment nicht festgestellt werden, sodass die Inaktivierung mit Formaldehyd bei den folgenden Analysen Anwendung fand.

1.3.3 Identifizierung von *Bacillus*-Endosporen mittels Raman-Spektroskopie und chemometrischer Methoden

Wie beschrieben gelang es, Einflüsse des häufig als Kultivierungszusatz verwendeten $MnSO_4$ auf die Raman-Spektren von *Bacillus*-Endosporen nachzuweisen. Außerdem wurde eine sichere Inaktivierungsmethode erarbeitet, die das Diskriminierungspotential des angewandten Raman-spektroskopischen Ansatzes nicht kompromittiert. Davon abgeleitete Schlussfolgerungen flossen in die nun hier beschriebenen Arbeiten ein. In diesen sollte ein Machbarkeitsnachweis erbracht werden, dass mithilfe der Raman-Mikrospektroskopie eine Identifizierung einer Vielzahl von *Bacillus*-Arten in Endosporenform im Allgemeinen und von Milzbrandsporen im Speziellen möglich ist. Für Bakterien in vegetativer Zellform

wurden derartige *proof-of-principles* bereits erbracht; für Endosporen stehen diese noch aus [111]. Unter den über 200 Spezies aerober endosporenbildender Bakterien ist die Gattung *Bacillus* die größte und umfasst ein Spektrum von Bakterien mit einer enormen physiologischen und genetischen Breite. Die zurzeit ungefähr 260 anerkannten *Bacillus*-Spezies besitzen einen stark variierenden GC-Gehalt (33-78 %) und eine teils deutlich ausdifferenzierte 16S-rRNA-Phylogenie [39, 136]. Um dieser Breite einigermaßen gerecht zu werden, muss die dem angestrebten Identifizierungsexperiment zugrunde liegende Raman-Spektren-Datenbank entsprechend breit aufgestellt sein. Die Mikroorganismen dafür stammten aus den Stammsammlungen des Friedrich-Loeffler-Institutes und der Deutschen Sammlung von Mikroorganismen und Zellkulturen GmbH (DSMZ), sodass eine Datenbank an Raman-Spektren mit 66 Stämmen von 14 *Bacillus*-Arten einschließlich *B. anthracis* erstellt werden konnte. Augenmerk wurde insbesondere auf die BC-Gruppe gelegt, da sie zum einen *B. anthracis*, zum anderen phylogenetisch sehr eng verwandte Spezies enthält. Eingeschlossen wurden außerdem Taxa, die aufgrund abweichender Physiologie in zusätzliche Gattungen überführt worden sind, nämlich die thermophilen *Geobacillus* spp. sowie *Paenibacillus* spp. Ungefähr 11 000 Spektren einzelner Endosporen konstituierten damit eine Datenbank, die in einem derartigen Umfang bisher nicht publiziert und zu Identifizierungsversuchen angewandt worden ist. Bei der Erstellung der Datenbank wurde neben der Einhaltung stringenter Kultivierungsparameter wie der Temperatur und einer generellen Medienzusammensetzung darauf geachtet, bei der Anzucht von Endosporen stets Mangansulfat als Sporulationsbeschleuniger dem Medium zuzusetzen (10 mg/l). Zudem mussten sämtliche Endosporenproben mit mindestens 10%iger Formaldehyd-Lösung über einen Zeitraum von wenigstens 1 h inaktiviert werden. Die Datenvorbehandlung bestand in der Reihenfolge aus Basislinien-, Spikekorrektur, Wellenzahlkalibration und Vektornormierung. Zuerst wurden die Raman-Spektren mithilfe einer HCA auf ihre spektrale Ähnlichkeit hin untersucht. Aus dem resultierenden Dendrogramm S-1 in [SS3] lässt sich erkennen, dass eine Zweiteilung der Daten erfolgte: In Cluster A sind vornehmlich die Mittelwertspektren von Endosporen der BC-Gruppe zu finden, in Cluster B mit lediglich zwei Ausnahmen nur Signaturen von Nicht-BC-Endosporen. Entsprechend wurde eine Klassifizierung der Daten in einem Zweistufenkonzept konstru-

iert. Zuerst ordnet ein *Top-Level*-Klassifizierer die Spektren entweder der BC- oder Nicht-BC-Gruppe zu, ehe zwei weitere Klassifizierer eine Zuordnung der Spektren auf Artebene vornehmen. Das Fließdiagramm 1 in [SS3] veranschaulicht diesen Prozess. An jedem Knotenpunkt agiert ein unabhängiger Klassifizierer, wobei eine SVM auf der obersten Ebene arbeitet, ebenso wie bei der Diskriminierung der BC-Spezies, während die Nicht-BC-Arten nach einer vorgeschalteten Dimensionsreduzierung durch eine PCA mittels einer LDA gelabelt werden. Eine Evaluierung der einzelnen Klassifizierer wurde via Kreuzvalidierung durchgeführt, wobei Trennungsraten von 93,2 % bis 97,1 % errechnet worden sind.

Die Praxisrelevanz der so erstellten drei Modelle wurde überprüft, indem 27 "unbekannte" Proben zu identifizieren versucht wurden. Hierbei handelte es sich um Endosporen, die gänzlich unabhängig von jenen der Modelle gezüchtet und gemessen worden sind. Alle gehörten einer Datenbankspezies an, allerdings stammten sie in sieben Fällen von Stämmen ab, die zuvor nicht zur Modellerstellung berücksichtigt worden sind. Damit sollte den Ansprüchen einer *Leave-one-strain-out*-Validierung Genüge getan werden. Bei *Bacillus*-Arten, die mit nicht mehr als zwei Stämme in der Datenbank registriert waren, wurde davon abgesehen. Wurden mehr als 85 % der Spektren einer Probe einer Klasse zugewiesen, so galt die Zuordnung als signifikant. Die Resultate dieser Identifizierung sind in Tabelle 2 in [SS3] angezeigt: Der *Top-level*-Klassifizierer bestimmte für alle 27 Testproben deren Zugehörigkeit zur BC- oder Nicht-BC-Gruppe korrekt, was einer mittleren Identifizierungsrate von 99,4 % entsprach. Von den 471 Raman-Spektren von *B. anthracis* wurde lediglich ein Spektrum der Nicht-BC-Gruppe zugeordnet. Die SVM zur Bestimmung der BC-Art identifizierte für alle zuvor als BC-Endosporen erkannte 15 Proben die korrekte Spezies mit einer minimalen Sensitivität von 88,4 % im Falle einer *B. thuringiensis*-Probe und einer durchschnittlichen Rate von 97,1 %. Obendrein wurden alle sechs *B. anthracis*-Proben als solche erkannt, selbst wenn im Falle des *B. anthracis* Vollum der Stamm im Modell nicht explizit integriert war. Nur 10 von 471 *B. anthracis*-Spektren wurden falsch identifiziert, sechs davon als *B. thuringiensis*. Erwähnenswert ist zudem, dass die Identifizierung von *B. anthracis* auch bei Stämmen Erfolg hatte, die nicht über eine volle Virulenz verfügten, wie *B. anthracis* 5261 (kein pXO1-Plasmid), *B. anthracis* Sterne (kein pXO2-Plasmid) oder *B. anthracis* A58 (weder pXO1 und pXO2 tragend).

Die LDA zur Identifizierung der mutmaßlichen 12 Nicht-BC-Proben vermochte mit einer mittleren Sensitivität von 98,6 % ebenso alle Proben korrekt ihrer Spezies zuzuordnen bei einer minimalen Rate von 93,1 % für eine *B. sphaericus*-Probe und 100 % in fünf weiteren Fällen. Selbst die *Bacillus*-verwandten Geobacilli und Paenibacilli wurden korrekt identifiziert. Gleiches gilt für die drei Proben der Spezies *B. pumilus*, *B. sphaericus* und *B. subtilis* jener Stämme, die nicht Teil der Datenbank waren.

Insgesamt erreichten die Identifizierungsraten die Werte der Kreuzvalidierung und eine Tendenz zur Überanpassung des Models war nicht feststellbar. Deshalb wurden die Endosporen aller 27 "unbekannten" Proben richtig identifiziert – unabhängig davon, ob es sich um Pathogene (etwa *B. anthracis* oder *B. cereus*), ubiquitäre Umweltkeime (*B. pumilus* oder *B. subtilis*) oder industriell genutzte Sporen (*B. licheniformis*) handelte.

1.3.4 Detektion von *B. anthracis* in Pulverproben

Ein ähnlicher datenbankbasierter Identifizierungsansatz mithilfe der Raman-Spektroskopie wurde auch verfolgt, um Endosporen in Realproben nachzuweisen. Es wurde sich primär auf Haushaltspulver konzentriert, da derartige Proben am häufigsten im nicht-klinischen Umfeld auf *B. anthracis* getestet werden müssen [137]. Ferner verursachen diese Probentypen aufgrund inhibitorischer Effekte bei PCR-Analysen häufig Probleme [61, 62, 138]. Das untersuchte Panel umfasste Backpulver, Baugips, Milchpulver, Natron, Schmerztabletten, Vogelsand und Waschpulver, welche jeweils mit Endosporen der Arten *B. anthracis*, *B. megaterium*, *B. mycoides*, *B. subtilis* und *B. thuringiensis* versetzt worden sind. Nach einer Verweildauer von mindestens 24 h wurden die Proben durch Behandlung mit Formaldehyd inaktiviert. Anschließend erfolgte die Extraktion der Sporen aus den Pulvern mithilfe einer Dichtegradientenzentrifugation und einigen nachfolgenden Waschschritten. Eine wässrige Suspension mit Polyvinylpyrrolidon beschichteter Siliciumdioxidpartikel (Percoll) stellte die Trennlösung dar und wurde in Anlehnung an die Literatur angewandt [139, 140]. Diese Trennlösung wurde gewählt, da sie pH-neutral ist, die Bakterienzellen während der Zentrifugation nur einem

geringen osmotischen Stress aussetzt, die Zellen nicht penetriert und ohne großen Aufwand wieder entfernbar ist. Durch die Polymerbeschichtung verlieren die Silikapartikel zudem ihre Zelltoxizität. Die Extraktionseffizienz des Verfahrens wurde anschließend durch eine Lebendkeimzahlbestimmung ermittelt. Hierfür wurden definierte Mengen an nicht inaktivierten *B. thuringiensis*-Sporen in jeweils 100 mg Backpulver oder Vogelsand eingebracht, wie beschrieben isoliert und das Extrakt schließlich durch serielles Ausplattieren quantifiziert. Tabelle S1 in [SS4] gibt Auskunft über die ermittelten Ausbeuten: Betrug die Anfangskonzentration circa 10^7 koloniebildende Einheiten (KbE oder *colony forming units*, CFU) pro 100 mg Matrix, so gingen überschlägig zwei Größenordnungen durch die Extraktion verloren, wogegen für die Startkonzentrationen von cirka 10^5, 10^3 und 10^2 KbE/100 mg noch ungefähr 90 % der Keime isoliert werden konnten. Dies gilt sowohl für die Backpulver- als auch Vogelsandproben und lässt ähnliche Ausbeuten darüber hinaus für die anderen untersuchten Matrices vermuten. Geht man von 1 g Proben aus, so ist bei den ermittelten Ausbeuten sichergestellt, stets ausreichend Endosporen, also annähernd 100 Einzelzellen, für eine aussagekräftige Raman-spektroskopische Analyse isolieren zu können. Dies gilt erst recht, wenn man die mittlere letale Dosis von *B. anthracis* gegenüber Menschen von 2 500 bis 55 000 KbE in Betracht zieht [17, 18].

Letztlich wurde von 5 723 einzelnen *Bacillus*-Endosporen Raman-Signaturen aufgenommen, deren Verteilung auf die fünf untersuchten Spezies der Tabelle S2a in [SS4] zu entnehmen ist. Jede *Bacillus*-Art wurde mindestens einmal aus jedem der sieben Pulver sowie direkt aus dem Nährmedium – nach vorheriger Inaktivierung – isoliert. Lediglich die *B. anthracis*-Endosporen entstammten nur aus Backpulver sowie Vogelsand. Ungefähr 1 µl der gewonnenen Sporensuspension wurde auf einen Quarzobjektträger pipettiert und kurz eintrocknen gelassen. Die Messungen erfolgten erneut partikelweise unter Dunkelfeldbeleuchtung (siehe Abbildung 1 in [SS4]). Wurden ungewollt Raman-Spektren von Matrixbestandteilen aufgenommen, konnten diese leicht als solche identifiziert und der Datenbankerstellung vorbehalten werden. Abbildung 2 in [SS4] verdeutlicht die großen Unterschiede von Spektren einiger häufig gemessener Matrixbestandteile im Vergleich mit Endosporen. Mithilfe des so konstruierten Modelldatensatzes aus Raman-Spektren von Endosporen gelang es durch eine LDA, Unterscheidungs-

funktionen zu berechnen, die eine Zuordnung der Raman-Spektren zu einer der fünf *Bacillus*-Arten mit einer Genauigkeit von 94,8 % bewerkstelligten, das heißt, 5 427 von den 5 723 gemessenen Endosporen wurden korrekt klassifiziert (Tabelle S3 in [SS4]). Die meisten Falsch-Positiven waren zwischen *B. mycoides* und *B. thuringiensis* zu finden – zwei Spezies der BC-Gruppe. Speziell *B. anthracis* wurde mit einer Trefferquote von 98,6 % korrekt erkannt (983 von 997). Erneut ist die Mehrheit der Falsch-Negativen sowohl in *B. mycoides* als auch *B. thuringiensis* zu verorten.

Um das Generalisierungspotential des aufgestellten LDA-Modells zu evaluieren, wurden weitere Pulverproben mit neu angezogenen Endosporen der fünf *Bacillus*-Arten gespikt, verarbeitet und analysiert (Tabelle S2b in [SS4]). Die 1 650 Raman-Spektren dieses unabhängigen Datensatzes wurden mit dem LDA-Modell zu 96,8 % korrekt ihren jeweiligen Klasse zugeordnet. Wie aus Tabelle 1 zu entnehmen ist, sind beispielsweise 241 von 242 *B. anthracis*-Spektren korrekt identifiziert worden; die Sensitivitäten schwankten zwischen 91,2 % für *B. thuringiensis* und 100 % für *B. subtilis*.

Zuletzt wurde die Robustheit des Identifizierungsansatzes ausgetestet, indem mit *B. anthracis* gespikte Kochsalzproben hergestellt und nach Vorbehandlung vermessen wurden. Raman-Spektren von Sporen aus dieser Matrix wurden im Modell bisher nicht implementiert, dennoch konnten 183 von 191 Endosporen als *B. anthracis* identifiziert werden (95,8 %).

1.4 Resümee

Im folgenden Abschnitt soll noch einmal der Inhalt der vorhergehenden Kapitel kurz zusammengefasst werden.

Es wurde eine Methodik erforscht, mithilfe derer sich binnen weniger Stunden Umweltproben wie Haushaltspulver oder Sand auf eine womögliche Kontamination mit pathogenen *Bacillus*-Endosporen wie *B. anthracis* und *B. cereus* überprüfen lassen. Insbesondere die zeitnahe Detektion des als Biowaffe geeigneten Milzbranderregers ist von besonderer gesellschaftlicher und wirtschaftlicher Bedeutung.

Basis des Ansatzes ist die Raman-Mikrospektroskopie, die in Kombination mit chemometrischen Verfahren zum ersten Mal zur Detektion und Identifikation verschiedener Arten bakterieller Endosporen in komplexen Matrices, wie sie üblicherweise in Umweltproben vorliegen, Verwendung fand. Eine zeitraubende Vorkultivierung ist dabei nicht erforderlich. Die geringen, für den Gesamtansatz notwendigen Aufwendungen in Material, Technik und Zeit erlauben eine Analyse vor Ort durch *first responder*. Dies ist ein großer Vorteil der erforschten Methode gegenüber der Vielzahl bereits etablierter Techniken zur Diagnose von Milzbranderregern. So können bereits sehr früh erforderliche Maßnahmen zum sachgerechten Umgang und der diagnostischen Aufarbeitung von Verdachtsproben abgeleitet werden. Weiterhin ermöglichen die Ergebnisse dieses Schnelltests, für eine nachfolgende konfirmative Analyse in Sicherheitslaboren, beispielsweise durch eine PCR, wertvolle Rückschlüsse zu ziehen.

Die erforschte Methode greift unmittelbar nach der Probengewinnung mit der Inaktivierung durch eine Formaldehydbehandlung, die sich als überlegen gegenüber einer Vielzahl anderer Inaktivierungsansätze erwiesen hat [SS2]. Geprüft wurde insbesondere auf ein ausreichend sporizides Potential und Kompatibilität zur Raman-spektroskopischen Analyse. Dieser Arbeitsschritt war erforderlich, da eine Beurteilung von Inaktivierungsmethoden unter solchen Gesichtspunkten zusammengenommen in bisherigen wissenschaftlichen Publikationen keine Berücksichtigung fand. Des Weiteren wurde ein Isolierungsverfahren erarbeitet, welches sich für sieben untersuchte Haushaltspulver als geeignet erwies, um Endosporen verschiedener Spezies möglichst effektiv und schonend aus den Matrices zu

extrahieren [SS4]. Auf gängige Ansätze konnte hierfür nicht zurückgegriffen werden, da sie zur Gewinnung diagnostisch relevanter Marker von Mikroorganismen mehrheitlich auf dem Aufschluss intrazellulärer Bestandteile (beispielsweise CaDPA für Lumineszenzmessungen, Nukleinsäuren für PCR) basieren. Als Folge werden die Bakterienzellen zerstört, was sie einer Raman-mikrospektroskopischen Analyse entzieht. Mittels formaldehyd-inaktivierten Endosporen wurden letztlich umfangreiche Datenbanken an Raman-Spektren aufgebaut, um durch chemometrische Methoden passgenaue Identifizierungsstrategien zu entwickeln. Dabei wurde auch in Betracht gezogen, dass ein Supplement an divalentem Mangan während der Kultivierung von Endosporen einen nicht zu vernachlässigenden Effekt auf deren Raman-Spektren ausübt [SS1]. Bisher existierten darüber keinerlei wissenschaftliche Publikationen. Des Weiteren wurden Vorbehandlungsstrategien gemessener Raman-Spektren von Endosporen erarbeitet, ebenso wie eine Möglichkeit, auch den Datenbanken unbekannte Stämme als Klasse "unbekannt" zu detektieren [SS2, SS3, SS4]. Eine Spektrenbibliothek von circa 11 000 Raman-Spektren von 66 *Bacillus*-und *Bacillus*-verwandten Stämmen, inklusive 17 *B. anthracis*-Stämme, wurde aufgebaut und zum Erstellen eines zweistufigen Klassifizierungssystems verwendet [SS3]. Dieses konnte 27 Endosporenproben korrekt auf Art-Ebene identifizieren – selbst dann, wenn die betreffenden Stämme nicht Teil der Datenbank waren. An einer letztlich erfolgreichen Analyse von Realproben, in denen teils pathogene Endosporen mit verschiedensten Haushaltspulvern vermischt wurden, konnte schließlich die Robustheit des erforschten Konzeptes bewiesen werden [SS4].

Literaturverzeichnis

1. R. Koch, "*Die Ätiologie der Milzbrand-Krankheit, begründet auf die Entwicklungsgeschichte des Bacillus Anthracis*", Cohns Beiträge zur Biologie der Pflanzen **1877**, *2*, 5-26.
2. M. Sterne, "*The use of anthrax vaccines prepared from avirulent (uncapsulated) variants of Bacillus anthracis*", Onderstepoort Journal of Veterinary Science and Animal Industry **1939**, *13*, 307-312.
3. World Organisation for Animal Health (OIE), "*World Animal Health Information Database (WAHID) - Version: 1.2*" (http://www.oie.int/wahis_2/public/wahid.php/Wahidhome/Home), Zugriff am: **28.09.2012**.
4. D. C. Dragon, D. E. Bader, J. Mitchell und N. Woollen, "*Natural Dissemination of Bacillus anthracis Spores in Northern Canada*", Applied and Environmental Microbiology **2005**, *71*, 1610-1615.
5. P. C. B. Turnbull, ed., "*Anthrax in humans and animals*", World Health Organization, Geneva, **2008**.
6. G. W. Christopher, T. J. Cieslak, J. A. Pavlin und E. M. Eitzen, "*Biological warfare - A historical perspective*", Jama-Journal of the American Medical Association **1997**, *278*, 412-417.
7. N. Khardori und T. Kanchanapoom, "*Overview of Biological Terrorism: Potential Agents and Preparedness*", Clinical Microbiology Newsletter **2005**, *27*, 1-8.
8. D. L. Noah, K. D. Huebner, R. G. Darling und J. F. Waeckerle, "*The history and threat of biological warfare and terrorism*", Emergency Medicine Clinics of North America **2002**, *20*, 255-271.
9. D. K. Bhalla und D. B. Warheit, "*Biological agents with potential for misuse: a historical perspective and defensive measures*", Toxicology and Applied Pharmacology **2004**, *199*, 71-84.
10. T. V. Inglesby, "*Anthrax as a biological weapon, 2002: Updated recommendations for management (vol 287, pg 2236, 2002)*", Jama-Journal of the American Medical Association **2002**, *288*, 1849-1849.
11. M. G. Booth, J. Hood, T. J. G. Brooks und A. Hart, "*Anthrax infection in drug users*", Lancet **2010**, *375*, 1345-1346.
12. N. E. Palmateer, C. N. Ramsay, L. Browning, D. J. Goldberg und S. J. Hutchinson, "*Anthrax Infection Among Heroin Users in Scotland During 2009–2010: A Case-Control Study by Linkage to a National Drug Treatment Database*", Clinical Infectious Diseases **2012**, *55*, 706-710.

13. T. Holzmann, D. Frangoulidis, M. Simon, P. Noll, S. Schmoldt, M. Hanczaruk, G. Grass, M. Pregler, A. Sing, S. Hörmansdorfer, H. Bernard, R. Grunow, R. Zimmermann, W. Schneider-Brachert, A. Gessner und U. Reischl, "*Fatal anthrax infection in a heroin user from southern Germany, June 2012*", Eurosurveillance **2012**, *17*, 2-6.
14. Bundesamt für Bevölkerungsschutz und Katastrophenhilfe, "*Vierter Gefahrenbericht der Schutzkommission beim Bundesminister des Innern*", *Schriften der Schutzkommission*, Bundesamt für Bevölkerungsschutz und Katastrophenhilfe, Bonn, **2011**.
15. R. Burger, "*Angemessene Vorbereitung gegen bioterroristische Anschläge*", Bundesgesundheitsblatt - Gesundheitsforschung - Gesundheitsschutz **2003**, *46*, 933-934.
16. R. M. Atlas, "*Bioterrorism: From Threat to Reality*", Annual Review of Microbiology **2002**, *56*, 167-185.
17. T. J. Cieslak und E. M. Eitzen, "*Clinical and Epidemiologic Principles of Anthrax*", Emerging Infectious Diseases **1999**, *5*, 552-555.
18. T. V. Inglesby, D. A. Henderson, J. G. Bartlett, M. S. Ascher, E. Eitzen, A. M. Friedlander, J. Hauer, J. McDade, M. T. Osterholm, T. O'Toole, G. Parker, T. M. Perl, P. K. Russell und K. Tonat, "*Anthrax as a Biological Weapon: Medical and Public Health Management. Working Group on Civilian Biodefense*", Jama-Journal of the American Medical Association **1999**, *281*, 1735-1745.
19. W. F. Klietmann und K. L. Ruoff, "*Bioterrorism: Implications for the Clinical Microbiologist*", Clinical Microbiology Reviews **2001**, *14*, 364-381.
20. Bundesamt für Bevölkerungsschutz und Katastrophenhilfe, "*Synopse zu ausgewählten Gefahrenberichten aus Deutschland, Europa und international*", *Schriften der Schutzkommission*, Bundesamt für Bevölkerungsschutz und Katastrophenhilfe, Bonn, **2012**.
21. D. Fritze, "*Taxonomy of the Genus Bacillus and Related Genera: The Aerobic Endospore-Forming Bacteria*", Phytopathology **2004**, *94*, 1245-1248.
22. G. M. Garrity, D. H. Bergey und W. B. Whitman, "*Bergey's manual of systematic bacteriology*", Springer, New York, NY [u.a.], **2001**.
23. J. Ravel und C. M. Fraser, "*Genomics at the genus scale*", Trends in Microbiology **2005**, *13*, 95-97.
24. D. G. Davies, "*The influence of temperature and humidity on spore formation and germination in Bacillus anthracis*", The Journal of hygiene **1960**, *58*, 177-186.
25. M. Hugh-Jones und J. Blackburn, "*The ecology of Bacillus anthracis*", Molecular Aspects of Medicine **2009**, *30*, 356-367.

26. P. Setlow, "*Spore germination*", Current Opinion in Microbiology **2003**, *6*, 550-556.
27. S. Ghosh, P. F. Zhang, Y. Q. Li und P. Setlow, "*Superdormant Spores of Bacillus Species Have Elevated Wet-Heat Resistance and Temperature Requirements for Heat Activation*", Journal of Bacteriology **2009**, *191*, 5584-5591.
28. W. L. Nicholson, N. Munakata, G. Horneck, H. J. Melosh und P. Setlow, "*Resistance of Bacillus Endospores to Extreme Terrestrial and Extraterrestrial Environments*", Microbiology and Molecular Biology Reviews **2000**, *64*, 548-572.
29. P. Setlow, "*Spores of Bacillus subtilis: their resistance to and killing by radiation, heat and chemicals*", Journal of Applied Microbiology **2006**, *101*, 514-525.
30. W. L. Nicholson, A. C. Schuerger und P. Setlow, "*The solar UV environment and bacterial spore UV resistance: considerations for Earth-to-Mars transport by natural processes and human spaceflight*", Mutation Research-Fundamental and Molecular Mechanisms of Mutagenesis **2005**, *571*, 249-264.
31. P. Keim, M. N. Van Ert, T. Pearson, A. J. Vogler, L. Y. Huynh und D. M. Wagner, "*Anthrax molecular epidemiology and forensics: using the appropriate marker for different evolutionary scales*", Infection, genetics and evolution: journal of molecular epidemiology and evolutionary genetics in infectious diseases **2004**, *4*, 205-213.
32. F. G. Priest, M. Barker, L. W. J. Baillie, E. C. Holmes und M. C. J. Maiden, "*Population Structure and Evolution of the Bacillus cereus Group*", Journal of Bacteriology **2004**, *186*, 7959-7970.
33. E. Helgason, O. A. Økstad, D. A. Caugant, H. A. Johansen, A. Fouet, M. Mock, I. Hegna und A.-B. Kolstø, "*Bacillus anthracis, Bacillus cereus, and Bacillus thuringiensis-One Species on the Basis of Genetic Evidence*", Applied and Environmental Microbiology **2000**, *66*, 2627-2630.
34. E. J. Bottone, "*Bacillus cereus, a Volatile Human Pathogen*", Clinical Microbiology Reviews **2010**, *23*, 382-398.
35. L. K. Nakamura, "*Bacillus pseudomycoides sp. nov*", International Journal of Systematic Bacteriology **1998**, *48*, 1031-1035.
36. L. K. Nakamura und M. A. Jackson, "*Clarification of the Taxomomy of Bacillus mycoides*", International Journal of Systematic Bacteriology **1995**, *45*, 46-49.
37. E. Schnepf, N. Crickmore, J. Van Rie, D. Lereclus, J. Baum, J. Feitelson, D. R. Zeigler und D. H. Dean, "*Bacillus thuringiensis and Its Pesticidal Crystal Proteins*", Microbiology and Molecular Biology Reviews **1998**, *62*, 775-806.

38. S. Lechner, R. Mayr, K. P. Francis, B. M. Pruss, T. Kaplan, E. Wiessner-Gunkel, G. Stewartz und S. Scherer, "*Bacillus weihenstephanensis sp. nov. is a new psychrotolerant species of the Bacillus cereus group*", International Journal of Systematic Bacteriology **1998**, *48*, 1373-1382.
39. A. B. Kolstø, N. J. Tourasse und O. A. Økstad, "*What Sets Bacillus anthracis Apart from Other Bacillus Species?*", Annual Reviews, Palo Alto, **2009**.
40. C. Ash und M. D. Collins, "*Comparative analysis of 23S ribosomal RNA gene sequences of Bacillus anthracis and emetic Bacillus cereus determined by PCR-direct sequencing*", FEMS Microbiology Letters **1992**, *94*, 75-80.
41. C. Ash, J. A. E. Farrow, M. Dorsch, E. Stackebrandt und M. D. Collins, "*Comparative Analysis of Bacillus anthracis, Bacillus cereus, and Related Species on the Basis of Reverse Transcriptase Sequencing of 16S rRNA*", International Journal of Systematic Bacteriology **1991**, *41*, 343-346.
42. P. Mikesell, B. E. Ivins, J. D. Ristroph und T. M. Dreier, "*Evidence for Plasmid-Mediated Toxin Production in Bacillus Anthracis*", Infection and Immunity **1983**, *39*, 371-376.
43. I. Uchida, T. Sekizaki, K. Hashimoto und N. Terakado, "*Association of the encapsulation of Bacillus anthracis with a 60 megadalton plasmid*", Journal of General Microbiology **1985**, *131*, 363-367.
44. M. Mock und A. Fouet, "*Anthrax*", Annual Review of Microbiology **2001**, *55*, 647-671.
45. A. R. Hoffmaster, J. Ravel, D. A. Rasko, G. D. Chapman, M. D. Chute, C. K. Marston, B. K. De, C. T. Sacchi, C. Fitzgerald, L. W. Mayer, M. C. J. Maiden, F. G. Priest, M. Barker, L. Jiang, R. Z. Cer, J. Rilstone, S. N. Peterson, R. S. Weyant, D. R. Galloway, T. D. Read, T. Popovic und C. M. Fraser, "*Identification of anthrax toxin genes in a Bacillus cereus associated with an illness resembling inhalation anthrax*", Proceedings of the National Academy of Sciences of the United States of America **2004**, *101*, 8449-8454.
46. C. K. Marston, J. E. Gee, T. Popovic und A. R. Hoffmaster, "*Molecular approaches to identify and differentiate Bacillus anthracis from phenotypically similar Bacillus species isolates*", Bmc Microbiology **2006**, *6*.
47. L. M. Irenge und J. L. Gala, "*Rapid detection methods for Bacillus anthracis in environmental samples: a review*", Applied Microbiology and Biotechnology **2012**, *93*, 1411-1422.
48. P. C. B. Turnbull, "*Definitive identification of Bacillus anthracis - a review*", Journal of Applied Microbiology **1999**, *87*, 237-240.

49. H. Peng, V. Ford, E. W. Frampton, L. Restaino, L. A. Shelef und H. Spitz, "*Isolation and enumeration of Bacillus cereus from foods on a novel chromogenic plating medium*", Food Microbiology **2001**, *18*, 231-238.
50. R. C. Spencer, "*Bacillus anthracis*", Journal of Clinical Pathology **2003**, *56*, 182-187.
51. N. Bannert, H. R. Gelderblom, M. Laue und M. Oezel, "*Elektronenmikroskopische Erregerdiagnostik bei vermuteten bioterroristischen Anschlägen*", Biologische Sicherheit, **2011**, 369-377.
52. A. Ascoli, "*Die Präzipitation bei Milzbrand*", Zentralblatt für Bakteriologie, Parasitenkunde, Infektionskrankheiten und Hygiene **1911**, *58*, 63-70.
53. S. R. Klee, H. Nattermann, S. Becker, M. Urban-Schriefer, T. Franz, D. Jacob und B. Appel, "*Evaluation of different methods to discriminate Bacillus anthracis from other bacteria of the Bacillus cereus group*", Journal of Applied Microbiology **2006**, *100*, 673-681.
54. A. B. Herzog, S. D. McLennan, A. K. Pandey, C. P. Gerba, C. N. Haas, J. B. Rose und S. A. Hashsham, "*Implications of Limits of Detection of Various Methods for Bacillus anthracis in Computing Risks to Human Health*", Applied and Environmental Microbiology **2009**, *75*, 6331-6339.
55. D. A. Rasko, M. J. Rosovitz, O. A. Økstad, D. E. Fouts, L. X. Jiang, R. Z. Cer, A. B. Kolstø, S. R. Gill und J. Ravel, "*Complete Sequence Analysis of Novel Plasmids from Emetic and Periodontal Bacillus cereus Isolates Reveals a Common Evolutionary History Among the B-cereus-Group Plasmids, Including Bacillus anthracis pXO1*", Journal of Bacteriology **2007**, *189*, 52-64.
56. S. R. Klee, M. Oezel, B. Appel, C. Boesch, H. Ellerbrok, D. Jacob, G. Holland, F. H. Leendertz, G. Pauli, R. Grunow und H. Nattermann, "*Characterization of Bacillus anthracis-like Bacteria Isolated from Wild Great Apes from Côte d'Ivoire and Cameroon*", Journal of Bacteriology **2006**, *188*, 5333-5344.
57. S. R. Klee, E. B. Brzuszkiewicz, H. Nattermann, H. Brüggemann, S. Dupke, A. Wollherr, T. Franz, G. Pauli, B. Appel, W. Liebl, E. Couacy-Hymann, C. Boesch, F. D. Meyer, F. H. Leendertz, H. Ellerbrok, G. Gottschalk, R. Grunow und H. Liesegang, "*The Genome of a Bacillus Isolate Causing Anthrax in Chimpanzees Combines Chromosomal Properties of B. cereus with B. anthracis Virulence Plasmids*", PLoS One **2010**, *5*, e10986.
58. X. M. Hu, G. Van der Auwera, S. Timmery, L. Zhu und J. Mahillon, "*Distribution, Diversity, and Potential Mobility of Extrachromosomal Elements Related to the Bacillus anthracis pXO1 and pXO2 Virulence Plasmids*", Applied and Environmental Microbiology **2009**, *75*, 3016-3028.

59. Y. A. Qi, G. Patra, X. D. Liang, L. E. Williams, S. Rose, R. J. Redkar und V. G. DelVecchio, "*Utilization of the rpoB gene as a Specific Chromosomal Marker for Real-Time PCR Detection of Bacillus anthracis*", Applied and Environmental Microbiology **2001**, *67*, 3720-3727.
60. A. A. Zasada, R. Gierczyński, N. Raddadi, D. Daffonchio und M. Jagielski, "*Some Bacillus thuringiensis Strains Share rpoB Nucleotide Polymorphisms Also Present in Bacillus anthracis*", Journal of Clinical Microbiology **2006**, *44*, 1606-1607.
61. I. G. Wilson, "*Inhibition and Facilitation of Nucleic Acid Amplification*", Applied and Environmental Microbiology **1997**, *63*, 3741-3751.
62. K. L. Opel, D. Chung und B. R. McCord, "*A Study of PCR Inhibition Mechanisms Using Real Time PCR*", Journal of Forensic Sciences **2010**, *55*, 25-33.
63. P. Rådström, R. Knutsson, P. Wolffs, M. Lövenklev und C. Löfström, "*Pre-PCR Processing - Strategies to Generate PCR-Compatible Samples*", Molecular Biotechnology **2004**, *26*, 133-146.
64. T. Notomi, H. Okayama, H. Masubuchi, T. Yonekawa, K. Watanabe, N. Amino und T. Hase, "*Loop-mediated isothermal amplification of DNA*", Nucleic Acids Research **2000**, *28*, e63.
65. Y. Mori, K. Nagamine, N. Tomita und T. Notomi, "*Detection of Loop-Mediated Isothermal Amplification Reaction by Turbidity Derived from Magnesium Pyrophosphate Formation*", Biochemical and Biophysical Research Communications **2001**, *289*, 150-154.
66. B. Hatano, T. Maki, T. Obara, H. Fukumoto, K. Hagisawa, Y. Matsushita, A. Okutani, B. Bazartseren, S. Inoue, T. Sata und H. Katano, "*LAMP Using a Disposable Pocket Warmer for Anthrax Detection, a Highly Mobile and Reliable Method for Anti-Bioterrorism*", Japanese Journal of Infectious Diseases **2010**, *63*, 36-40.
67. L. Dugan, J. Bearinger, A. Hinckley, C. Strout und B. Souza, "*Detection of Bacillus anthracis from spores and cells by loop-mediated isothermal amplification without sample preparation*", Journal of Microbiological Methods **2012**, *90*, 280-284.
68. E. Helgason, N. J. Tourasse, R. Meisal, D. A. Caugant und A. B. Kolstø, "*Multilocus Sequence Typing Scheme for Bacteria of the Bacillus cereus Group*", Applied and Environmental Microbiology **2004**, *70*, 191-201.
69. D. A. Rasko, P. L. Worsham, T. G. Abshire, S. T. Stanley, J. D. Bannan, M. R. Wilson, R. J. Langham, R. S. Decker, L. X. Jiang, T. D. Read, A. M. Phillippy, S. L. Salzberg, M. Pop, M. N. Van Ert, L. J. Kenefic, P. S. Keim, C. M. Fraser-Liggett und J. Ravel, "*Bacillus anthracis comparative genome analysis in support of the Amerithrax investigation*", Proceedings of the National Academy of Sciences of the United States of America **2011**, *108*, 5027-5032.

70. P. Keim, A. Kalif, J. Schupp, K. Hill, S. E. Travis, K. Richmond, D. M. Adair, M. HughJones, C. R. Kuske und P. Jackson, "*Molecular Evolution and Diversity in Bacillus anthracis as Detected by Amplified Fragment Length Polymorphism Markers*", Journal of Bacteriology **1997**, *179*, 818-824.
71. D. King, V. Luna, A. Cannons, J. Cattani und P. Amuso, "*Performance Assessment of Three Commercial Assays for Direct Detection of Bacillus anthracis Spores*", Journal of Clinical Microbiology **2003**, *41*, 3454-3455.
72. P. M. Pellegrino, N. F. Fell und J. B. Gillespie, "*Enhanced spore detection using dipicolinate extraction techniques*", Analytica Chimica Acta **2002**, *455*, 167-177.
73. J. Fichtel, J. Köster, B. Scholz-Böttcher, H. Sass und J. Rullkötter, "*A highly sensitive HPLC method for determination of nanomolar concentrations of dipicolinic acid, a characteristic constituent of bacterial endospores*", Journal of Microbiological Methods **2007**, *70*, 319-327.
74. A. N. Nackos, T. V. Truong, T. C. Pulsipher, J. A. Kimball, H. D. Tolley, R. A. Robison, C. H. Bartholomew und M. L. Lee, "*One-step conversion of dipicolinic acid to its dimethyl ester using monomethyl sulfate salts for GC-MS detection of bacterial endospores*", Analytical Methods **2011**, *3*, 245-258.
75. K. L. Ai, B. H. Zhang und L. H. Lu, "*Europium-Based Fluorescence Nanoparticle Sensor for Rapid and Ultrasensitive Detection of an Anthrax Biomarker*", Angewandte Chemie, International Edition **2009**, *48*, 304-308.
76. L. W. J. Baillie, M. N. Jones, P. C. B. Turnbull und R. J. Manchee, "*Evaluation of the Biolog system for the identification of Bacillus anthracis*", Letters in Applied Microbiology **1995**, *20*, 209-211.
77. Y. J. Song, R. F. Yang, Z. B. Guo, M. L. Zhang, X. H. Wang und F. Zhou, "*Distinctness of spore and vegetative cellular fatty acid profiles of some aerobic endospore-forming bacilli*", Journal of Microbiological Methods **2000**, *39*, 225-241.
78. D. Li, T. V. Truong, T. M. Bills, B. C. Holt, D. N. VanDerwerken, J. R. Williams, A. Acharya, R. A. Robison, H. D. Tolley und M. L. Lee, "*GC/MS Method for Positive Detection of Bacillus anthracis Endospores*", Analytical Chemistry **2012**, *84*, 1637-1644.
79. P. Lasch, W. Beyer, H. Nattermann, M. Stämmler, E. Siegbrecht, R. Grunow und D. Naumann, "*Identification of Bacillus anthracis by Using Matrix-Assisted Laser Desorption Ionization-Time of Flight Mass Spectrometry and Artificial Neural Networks*", Applied and Environmental Microbiology **2009**, *75*, 7229-7242.

80. J. Chenau, F. Fenaille, E. Ezan, N. Morel, P. Lamourette, P. L. Goossens und F. Becher, "*Sensitive Detection of Bacillus anthracis Spores by Immunocapture and Liquid Chromatography-Tandem Mass Spectrometry*", Analytical Chemistry **2011**, *83*, 8675-8682.
81. S. Sauer und M. Kliem, "*Mass spectrometry tools for the classification and identification of bacteria*", Nature Reviews Microbiology **2010**, *8*, 74-82.
82. P. A. Demirev und C. Fenselau, "*Mass spectrometry in biodefense*", Journal of Mass Spectrometry **2008**, *43*, 1441-1457.
83. C. J. Ehrhardt, V. Chu, T. Brown, T. L. Simmons, B. K. Swan, J. Bannan und J. M. Robertson, "*Use of Fatty Acid Methyl Ester Profiles for Discrimination of Bacillus cereus T-Strain Spores Grown on Different Media*", Applied and Environmental Microbiology **2010**, *76*, 1902-1912.
84. S. C. Wunschel, K. H. Jarman, C. E. Petersen, N. B. Valentine, K. L. Wahl, D. Schauki, J. Jackman, C. P. Nelson und E. White, "*Bacterial Analysis by MALDI-TOF Mass Spectrometry: An Inter-Lab Oratory Comparison*", Journal of the American Society for Mass Spectrometry **2005**, *16*, 456-462.
85. P. Chen, Y. Lu und P. B. Harrington, "*Biomarker Profiling and Reproducibility Study of MALDI-MS Measurements of Escherichia coli by Analysis of Variance-Principal Component Analysis*", Analytical Chemistry **2008**, *80*, 1474-1481.
86. T. L. Williams, D. Andrzejewski, J. O. Lay und S. M. Musser, "*Experimental Factors Affecting the Quality and Reproducibility of MALDI TOF Mass Spectra Obtained from Whole Bacteria Cells*", Journal of the American Society for Mass Spectrometry **2003**, *14*, 342-351.
87. K. Maquelin, L. P. Choo-Smith, C. Kirschner, N. A. Ngo-Thi, D. Naumann und G. J. Puppels, "*Vibrational Spectroscopic Studies of Microorganisms*", John Wiley & Sons, Ltd, **2006**.
88. C. V. Raman, "*A Change of Wave-length in Light Scattering*", Nature **1928**, *121*, 619-619.
89. C. V. Raman und K. S. Krishnan, "*A New Type of Secondary Radiation* ", Nature **1928**, *121*, 501-502.
90. C. V. Raman und K. S. Krishnan, "*Polarisation of Scattered Light-quanta* ", Nature **1928**, *122*, 169-169.
91. D. Naumann, "*Infrared Spectroscopy in Microbiology*", John Wiley & Sons, Ltd, **2000**.
92. M. Harz, P. Rösch und J. Popp, "*Vibrational spectroscopy - A Powerful Tool for the Rapid Identification of Microbial Cells at the Single-cell Level*", Cytometry, Part A **2009**, *75A*, 104-113.
93. T. Fearn, "*Discriminant Analysis*", John Wiley & Sons, Ltd, **2006**.
94. R. Petry, M. Schmitt und J. Popp, "*Raman Spectroscopy - A Prospective Tool in the Life Sciences*", ChemPhysChem **2003**, *4*, 14-30.

95. J. L. McHale, "*Resonance Raman Spectroscopy*", John Wiley & Sons, Ltd, **2006**.
96. D. A. Long, "*The Raman effect: a unified treatment of the theory of Raman scattering by molecules*", Wiley, Chichester [u.a.], **2002**.
97. W. H. Nelson, R. Dasari, M. Feld und J. F. Sperry, "*Intensities of calcium dipicolinate and Bacillus subtilis spore Raman spectra excited with 244 nm light*", Applied Spectroscopy **2004**, *58*, 1408-1412.
98. E. Ghiamati, R. Manoharan, W. H. Nelson und J. F. Sperry, "*UV Resonance Raman Spectra of Bacillus Spores*", Applied Spectroscopy **1992**, *46*, 357-364.
99. E. C. López-Díez und R. Goodacre, "*Characterization of Microorganisms Using UV Resonance Raman Spectroscopy and Chemometrics*", Analytical Chemistry **2004**, *76*, 585-591.
100. E. C. Le Ru, E. Blackie, M. Meyer und P. G. Etchegoin, "*Surface Enhanced Raman Scattering Enhancement Factors: a Comprehensive Study*", Journal of Physical Chemistry C **2007**, *111*, 13794-13803.
101. K. Kneipp, M. Moskovits und H. Kneipp, "*Surface-Enhanced Raman Scattering: Physics and Applications*", Springer-Verlag, [s. l.], **2006**.
102. X. Zhang, C. R. Yonzon und R. P. Van Duyne, "*An electrochemical surface-enhanced Raman spectroscopy approach to anthrax detection*", Proceedings of SPIE - The International Society for Optical Engineering **2003**, *5221*, 82-91.
103. S. Farquharson, A. D. Gift, P. Maksymiuk und F. E. Inscore, "*Rapid Dipicolinic Acid Extraction from Bacillus Spores Detected by Surface-Enhanced Raman Spectroscopy*", Applied Spectroscopy **2004**, *58*, 351-354.
104. S. E. J. Bell, J. N. Mackle und N. M. S. Sirimuthu, "*Quantitative surface-enhanced Raman spectroscopy of dipicolinic acid-towards rapid anthrax endospore detection*", Analyst (Cambridge, United Kingdom) **2005**, *130*, 545-549.
105. X. Zhang, M. A. Young, O. Lyandres und R. P. Van Duyne, "*Rapid Detection of an Anthrax-Biomarker by Surface-Enhanced Raman Spectroscopy*", Journal of the American Chemical Society **2005**, *127*, 4484-4489.
106. A. Alexander Troy und M. Le Dianna, "*Characterization of a commercialized SERS-active substrate and its application to the identification of intact Bacillus endospores*", Applied Optics **2007**, *46*, 3878-3890.
107. J. Guicheteau, L. Argue, D. Emge, A. Hyre, M. Jacobson und S. Christesen, "*Bacillus Spore Classification via Surface Enhanced Raman Spectroscopy and Principal Component Analysis*", Applied Spectroscopy **2008**, *62*, 267-272.

108. W. F. Pearman und A. W. Fountain, "*Classification of Chemical and Biological Warfare Agent Simulants by Surface-Enhanced Raman Spectroscopy and Multivariate Statistical Techniques*", Applied Spectroscopy **2006**, *60*, 356-365.
109. L. Baia, K. Gigant, U. Posset, G. Schottner, W. Kiefer und J. Popp, "*Confocal Micro-Raman Spectroscopy: Theory and Application to a Hybrid Polymer Coating*", Applied Spectroscopy **2002**, *56*, 536-540.
110. G. J. Puppels, F. F. M. Demul, C. Otto, J. Greve, M. Robertnicoud, D. J. Arndt-Jovin und T. M. Jovin, "*Studying single living cells and chromosomes by confocal Raman microspectroscopy*", Nature **1990**, *347*, 301-303.
111. P. Rösch, M. Harz, M. Schmitt, K.-D. Peschke, O. Ronneberger, H. Burkhardt, H.-W. Motzkus, M. Lankers, S. Hofer, H. Thiele und J. Popp, "*Chemotaxonomic Identification of Single Bacteria by Micro-Raman Spectroscopy: Application to Clean-Room-Relevant Biological Contaminations*", Applied and Environmental Microbiology **2005**, *71*, 1626-1637.
112. M. Harz, M. Kiehntopf, S. Stöckel, P. Rösch, E. Straube, T. Deufel und J. Popp, "*Direct analysis of clinical relevant single bacterial cells from cerebrospinal fluid during bacterial meningitis by means of micro-Raman spectroscopy*", Journal of Biophotonics **2009**, *2*, 70-80.
113. S. Meisel, S. Stöckel, M. Elschner, F. Melzer, P. Rösch und J. Popp, "*Raman Spectroscopy as a Potential Tool for Detection of Brucella spp. in Milk*", Applied and Environmental Microbiology **2012**, *78*, 5575-5583.
114. A. P. Esposito, C. E. Talley, T. Huser, C. W. Hollars, C. M. Schaldach und S. M. Lane, "*Analysis of Single Bacterial Spores by Micro-Raman Spectroscopy*", Applied Spectroscopy **2003**, *57*, 868-871.
115. D. Chen, S. S. Huang und Y. Q. Li, "*Real-Time Detection of Kinetic Germination and Heterogeneity of Single Bacillus Spores by Laser Tweezers Raman Spectroscopy*", Analytical Chemistry **2006**, *78*, 6936-6941.
116. J. De Gelder, P. Scheldeman, K. Leus, M. Heyndrickx, P. Vandenabeele, L. Moens und P. De Vos, "*Raman spectroscopic study of bacterial endospores*", Analytical and Bioanalytical Chemistry **2007**, *389*, 2143-2151.
117. S. S. Huang, D. Chen, P. L. Pelczar, V. R. Vepachedu, P. Setlow und Y. Q. Li, "*Levels of Ca^{2+}-dipicolinic acid in individual Bacillus spores determined using microfluidic Raman tweezers*", Journal of Bacteriology **2007**, *189*, 4681-4687.

118. L. B. Kong, P. F. Zhang, G. W. Wang, J. Yu, P. Setlow und Y.-q. Li, "*Characterization of bacterial spore germination using phase-contrast and fluorescence microscopy, Raman spectroscopy and optical tweezers*", Nature Protocols **2011**, *6*, 625-639.
119. L. B. Kong, P. Setlow und Y. Q. Li, "*Analysis of the Raman spectra of Ca^{2+}-dipicolinic acid alone and in the bacterial spore core in both aqueous and dehydrated environments*", Analyst (Cambridge, United Kingdom) **2012**, *137*, 3683-3689.
120. P. Zhang, L. Kong, G. Wang, M. Scotland, S. Ghosh, B. Setlow, P. Setlow und Y. Q. Li, "*Analysis of the slow germination of multiple individual superdormant Bacillus subtilis spores using multifocus Raman microspectroscopy and differential interference contrast microscopy*", Journal of Applied Microbiology **2012**, *112*, 526-536.
121. J. W. Chan, A. P. Esposito, C. E. Talley, C. W. Hollars, S. M. Lane und T. Huser, "*Reagentless Identification of Single Bacterial Spores in Aqueous Solution by Confocal Laser Tweezers Raman Spectroscopy*", Analytical Chemistry **2004**, *76*, 599-603.
122. S. Farquharson, G. Lawrence, K. Victor, S. Wayne, F. S. Jay und F. Gerard, "*Detecting Bacillus cereus spores on a mail sorting system using Raman spectroscopy*", Journal of Raman Spectroscopy **2004**, *35*, 82-86.
123. A. Tripathi, R. E. Jabbour, P. J. Treado, J. H. Neiss, M. P. Nelson, J. L. Jensen und A. P. Snyder, "*Waterborne Pathogen Detection Using Raman Spectroscopy*", Applied Spectroscopy **2008**, *62*, 1-9.
124. K. S. Kalasinsky, T. Hadfield, A. A. Shea, V. F. Kalasinsky, M. P. Nelson, J. Neiss, A. J. Drauch, G. S. Vanni und P. J. Treado, "*Raman Chemical Imaging Spectroscopy Reagentless Detection and Identification of Pathogens: Signature Development and Evaluation*", Analytical Chemistry **2007**, *79*, 2658-2673.
125. R. L. McCreery, "*Raman spectroscopy for chemical analysis*", *Chemical analysis v. 157*, John Wiley & Sons, New York, **2000**.
126. D. Hutsebaut, K. Maquelin, P. De Vos, P. Vandenabeele, L. Moens und G. J. Puppels, "*Effect of Culture Conditions on the Achievable Taxonomic Resolution of Raman Spectroscopy Disclosed by Three Bacillus Species*", Analytical Chemistry **2004**, *76*, 6274-6281.
127. M. Harz, P. Rösch, K. D. Peschke, O. Ronneberger, H. Burkhardt und J. Popp, "*Micro-Raman spectroscopic identification of bacterial cells of the genus Staphylococcus and dependence on their cultivation conditions*", Analyst (Cambridge, United Kingdom) **2005**, *130*, 1543-1550.
128. J. Charney, W. P. Fisher und C. P. Hegarty, "*Managanese as an essential element for sporulation in the genus Bacillus*", Journal of Bacteriology **1951**, *62*, 145-148.

129. Q. Que und J. D. Helmann, "*Manganese homeostasis in Bacillus subtilis is regulated by MntR, a bifunctional regulator related to the diphtheria toxin repressor family of proteins*", Molecular Microbiology **2000**, *35*, 1454-1468.
130. R. Slepecky und J. W. Foster, "*Alterations in metal content of spores of Bacillus megaterium and the effect on some spore properties*", Journal of Bacteriology **1959**, *78*, 117-123.
131. M. Kalinowska, M. Borawska, R. Świsłocka, J. Piekut und W. Lewandowski, "*Spectroscopic (IR, Raman, UV, 1H and 13C NMR) and microbiological studies of Fe(III), Ni(II), Cu(II), Zn(II) and Ag(I) picolinates*", Journal of Molecular Structure **2007**, *834-836*, 419-425.
132. G. Świderski, M. Kalinowska, S. Wojtulewski und W. Lewandowski, "*Experimental (FT-IR, FT-Raman, ^{1}H NMR) and theoretical study of magnesium, calcium, strontium, and barium picolinates*", Spectrochimica Acta Part A: Molecular and Biomolecular Spectroscopy **2006**, *64A*, 24-33.
133. Robert Koch-Institut, "*Liste der vom Robert Koch-Institut geprüften und anerkannten Desinfektionsmittel und -verfahren (15. Ausgabe)*", Bundesgesundheitsblatt - Gesundheitsforschung - Gesundheitsschutz **2007**, *50*, 1332-1356.
134. P. C. B. Turnbull, "*Guidelines for the Surveillance and Control of Anthrax in Humans and Animals*", World Health Organization, Geneva, **2008**.
135. D. G. Black, T. M. Taylor, H. J. Kerr, S. Padhi, T. J. Montville und P. M. Davidson, "*Decontamination of Fluid Milk Containing Bacillus Spores Using Commercial Household Products*", Journal of Food Protection **2008**, *71*, 473-478.
136. J. P. M. Euzéby, "*List of Prokaryotic names with Standing in Nomenclature (LPSN)*" (http://www.bacterio.cict.fr/), Zugriff am: **25.09.2012**.
137. V. A. Luna, D. King, C. Davis, T. Rycerz, M. Ewert, A. Cannons, P. Amuso und J. Cattani, "*Novel Sample Preparation Method for Safe and Rapid Detection of Bacillus anthracis Spores in Environmental Powders and Nasal Swabs*", Journal of Clinical Microbiology **2003**, *41*, 1252-1255.
138. L. Rossen, P. Nørskov, K. Holmstrøm und O. F. Rasmussen, "*Inhibition of PCR by components of food samples, microbial diagnostic assays and DNA-extraction solutions*", International Journal of Food Microbiology **1992**, *17*, 37-45.
139. H. Fukushima, K. Katsube, Y. Hata, R. Kishi und S. Fujiwara, "*Rapid Separation and Concentration of Food-Borne Pathogens in Food Samples Prior to Quantification by Viable-Cell Counting and Real-Time PCR*", Applied and Environmental Microbiology **2007**, *73*, 92-100.
140. H. Pertoft, "*Fractionation of cells and subcellular particles with Percoll*", Journal of Biochemical and Biophysical Methods **2000**, *44*, 1-30.

[SS1] S. Stöckel, S. Meisel, R. Böhme, M. Elschner, P. Rösch und J. Popp, "*Effect of supplementary manganese on the sporulation of Bacillus endospores analysed by Raman spectroscopy*", Journal of Raman Spectroscopy **2009**, *40*, 1469-1477.

[SS2] S. Stöckel, W. Schumacher, S. Meisel, M. Elschner, P. Rösch und J. Popp, "*Raman Spectroscopy-Compatible Inactivation Method for pathogenic Endospores*", Applied and Environmental Microbiology **2010**, *76*, 2895-2907.

[SS3] S. Stöckel, S. Meisel, M. Elschner, P. Rösch und J. Popp, "*Identification of Bacillus Anthracis via Raman Spectroscopy and Chemometric Approaches*", Analytical Chemistry, DOI: 10.1021/ac302250t.

[SS4] S. Stöckel, S. Meisel, M. Elschner, P. Rösch und J. Popp, "*Raman Spectroscopic Detection of Anthrax Endospores in Powder Samples*", Angewandte Chemie, International Edition **2012**, *51*, 5339-5342.

2 Publikationen und Konferenzbeiträge

2.1 Publikationen

2.1.1 Effect of supplementary manganese on the sporulation of *Bacillus* endospores analysed by Raman spectroscopy

Journal of Raman Spectroscopy **2009**, 40, 1469-1477

Stephan Stöckel:	Kultivierung und Aufarbeitung von Mikroorganismen, Raman-Messungen, Datenauswertung, Manuskripterstellung
Susann Meisel:	Kultivierung und Aufarbeitung von Mikroorganismen, Raman-Messungen, Datenauswertung, Beiträge zum Manuskript
René Böhme:	quantenchemische Berechnungen, Beiträge zum Manuskript
Mandy Elschner:	Bereitstellung von Mikroorganismen, Konzept- und Ergebnisdiskussion, Revision und Überarbeitung des Manuskripts
Petra Rösch:	Konzept- und Ergebnisdiskussion, Revision und Überarbeitung des Manuskripts
Jürgen Popp:	Projektleitung, Konzept- und Ergebnisdiskussion, Revision und Überarbeitung des Manuskripts

Research Article

Journal of RAMAN SPECTROSCOPY

Received: 29 October 2008 Accepted: 13 March 2009 Published online in Wiley Interscience: 29 April 2009

(www.interscience.wiley.com) DOI 10.1002/jrs.2292

Effect of supplementary manganese on the sporulation of *Bacillus* endospores analysed by Raman spectroscopy

S. Stöckel,[a] S. Meisel,[a] R. Böhme,[a] M. Elschner,[b] P. Rösch[a] and J. Popp[a,c]*

It is a common practice in microbiology to induce and accelerate sporulation of spore-forming bacteria by adding small amounts of divalent manganese to the cultivation medium. By micro-Raman spectroscopy the effect of supplementary divalent manganese during the growth and sporulation of *Bacillus* spp. bacteria was studied. The spectral alterations in the Raman spectra of single endospores due to this cultivation parameter comprised slight alterations of the bands attributed to intracellular, abundantly present calcium dipicolinate (CaDPA). Those signals suffered a loss of intensity or partial band broadening because of the appearance of new weak signals next to them. Exclusively in Raman spectra of single *B. sphaericus* endospores, the band at 1485 cm^{-1} vanished. The theoretical spectra of CaDPA and manganese dipicolinate (MnDPA) were calculated and compared with the experimental spectra to prove the hypothesis that, while the overall intracellular DPA content decreased, an intracellular assembly of MnDPA in the endospores might also occur. Band shifts of the COO^- vibrations in the salt's spectra as well as in the endospore's spectra, and the decrease of the two CaDPA bands, confirmed this proposal. The appearance of the 1030 cm^{-1} band in all *Bacillus* spectra as well as the disappearance of the 1485 cm^{-1} band in the *B. sphaericus* spectra still needs to be clarified. With the help of two multivariate chemometric methods, these spectral alterations allowed discrimination between single endospores of different *Bacillus* strains cultivated on normal nutrient agar (NA) and those grown on NA with $MnSO_4 \cdot xH_2O$ addition. With these investigations, a possible strategy is shown to trace back the cultivation environment of matured single endospores. Utilizing the joint concept of micro-Raman spectroscopy and chemometric analysis, the differentiation between natively grown endospores and those cultivated in a laboratory with the help of manganous salts as a common sporulation accelerator seems accomplishable.

Keywords: *Bacillus*; bacteria; chemometric analysis; endospores; micro-Raman spectroscopy

Introduction

Under environmental stress, vegetative cells of a few Gram-positive bacteria, mainly of the genera *Bacillus* and *Clostridium*, can undergo a complex developmental process culminating in the production of endospores. These metabolically dormant, non-reproducing microorganisms ensure the preservation and propagation of the genetic information contained within the bacterium by providing the cell with the ability to withstand adverse conditions disadvantageous for vegetative life, until exogenous small molecules (called *germinants*) break the dormancy and trigger the germination, which finally culminates in restoring vegetative growth again. This spatial and temporal escape strategy has proven to be very successful not the least because of the endospore's extraordinarily high resistance to inactivation by various physical insults including radiation (UV and gamma), heat (wet and dry), desiccation and toxic chemicals.[1,2]

So, spore-forming bacteria managed to advance into a bewildering array of ecological niches and habitats, and many of them are ubiquitous in nature.

While a large majority of *Bacillus* species are harmless saprophytes, some of them demonstrate several pathogenic effects. The soil bacterium *B. anthracis* is the aetiological agent of the acute fatal disease anthrax in mammals. While usually soil- and dust-exposed grazing herbivores are afflicted, anthrax is also a zoonotic infection of humans, making *B. anthracis* a potential biological warfare agent. If, for example, more than 10^4 *B. anthracis* endospores are inhaled, medical treatment has to commence within 24–48 h.[3]

B. cereus as an ubiquitous soil-borne bacterium is considered to be an opportunistic pathogen and common cause of food poisoning.[4] *Bacillus* (*Paenibacillus*) *larvae*, the causative agent of the American foulbrood disease (AFB) of honeybees,[5] as well as *B. popilliae*, *B. lenitmorbus*, or *B. sphaericus* are pathogens of specific groups of insects.[6] Also *B. thuringiensis* forms upon sporulation crystals of proteinaceous insecticidal endotoxins.

As a matter of fact, especially *B. thuringiensis* and *B. sphaericus* are successfully utilized as natural pesticides (biopesticides) capable of causing either plant pests or human health hazards.[7] About 30–100% of spore formers in phyllosphere samples were found to be *B. thuringiensis*.[8]

Owing to the endospores' omnipresence, their exploitability in mankind's interest and their potential to act as delivery vehicles for animal pathogens, a wide range of endeavours have

* *Correspondence to: J. Popp, Institute of Physical Chemistry, Friedrich Schiller University Jena, D-07743 Jena, Germany. E-mail: juergen.popp@uni-jena.de*

a *Institute of Physical Chemistry, Friedrich Schiller University Jena, D-07743 Jena, Germany*

b *Friedrich Loeffler Institute, Federal Research Institute for Animal Health, Institute of Bacterial Infections and Zoonoses, D-07743 Jena, Germany*

c *Institute of Photonic Technology, D-07745 Jena, Germany*

been made to fathom various aspects of spore-forming bacteria. The attention has been focused, *inter alia*, on the processes of sporulation,[9–11] germination,[12–14] the structure and composition of the endospores along with extrachromosomally encoded phenotypes such as the *Bacillus anthracis* toxins,[15–17] the assessment of various inactivation methods[18–20] and the investigation of the phylogenetic relationship of *Bacilli* species by means of gene sequencing.[21,22]

In addition, a host of different detection and identification strategies have been developed impelled by the demand for biological warfare detection. The quantitative determination of endospores in their native matrices mainly relies on the fluorimetric determination of calcium dipicolinate (CaDPA), which is the calcium chelate of dipicolinic acid (2,6-pyridinedicarboxylic acid) and a major constituent in endospores, accounting for 5–15% of its molecular weight.[2] The terbium dipicolinate fluorescence method has been described as the most sensitive technique, allowing the determination of nanomolar concentrations.[23] But mass spectroscopic and electrophoretic methods also need to be reckoned with.

Methods aiming for the detection, identification and classification of bacterial endospores and other biological organisms also comprise a vast number of different technologies and combinations thereof: e.g. DNA sequencing[24] or single-nucleotide polymorphism (SNPs) assays[25] as genetic analysis, different microscopic approaches (such as atomic force microscopy[26] or fluorescence microscopy[27,28]), mass spectroscopy and vibrational spectroscopy, among which infrared[29–31] and Raman spectroscopy together with chemometrical analysis can play a key role. With these optical detection methods, an appreciable reduction of preparation and analysis time is achievable compared to the currently established methods based on microbiology, immunoassay, as well as genetic and molecular-based approaches for identification.

Several Raman-based methods dealing with bacterial spores have already verified their feasibility in this respect, relying on normal Raman,[9,32–36] UV-resonance Raman,[37,38] surface-enhanced Raman (SERS)[39,40] and nonlinear Raman spectroscopies[41,42] as well as Raman imaging.[43–46] In some of these publications, the possibility to perform the detection and identification at the single organism level via a micro-Raman setup was exploited, making cultivation steps prior to the actual measurements redundant.

But still one point must not be ignored: varying culturing environments (temperature, nutrition, age of cells, etc.) lead to variations in the biochemical composition of microbial cells, and since the Raman spectra of single cells are strongly affected by their individual physiological states,[47,48] an underestimation of the cultivation parameters might lead to a decrease in the identification accuracy and taxonomic resolution.[49] And that is even more worth considering when dealing with native endospores extracted from their natural habitat. In these cases, the actual circumstances under which the single endospores grow and sporulate are unknown.[6]

Moreover, the mechanisms by which supplements besides the essential nutrients influence the sporulation are still not well understood. One example is divalent manganese. It is considered to be essential for sporulation and the biosynthesis of other metabolites and structures in spore-forming bacteria.[50,51] Because of its effect to induce sporulation, it is a common practice in microbiology to add bivalent manganese to the cultivation broth or agar plates in a concentration higher than required for bacterial growth (up to several hundred micrograms per litre). For example, almost all Raman spectroscopists dealing with bacterial spores resort to manganese-augmented media like the Leighton–Doi (2× SG) medium,[52] the G-Medium,[53] or the new sporulation medium (NSM).[54] But to the best of our knowledge none of these authors examined thoroughly the possible consequences the supplementary manganese could have on the Raman spectra of their analysed microorganisms. Maybe the comparability of these spectra from laboratory spores with those from native cells is unintentionally compromised.

Raman spectroscopy itself can be used for the elucidation of the effect a boosted Mn(II) presence can have during the growth and sporulation process on single endospores. These considerations are the motivation for this work, where single endospores of several different *Bacillus* spp. are studied in respect to a manganese supplementation during their cultivation by means of micro-Raman spectroscopy and the subsequent multivariate analysis.

Experimental

Spectroscopic instrumentation

The Raman spectroscopic measurements were carried out with a micro-Raman setup (HR LabRam inverse, Horiba Jobin Yvon). A frequency-doubled Nd : YAG laser (Coherent Compass) provided the excitation light with a wavelength at 532 nm and 1.5 mW power on the sample. The integration time for a single endospore spectra amounted to 30 s. A Leica PLFluoar L100× objective focused the laser light onto the sample within a focus of less than 1 μm in diameter. The spectrometer had an entrance slit of 100 μm and a focal length of 800 mm and was equipped with a 300 or 1800 lines/mm grating. A CCD camera operating at 220 K was utilized over a range of 298–3373 cm^{-1}. Calibration was performed relative to TiO_2 as reference. The resolution of the spectra is approximately between 10 cm^{-1} (300 lines/mm grating) and 1.5 cm^{-1} (1800 lines/mm grating). In all measurements except for the ones of the DPA salts, the 300 lines/mm grating was employed.

Strains and culturing conditions

The strains *B. atrophaeus* DSM 675, *B. mycoides* DSM 299, *B. sphaericus* DSM 28, *B. sphaericus* DSM 1867, *B. subtilis* DSM 6399 and *B. thuringiensis* DSM 350 were purchased from the German Collection of Microorganisms and Cell Cultures (DSMZ, Braunschweig, Germany). All the strains except *B. mycoides* DSM 299 (25 °C) were grown on nutrient agar (NA, peptone 5.0 g/l, meat extract 3.0 g/l, agar 15 g/l, distilled water 1000 ml, pH 7.0), on a case-by-case basis with or without supplementary 10 mg of MnSO4 · *x*H2O, at 30 °C for 10 days to ensure a maximum yield of mature endospores.

Sample preparation

Using a 1-μl inoculation loop, a part of the cultivated strains was scraped from plates, suspended and washed twice in 100 μl distilled water, and finally 1 μl of the endospore suspension was applied to a fused silica plate. Of all analysed bacterial strains, the Raman spectra from at least two independent cultures from separately prepared batches of media were recorded. Also, cells were harvested from the perimeter and from the centre of the agar plates in order to account for inhomogeneities of the culturing conditions within an agar plate (nutritient distribution,

temperature gradients, etc.). Only single, well-separated and morphologically flawless cells (according to the bright field image) were measured.

CaDPA was prepared by the method described in the literature[55] by mixing solutions of 0.1 M $CaCl_2$ and 0.1 M sodium dipicolinate (Na_2DPA), heating in a boiling water bath and subsequent cooling. Since dipicolinic acid is rather insoluble in cold water, Na_2DPA was prepared earlier from dipicolinic acid (Sigma-Aldrich, Munich, Germany). Manganese dipicolinate (MnDPA) was prepared according to the method of Windle and Sacks.[56]

Quantum chemical calculations

The RI-DFT calculations of CaDPA and MnDPA were performed with the program package Turbomole 5.7.1 on BP86/def2-TZVP level. For the calculation of the Raman spectra, the vibrational spectroscopy package SNF was used. The output spectra were convoluted with a Lorentzian profile of 10 cm^{-1} width to better match the experimental spectra.

Multivariate analysis

Matlab R2006b (The Mathworks, Natick, MA, USA) and the Opus Ident Software Package 6.5 (Bruker Optik GmbH, Ettlingen, Germany) were utilized for data pre-processing and multivariate analysis. The pre-processing of the spectra comprised a baseline correction (weighted least square) and vector normalization. If not otherwise noted, the spectral region between 682 and 1801 cm^{-1} was included. For the principal component analysis (PCA), the spectra were also mean-centred and the model cross-validated afterwards (leave-one-out).

Results and Discussion

In order to ascertain whether an elevated manganese supply during the sporulation process affects the Raman spectra of endospores to an appreciable extent, a hierarchical cluster analysis (HCA) was performed on 206 pre-processed single endospore spectra of six *Bacillus* species and strains (*B. thuringiensis* DSM 350, *B. mycoides* DSM 299, *B. subtilis* DSM 6399, *B. atrophaeus* DSM 675, *B. sphaericus* DSM 28 and *B. sphaericus* DSM 1867), half of which (15–25 spectra) were cultivated on manganese-augmented NA agar plates (notations tagged with a '+'), and the other half not (notations tagged with a '−'). The dendrogram is given in Fig. 1. For most of the samples, all Raman spectra of one sample are grouped in the same cluster – the three outliers are marked with an asterisk and belong to *B. thuringiensis* spectra, which are wrongly classified according to their cultivation. Small heterogeneities within these subgroups may arise from differences in the spore composition of the particular culture, emerging, e.g., from fluctuating CaDPA contents in single spores among a population.[34]

In the dendrogram, two major groups A and B can be seen, and both are further subdivided into four and two sub-clusters, respectively. Group A is comprised of spectra of *B. thuringiensis* (abbreviated as Bthu350+ and Bthu350−) and *B. mycoides* (Bmyc299+ and Bmyc299−) as well as those of *B. subtilis* (Bsub6399+ and Bsub6399−) and *B. atrophaeus* (Batr675+ and Batr675−). The species-mediated clustering is almost flawless, since all four species are clearly separated from each other. And according to their phylogenetic relationship, this makes perfect sense: the genetically near neighbours *B. thuringiensis* and *B. mycoides* are joined together in one sub-cluster. Inferred from the nucleotide sequences of the 150 bp 3′ end 16S rDNA and the 70 bp 5′ 16S–23S internal transcribed spacers (ITS) region, both are phylogenetically very similar.[22] And, indeed, the phenotypic and genotypic similarities of both recently led to the proposal to regroup them together with *B. anthracis* and *B. cereus* into a single species on the basis of genetic evidence.[21] Spectra of *B. subtilis* and *B. atrophaeus* are grouped together in one sub-cluster, too, but are still clearly subdivided. Here again, both share great similarities in their genetic makeup.[22] After the species-relevant classification, the cultivation parameters come into play: each of the species-pure clusters is then again divided into clusters of spectra of endospores with manganese-mediated sporulation ('+' tags) and those without ('−' tags).

Spectra of both *B. sphaericus* strains (Bsph28, Bsph1867) combine together to build group B. While in group A initially a clear distinction according to species differences is achieved, in group B, on the other hand, the two sub-clusters emerge from the different contents of manganese in the otherwise same growth media. Both strains grown on manganese-rich media ('+' tag) are clearly separated from those cultivated without this sporulation accelerator ('−' tag). The last classification step then occurs among both *B. sphaericus* clusters, when even at the strain level the spectra are pooled together correctly.

From the results of this HCA, it is to be assumed that two different factors account for the classification: that is, the differences at the species and even strain level and the presence/absence of supplementary divalent manganese during the sporulation process. But obviously these two factors make an impact on the spectra with non-constant weight. In group A, the dominating factor is the species specificity followed by influence of the growth media. This is in clear distinction to group B, where first the culturing conditions cause the clustering, and only thereafter the strain-mediated characteristics complete the classification.

Hence, albeit to a variable extent, the addition of manganese to the otherwise unaltered growth media influences measurably the spectra of single endospores grown in these media. But still a comprehensive partitioning of the spectra in compliance with phylogenetic similarities is achieved. But it is strange why the pronounced separation of both of the B. *sphaericus* strains occurred. Not as probably expected, these clusters were not put into the group comprising the genetically related *B. atrophaeus* and *B. subtilis*. Since the main classification feature of the *B. sphaericus* strains obviously arises from the cultivation parameter, this also might be the reason for the isolation of these very strains from the others.

In order to get qualitative information about the changes that form the basis of this division, all the following analyses were performed. It is necessary to understand whether these alterations, which apparently occur within the endospores themselves, are provoked by manganese, which is directly integrated into the endospores. Alternatively, some metabolic changes without direct participation of manganese during the sporulation process might initiate these changes just by the mere elevated presence of this metal. Of course, a combination of both processes is also imaginable.

To follow the first idea of an increased uptake of manganese by the spores, it is an apparent approach to propose that similar to the divalent Ca^{2+} ion in case of the CaDPA, the Mn^{2+} ion also might be sequestered by the bidentate intra-spore dipicolinate chelators to give MnDPA. Thus, to get some knowledge of possible spectral diversities in the Raman spectra between these two salts,

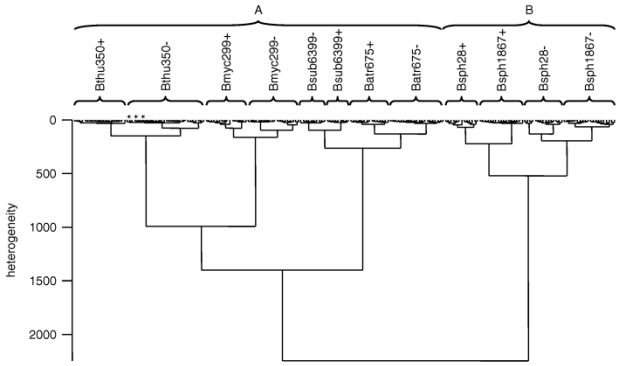

Figure 1. Dendrogram obtained from a hierarchical cluster analysis performed on Raman spectra of single endospores of the strains *B. thuringiensis* DSM 350 (Bthu350), *B. mycoides* DSM 299 (Bmyc299), *B. subtilis* DSM 6399 (Bsub6399), *B. atrophaeus* DSM 675 (Batr675), *B. sphaericus* DSM 28 (Bsph28) and *B. sphaericus* DSM (Bsph1867). Spectra of endospores grown on Mn^{2+} supplemented NA are denoted with a (+), those grown on normal NA with a (−); Asterisks designate wrongly classified spectra.

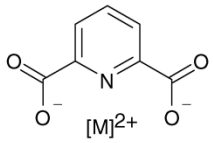

Figure 2. Sketched structure in C_{2V} symmetry of the calculated dipicolinate salts with divalent metal ions: M = Ca, Mn.

the spectra of the pure substances in crystalline solid form were recorded, and DFT calculations performed on both. The calculated structures exhibit a planar structure in a C_{2V} symmetry, which is sketched in Fig. 2. For the Raman measurements of the salts, a grating with 1800 lines/mm was used instead of the usual 300 lines/mm to get maximum spectral resolution. The results are presented in Fig. 3, and a tentative band assignment is given in Table 1.

The agreement between the experimental and calculated spectra is insufficient, which is nevertheless acceptable, since only isolated DPA molecules in the gas phase with perfect C_{2V} symmetry were considered in the calculations. Therefore solvent effects or intermolecular interactions were ignored. But a striking feature still stands out: all three carboxylate modes are subject to partly significant band shifts if the metal ion is changed. This takes effect in both the experimental and theoretical spectra. First, the C–COO^- stretching mode located at 820 cm^{-1} (787 cm^{-1} calculated) in the CaDPA spectrum moves to 817 cm^{-1} (784 cm^{-1}). Equally, the symmetric valence vibration of the COO^- group is shifted to lower wavenumbers as a result of the metal exchange, even though to different extents. In the experimental spectra, the shift spans 6 cm^{-1} from 1400 to 1394 cm^{-1}, whereas in the calculations by 33 cm^{-1} from 1270 to 1237 cm^{-1}. On the contrary, the band of the asymmetric COO^- valence vibration is shifted to higher wavenumbers: in the experimental spectra from 1582 to 1592 cm^{-1} and in the theoretical ones from 1684 to 1708 cm^{-1}. By carrying out theoretical and experimental studies on picolinates with different metal ions, Kalinowska *et al.*[59] and Świderski *et al.*[60] corroborated that the difference between the symmetric and asymmetric valence vibrations of the carboxylate

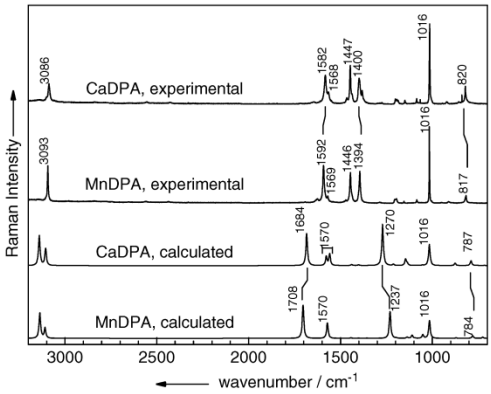

Figure 3. Experimental and calculated Raman spectra of CaDPA and MnDPA. The experimental spectra were recorded using a 1800 lines/mm grating.

groups correlates with the type of metal–ligand bonding.[61] The metal cations seem to influence the carboxylic anion as well as the aromatic ring structure, depending on their mass and ionic potential and also on other yet unknown parameters.

All the other bands emerging from aromatic ring vibrations maintain their position, including the prominent ring-breathing vibration at 1016 cm^{-1} as well as both the stretching vibrations at 1447 and 1568 cm^{-1}.

To confirm whether these findings can be used for the examination of real biological systems, the Raman spectra of single *Bacillus* endospores were thoroughly evaluated using an increased manganese presence during their cultivation. Figure 4 exemplifies the methodology on *B. mycoides* endospores. Here both the spectra at the top end are baseline-corrected mean endospore spectra of cells grown on the manganese-enriched medium (Fig. 4A) or on normal NA agar (Fig. 4B): each of them was calculated from 20 baseline-corrected spectra and for the prominent C–H band at 2939 cm^{-1} normalized Raman spectra

Table 1. Tentative band assignment for the experimental and calculated theoretical Raman spectra of CaDPA and MnDPA

Wavenumber (cm^{-1})				
CaDPA exp.	MnDPA exp.	CaDPA calc.	MnDPA calc.	Band assignment
820	817	787	784	C–COO^- stretch[44]
1016	1016	1016	1016	Ring breathing of pyridine ring[44]
1400	1394	1270	1237	COO^- sym. stretch[44,57]
1447	1446	1570	1570	Pyridine ring vibration[57]
1568	1569			Pyridine ring vibration[57]
1582	1592	1684	1708	COO^- asym. stretch[44,57,58]

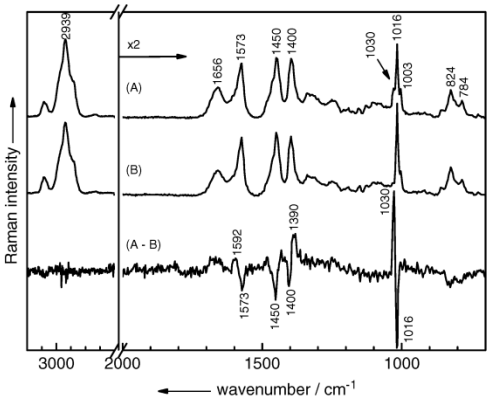

Figure 4. Baseline-corrected mean Raman spectra, each calculated with 20 single endospore spectra of *B.mycoides* DSM 299: (A) grown on Mn^{2+}-enriched NA, (B) grown on normal NA, (A – B) difference spectrum.

from single endospores. Afterwards, the mean spectrum of the normally grown endospores was subtracted from the mean spectrum of the manganese exposed endospores (Fig. 4A–B).

At first glance, the mean spectra (A) and (B) show no remarkable differences in the fingerprint region. All typical CaDPA-associated bands are clearly visible, e.g., 824, 1016, 1400, 1450 or 1573 cm^{-1}. Other contributions arise exclusively due to proteins (1003 cm^{-1} ring-breathing vibration of phenylalanine, 1659 cm^{-1} amide I vibration) or DNA/RNA moieties (784 cm^{-1} O–P–O stretching of cytosine/uracil). And some bands of those biomolecules may overlap with the CaDPA signals: e.g. at 824 cm^{-1} the ring-breathing mode of tyrosine with the carboxylate stretching mode, and at 1450 cm^{-1} the deformation mode of $CH_{2/3}$, as well as at 1570 cm^{-1} the ring vibrations of guanine and adenine with the pyridine ring vibrations of the DPA.

The most remarkable features of the difference spectrum (Fig. 4A–B) are the bands at 1016 and 1030 cm^{-1}, which is not surprising since the latter is clearly visible in the mean endospore spectrum (Fig. 4A), and the higher intensity of the 1016 cm^{-1} in (Fig. 4B) is also obvious. But even more intriguing are the other differences, which are clearly visible only in the difference spectra. Apparently, the bands at 1400, 1450 and 1573 cm^{-1} are accentuated especially in the Raman spectra of normally grown endospores, while, on the other hand, the signals at 1390 cm^{-1} and to a lesser extent at 1592 cm^{-1} arise in spectra of the manganese-influenced group. They reveal themselves, at best, as shoulders in the Raman spectrum (Fig. 4A). Bands of other intracellular biological building blocks than those of the dipicolinates demonstrate no significant information to the difference spectrum.

To put these findings onto a broader basis, a PCA was performed on baseline-corrected, vector-normalized and mean-centred Raman spectra of four *B. mycoides* ensembles, comprising at least 13 single-cell spectra from one of four independent cultures, two of them grown on manganese-rich media. In this way, physiological variations due to differences in microbial growth were attempted to be covered. Figure 5 displays the outcomes. Along the principal component 2 (PC2), the sample score plot (Fig. 5a) clearly separates the spectra of the normally grown endospores with the positive scores from the others, which possess mainly negative scores on PC2; this is true for both ensembles of each group. Seemingly, the PCA discriminates the spectra according to the presence/absence of manganese during the cultivation along PC2. Also, the associated loading plot (Fig. 5b) reinforces this observation. A comparison of the score and loading plots provides information about the Raman bands that are responsible for the spectral differences. Here the Raman shifts with a high score for this factor are the ones at 1016, 1400, 1451 and 1573 cm^{-1}. These contribute highly to all the spectra with a high score for PC2 in the score plot: that is, to the spectra of the normally grown endospores. The three bands at 1030, 1389 and 1592 cm^{-1} therefore correspond to the spectra with negative scores in the score plot, which all the spectra of manganese-perturbed cells indeed have.

The results of this chemometric analysis affirm the outcomes of the preceding analysis of not only the single cells but also of the experimental and theoretical explorations on the two dipicolinates. The decrease in intensity of the CaDPA Raman signals at 1016, 1400, 1450 and 1573 cm^{-1} in the spectra of endospores exposed to increased $MnSO_4$ concentration is attributable to the loadings in the PCA of these cells, which is also visible in the difference spectra in Fig. 4. Therefore, the first effect of supplementary manganese on endospores is a lower overall content of intracellular DPA. Since the sporulation time is significantly shortened for the bacteria grown in manganese-enriched media, the overall content of DPA salt in the endospores, which correlates with the sporulation time,[9] is also decreased.

On the other hand, the simultaneous intensity gain of the MnDPA-correlated bands suggests a partial substitution of the remaining CaDPA through MnDPA when supplementary divalent manganese is present during the sporulation process.

The exchange of the metal ions provoked at least three different band shifts, which correspond to vibrations of the carboxylate groups. And exactly these alterations manifest themselves in the spectra of native endospores grown on manganese-supplemented

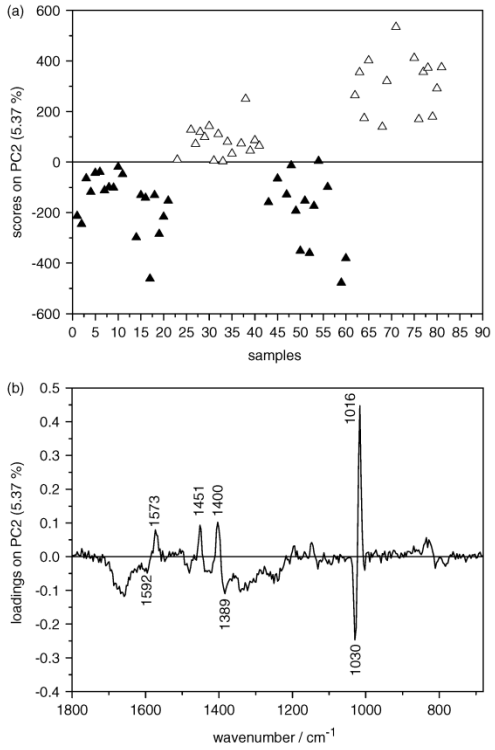

Figure 5. Principal component analysis performed on single endospore Raman spectra of *B. mycoides* DSM 299: filled triangle (▲), grown on Mn^{2+} enriched NA; open triangle (△), grown on normal NA. (a) Scores sample plot and (b) loadings plot of PC2.

media in the form of new bands at around 1390 and 1592 cm^{-1}, which is in concordance with the calculated DPA spectra. A signal shift of the deformation mode at 821 cm^{-1} may occur in the endospore spectra but it is hardly identifiable. But the two bands, together with the one at 1030 cm^{-1}, ensure a decent separation of spectra according to the cultivation factor manganese. While the origin of the 1030 cm^{-1} signal is still to be clarified (de Gelder *et al.*[9] tentatively assigned it to a symmetric stretching vibration of PO_2^-), the two other bands seem to arise from MnDPA built into the endospores while they were forming.

To validate the extent to which the manganese induced acceleration of endospores hampers the taxonomic resolution, endospores of the two phylogenetically well-separated *Bacillus* species, i.e. *B. thuringiensis* and *B. atrophaeus*, were analysed together.[22] The conditions under which they were cultivated were kept constant except for the manganese concentration: some endospores grew under normal conditions (abbreviated Batr− and Bthu−) and some with $MnSO_4$ added to the medium (Batr+ and Bthu+). Then again, a PCA was employed on approximately 20 spectra of each of the four fractions with the above-mentioned parameters. In Fig. 6a, four representative single-cell spectra of each class are given alongside the results of the PCA. The spectra of Bthu350+ and Batr675+ nicely demonstrate the aforementioned spectral features: the clearly visible new peak at 1030 cm^{-1} plus the shoulders at 1389 and 1592 cm^{-1}. Bthu350− and Batr675−, however, possess higher band intensities for the CaDPA bands. To visualize the discrimination power provided by these spectral alterations, each of the individual spectra is represented in the principal component score plot of the PCA, a two-dimensional projection of PC2 *versus* PC1 scores in Fig. 6b. In this projection, spectra of the same species exhibit distinct clusters that are reasonably well discriminated relative to the other species along PC1. These two groups are further subdivided into spectra of Batr− and Bthu− in quadrants I and II (positive scores on PC2) and Batr+ and Bthu+ in quadrants III and IV (negative scores). Therefore, PC2 gathers the variance due to the spectral changes caused by the $MnSO_4$ addition to the medium, which is in concordance with its loadings plot in Fig. 6d. Here the marker bands for the manganese influence at 1030, 1389 and 1593 cm^{-1} possess negative loadings *en bloc*, which fits to the negative scores of the Batr+ and Bthu+ spectra. Those with positive loadings seem to be the ones at 1016, 1400, 1448 and 1573 cm^{-1}, all correlated to normally grown endospores earlier. Therefore it makes perfect sense that all Batr− and Bthu− spectra possess positive scores on PC2.

The loadings plot of PC1 (Fig. 6c), however, bears reference to signals without any direct relevance to neither the dipicolinates nor other specific cell contents nor any single clearly distinguishable bands in the single-cell spectra. Ergo PC2 describes the trends in spectra caused by the manganese influence during sporulation; PC1 delivers the chemotaxonomic resolution at the species level between the *B. atrophaeus* and *B. thuringiensis* strains.

Among all the *Bacillus* species that were analysed in this work, *B. sphaericus* revealed a unique feature. An attempt was made to achieve discrimination between the two different *B. sphaericus* strains DSM 28 and DSM 1867 against the backdrop of elevated manganese supply during the cultivation. In Fig. 7a, spectra of single endospores are displayed, representing these four groups: *B. sphaericus* DSM 28 cultivated with or without added $MnSO_4$ in the media (Bsph 28+ and Bsph 28−) and the same for *B. sphaericus* DSM 1867 (Bsph 1867+ and Bsph 1867−). Besides the aforementioned spectral variances (new band at 1031 cm^{-1} and shoulders at 1591 and 1389 cm^{-1}), in these spectra the Raman band at 1485 cm^{-1} undergoes an astounding modification. In both of the spectra of normally grown endospores, this signal is clearly detectable, but it completely vanishes in the Raman spectra of endospores that were cultivated on manganese-enriched media. We could observe this alteration also in two other *B. sphaericus* strains (DSM 396 and DSM 488; data not shown). The origin of this band is, to the authors' best knowledge, unknown.

When spectral data of these endospores were analysed via PCA, there was a significant differentiation between cells that had been treated with manganese and cells that had not. All spectra were again pre-processed in the same manner as before, but this time the second derivative of the spectra was used and the band region of the $CH_{2/3}$ stretching vibrations was incorporated. This modification of the pre-processing was needed to yield the best discrimination results.

Figure 7b displays the first and fifth principal component plot for both the *B. sphaericus* strains. The Raman spectra are distributed on the basis of the first principal component (normally grown samples have mainly negative scores, thus are located in quadrants II and III) and the fifth component (spectra of strain DSM 1867 have mainly positive scores, those of DSM 28 negative). However, the chemotaxonomic differentiation is more vague compared to that caused by variable manganese exposure. The corresponding

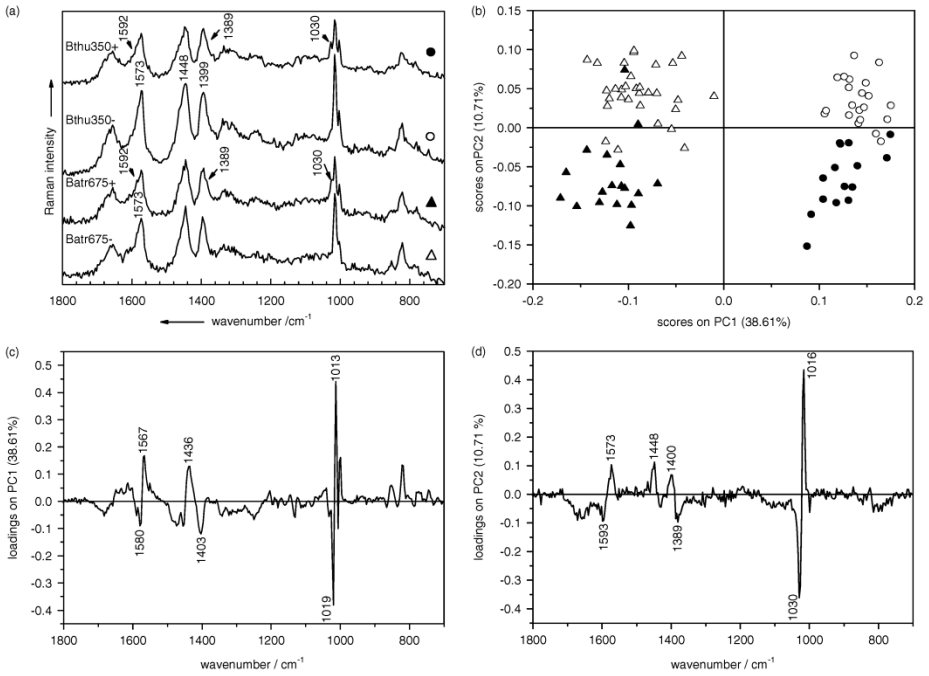

Figure 6. Principal component analysis performed on single endospore Raman spectra of *B. thuringiensis* DSM 350 (Bthu350): filled circle (●), grown on Mn^{2+} enriched NA; open circle (○), grown on normal NA and *B. atrophaeus* DSM 675 (Batr675): filled triangle (▲), grown on Mn^{2+}-enriched NA; open triangle (△), grown on normal NA. (a) Representative single endospore spectra, (b) scores plot of PC1 and PC2, (c) loadings plot of PC1, (d) loadings plot of PC2.

PC5 accounts for only 4.34% of the total variance, suggesting the Raman signatures of those two strains differ only to a minor degree, whereas PC1, accounting for 22.84% of the total variability, clearly separates the spectra of differently cultured endospores, independent of the strain. This is easily comprehensible by taking a look at the PC1's loading plot in Fig. 7c. This time, the negative amplitudes in the loadings plot correspond to the spectra with the positive scores on PC1 in the scores plot, as the second derivatives of the spectra were employed earlier, in which all bands were transformed into negative signals. Therefore, the typical marker bands for the presence of supplementary manganese during sporulation (1032, 1387 and 1592 cm^{-1}) have negative loadings but have to be assigned to the spectra of manganese-influenced endospores (Bsph28+ and Bsph1867+), which all have positive scores on PC1. Likewise, the spectra designated with Bsph28− and Bsph1867− have negative scores on PC1, which has positive loadings on the bands 1403 and 1573 cm^{-1}. Additionally, the band at 1485 cm^{-1} also strongly contributes to the positive loadings of PC1, which is a remarkable feature of *B. sphaericus* endospores grown on normal media. This unique signal re-emphasizes the already high discriminatory power of the PCA model based on the mentioned marker bands.

The significance of the PC5's loading plot in Fig. 7d suffers seemingly from a substantial contribution of noise. However, the amplitude of the signals in the CH-region at 2800–3200 cm^{-1} implies an involvement of this spectral region in the species-level differentiation and thus justifies the use of this region for this PCA model.

Now looking back to the dendrogram in Fig. 1, its remarkable classification of single endospore spectra correlating to the two parameters of phylogenetic position and cultivation conditions, i.e. with or without $MnSO_4$ added to the media's recipe, is easily understandable. Among all the six analysed *Bacillus* strains, the characteristic alterations in their spectra occur consistently when $MnSO_4$ is added. This species-independent universality suggests that the changes in the molecular makeup are based on ubiquitous processes and intracellular substances that are common for all the *Bacillus* endospores. Additionally, the alterations have to affect abounding substances inside the bacterial spores if the changes are to be perceived after all and which are superimposed by strain- or even species-specific features. And one of these similarities is the highly abundant CaDPA in the cells. Therefore, an involvement of this salt in the compositional changes inside the cells is very likely. A smaller content of intra-spore DPA, and the formation of MnDPA as a substitute of CaDPA, may explain the band shifts and the decrease in intensity of the CaDPA band, which are implied in this work. But clearly this interpretation is not altogether complete, for it is quite intriguing to note that the most distinct alteration, the Raman band at 1030 cm^{-1}, is not explainable yet. But since the exact constitution of CaDPA in endospores has not been figured out or synthesized as of now – a glassy like state is the latest assumption[62] – there is an ample scope of interpretation

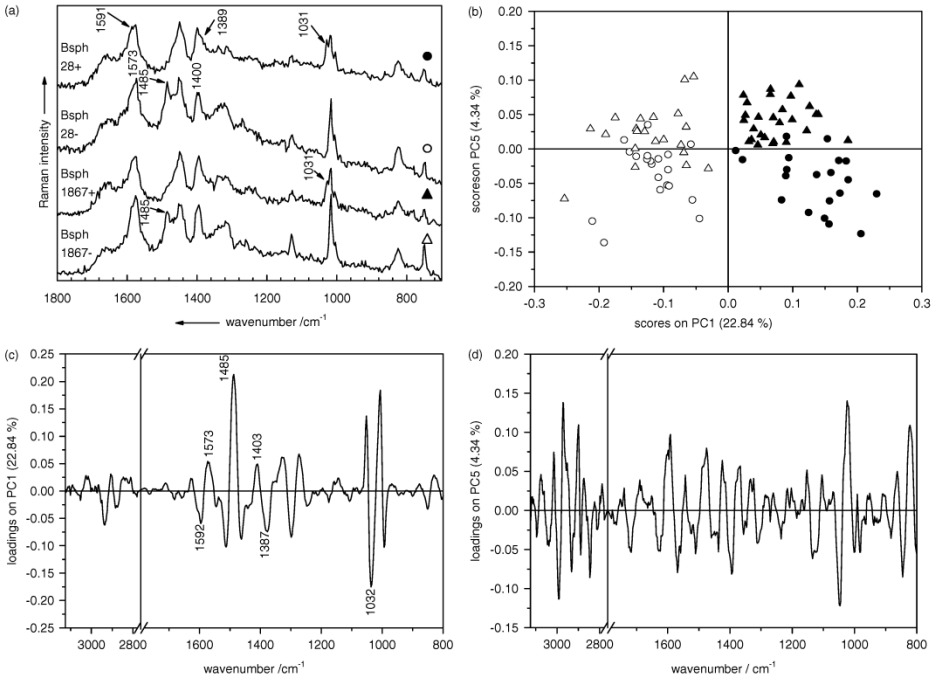

Figure 7. Principal component analysis performed on single endospore second derivative Raman spectra of *B. sphaericus* DSM 28 (Bsph28): filled circle (●), grown on Mn^{2+} enriched NA; open circle (○), grown on normal NA and *B. sphaericus* DSM 1867 (Bsph1867): filled triangle (▲), grown on Mn^{2+}-enriched NA; open triangle (△), grown on normal NA; (a) Representative single endospore spectra, (b) scores plot of PC1 and PC2, (c) loadings plot of PC1, (d) loadings plot of PC2.

left. Also the species-specific intracellular alterations shown on the example of *B. sphaericus* and its manganese-sensitive Raman signal at 1485 cm^{-1} point towards other metabolic changes that have not been elucidated yet. However, this additional spectral anomaly made sure that the *B. sphaericus* spectra built a cluster on their own in the HCA (Fig. 1), which were at first classified as due to cultivation conditions and only thereafter according to strain specificities.

Conclusions

Adding a considerable amount of manganous salts (up to several hundred micrograms per litre) to culture media for spore-forming bacteria is common practice in microbiology to accelerate the sporulation process and to achieve a maximum yield of endospores in a short time.

In this work, single *Bacillus* spp. endospores of six different strains were studied by means of micro-Raman spectroscopy. Significant variations in the spectra occurred between endospores grown on normal and $MnSO_4$-supplemented nutritient agar (10 mg MnSO4 · *x*H2O per litre). Within all strains in the spectra of endospores cultivated on the manganese-rich agar, the CaDPA-associated signals at 1016, 1400 and 1572 cm^{-1} experience a decrease in intensity, and, furthermore, a band-broadening due to additional bands at 1030, 1390 and 1592 cm^{-1}, respectively. Exclusively in both of the analysed *B. sphaericus* strains, the signal at 1485 cm^{-1} appears only in Raman spectra of endospores that grew on agar devoid of additional $MnSO_4$.

Parts of these spectral alterations seem to be explainable by the hypothesis that, firstly, the overall content of intracellular DPA is smaller and, secondly, a partial substitution of the remaining intracellular CaDPA with MnDPA occurs when spore-forming bacteria are provided with a significant concentration of manganese in excess of the quantity normally required for vegetative growth. Firstly, the intensity loss of the CaDPA bands fits into this model. Secondly, the comparison of the experimental Raman spectra and the DFT-calculated Raman spectra of the pure salts confirm this hypothesis: Bands assignable to COO^- vibrations are subject to multidirectional band shifts when the metal ion is changed from Ca^{2+} to Mn^{2+}, which may explain the occurrence of the shoulder-like bands in endospore spectra at 1390 and 1592 cm^{-1}. These two can then directly be designated to vibrations of MnDPA. The appearance of the signal at 1030 cm^{-1} and the vanishing band at 1485 cm^{-1} in *B. sphaericus* spectra defy any explanation so far.

However, utilizing multivariate chemometric analysis (PCA, HCA), these spectral alterations were exploited to discriminate between the endospores based on their growth history. Out of a pool of spectra, comprising those from endospores of different species cultivated with or without an additional manganese supply, the PCA and HCA formed distinct clusters/groups

according to species affiliation and presence/absence of $MnSO_4$ during sporulation. The PCA loading plots indicate that the aforementioned bands heavily contribute to the variance or information of the relevant principal components, along which the discrimination according to the addition of $MnSO_4$ to the cultivation medium takes place.

In conclusion, we showed in the present work the power of the combined concept micro-Raman spectroscopy and subsequent chemometric analysis to trace back whether a single endospore grew in its native habitat (soil, decaying organic matter, etc.) or was prepared by human hand in the laboratory, provided a manganese-enriched nutrient sporulation medium was used.

Acknowledgements

Funding of the research projects 'Pathosafe' FKZ 13N9547 and FKZ 13N9549 within the framework from the Federal Ministry of Education and Research, Germany (BMBF) and of the Graduiertenkolleg 1257 'Alteration and element mobility at the microbe-mineral interface' from the German Research Foundation (DFG) is gratefully acknowledged.

References

[1] W. L. Nicholson, N. Munakata, G. Horneck, H. J. Melosh, P. Setlow, *Microbiol. Mol. Biol. Rev.* **2000**, *64*, 548.
[2] P. Setlow, *J. Appl. Microbiol.* **2006**, *101*, 514.
[3] D. R. Walt, D. R. Franz, *Anal. Chem.* **2000**, *72*, 738A.
[4] M.-J. Lee, D.-H. Bae, D.-H. Lee, K.-H. Jang, D.-H. Oh, S.-D. Ha, *J. Microbiol. Biotechnol.* **2006**, *16*, 639.
[5] M. A. Hornitzky, *J. Apic. Res.* **1998**, *37*, 267.
[6] W. L. Nicholson, *Cell. Mol. Life Sci.* **2002**, *59*, 410.
[7] M. A. El-Bendary, *J. Basic Microbiol.* **2006**, *46*, 158.
[8] S. N. Chatterjee, T. Bhattacharya, T. K. Dangar, G. Chandra, *Afr. J. Biotechnol.* **2007**, *6*, 1587.
[9] J. De Gelder, P. Scheldeman, K. Leus, M. Heyndrickx, P. Vandenabeele, L. Moens, P. De Vos, *Anal. Bioanal. Chem.* **2007**, *389*, 2143.
[10] B.-L. Liu, Y.-M. Tzeng, *Biotechnol. Bioeng.* **2000**, *68*, 11.
[11] I. Grainge, *Curr. Biol.* **2008**, *18*, R871.
[12] A. Moir, *J. Appl. Microbiol.* **2006**, *101*, 526.
[13] M. Plomp, T. J. Leighton, K. E. Wheeler, H. D. Hill, A. J. Malkin, *Proc. Natl. Acad. Sci. U.S.A.* **2007**, *104*, 9644.
[14] D. Chen, S.-S. Huang, Y.-Q. Li, *Anal. Chem.* **2006**, *78*, 6936.
[15] H. Liu, N. H. Bergman, B. Thomason, S. Shallom, A. Hazen, J. Crossno, D. A. Rasko, J. Ravel, T. D. Read, S. N. Peterson, J. Yates, P. C. Hanna III, *J. Bacteriol.* **2004**, *186*, 164.
[16] A. O. Henriques, C. P. Moran Jr, *Annu. Rev. Microbiol.* **2007**, *61*, 555.
[17] M. Plomp, T. J. Leighton, K. E. Wheeler, M. E. Pitesky, A. J. Malkin, *Langmuir* **2005**, *21*, 10 710.
[18] D. L. Perkins, C. R. Lovell, B. V. Bronk, B. Setlow, P. Setlow, M. L. Myrick, *Appl. Spectrosc.* **2004**, *58*, 749.
[19] G. McDonnell, A. D. Russell, *Clin. Microbiol. Rev.* **1999**, *12*, 147.
[20] P. Lasch, H. Nattermann, M. Erhard, M. Staemmler, R. Grunow, N. Bannert, B. Appel, D. Naumann, *Anal. Chem.* **2008**, *80*, 2026.
[21] E. Helgason, O. A. Okstad, D. A. Caugant, H. A. Johansen, A. Fouet, M. Mock, I. Hegna, A.-B. Kolsto, *Appl. Environ. Microbiol.* **2000**, *66*, 2627.
[22] D. Xu, J.-C. Cote, *Int. J. Syst. Evol. Microbiol.* **2003**, *53*, 695.
[23] J. Fichtel, J. Koester, J. Rullkoetter, H. Sass, *FEMS Microbiol. Ecol.* **2007**, *61*, 522.
[24] T. D. Read, S. L. Salzberg, M. Pop, M. Shumway, L. Umayam, L. Jiang, E. Holtzapple, J. D. Busch, K. L. Smith, J. M. Schupp, D. Solomon, P. Keim, C. M. Fraser, *Science (Washington, D.C.)* **2002**, *296*, 2028.
[25] M. N. Van Ert, W. R. Easterday, T. S. Simonson, J. M. U'Ren, T. Pearson, L. J. Kenefic, J. D. Busch, L. Y. Huynh, M. Dukerich, C. B. Trim, J. Beaudry, A. Welty-Bernard, T. Read, C. M. Fraser, J. Ravel, P. Keim, *J. Clin. Microbiol.* **2007**, *45*, 47.
[26] A. Zolock Ruth, G. Li, C. Bleckmann, L. Burggraf, C. Fuller Douglas, *Micron (Oxford, England: 1993)* **2006**, *37*, 363.
[27] M. Krause, B. Beyer, C. Pietsch, B. Radt, M. Harz, P. Rösch, J. Popp, *Proc. SPIE* **2008**, *6991*, 69 910E/1.
[28] M. Krause, B. Radt, P. Rösch, J. Popp, *J. Raman Spectrosc.* **2007**, *38*, 369.
[29.] D. Naumann, in *Encyclopedia of Analytical Chemistry* (Ed.: R. A. Meyers), John Wiley and Sons: Chichester, **2000**, p 102.
[30] D. Naumann, S. Keller, D. Helm, C. Schultz, B. Schrader, *J. Mol. Struct.* **1995**, *347*, 399.
[31] C. Kirschner, K. Maquelin, P. Pina, N. A. N. Thi, L. P. Choo-Smith, G. D. Sockalingum, C. Sandt, D. Ami, F. Orsini, S. M. Doglia, P. Allouch, M. Mainfait, G. J. Puppels, D. Naumann, *J. Clin. Microbiol.* **2001**, *39*, 1763.
[32] J. W. Chan, A. P. Esposito, C. E. Talley, C. W. Hollars, S. M. Lane, T. Huser, *Anal. Chem.* **2004**, *76*, 599.
[33] A. P. Esposito, C. E. Talley, T. Huser, C. W. Hollars, C. M. Schaldach, S. M. Lane, *Appl. Spectrosc.* **2003**, *57*, 868.
[34] S.-S. Huang, D. Chen, P. L. Pelczar, V. R. Vepachedu, P. Setlow, Y.-Q. Li, *J. Bacteriol.* **2007**, *189*, 4681.
[35] P. Rösch, M. Harz, M. Schmitt, K.-D. Peschke, O. Ronneberger, H. Burkhardt, H.-W. Motzkus, M. Lankers, S. Hofer, H. Thiele, J. Popp, *Appl. Environ. Microbiol.* **2005**, *71*, 1626.
[36] P. Rösch, M. Harz, K.-D. Peschke, O. Ronneberger, H. Burkhardt, J. Popp, *Biopolymers* **2006**, *82*, 312.
[37] E. Ghiamati, R. Manoharan, W. H. Nelson, J. F. Sperry, *Appl. Spectrosc.* **1992**, *46*, 357.
[38] W. H. Nelson, R. Dasari, M. Feld, J. F. Sperry, *Appl. Spectrosc.* **2004**, *58*, 1408.
[39] J. Guicheteau, L. Argue, D. Emge, A. Hyre, M. Jacobson, S. Christesen, *Appl. Spectrosc.* **2008**, *62*, 267.
[40] X. Zhang, M. A. Young, O. Lyandres, R. P. Van Duyne, *J. Am. Chem. Soc.* **2005**, *127*, 4484.
[41] G. I. Petrov, R. Arora, V. V. Yakovlev, X. Wang, A. V. Sokolov, M. O. Scully, *Proc. Natl. Acad. Sci. U.S.A.* **2007**, *104*, 7776.
[42] D. Pestov, X. Wang, G. O. Ariunbold, R. K. Murawski, V. A. Sautenkov, A. Dogariu, A. Sokolov, M. O. Scully, *Proc. Natl. Acad. Sci. U.S.A.* **2008**, *105*, 422.
[43] M. F. Escoriza, J. M. VanBriesen, S. Stewart, J. Maier, P. J. Treado, *J. Microbiol. Methods* **2006**, *66*, 63.
[44] K. S. Kalasinsky, T. Hadfield, A. A. Shea, V. F. Kalasinsky, M. P. Nelson, J. Neiss, A. J. Drauch, G. S. Vanni, P. J. Treado, *Anal. Chem.* **2007**, *79*, 2658.
[45] A. Tripathi, R. E. Jabbour, P. J. Treado, J. H. Neiss, M. P. Nelson, J. L. Jensen, A. P. Snyder, *Appl. Spectrosc.* **2008**, *62*, 1.
[46] P. Rösch, M. Harz, K.-D. Peschke, O. Ronneberger, H. Burkhardt, A. Schuele, G. Schmauz, M. Lankers, S. Hofer, H. Thiele, H.-W. Motzkus, J. Popp, *Anal. Chem.* **2006**, *78*, 2163.
[47] M. Harz, P. Rösch, K. D. Peschke, O. Ronneberger, H. Burkhardt, J. Popp, *Analyst (Cambridge, U.K.)* **2005**, *130*, 1543.
[48] K. C. Schuster, E. Urlaub, J. R. Gapes, *J. Microbiol. Methods* **2000**, *42*, 29.
[49] D. Hutsebaut, K. Maquelin, P. De Vos, P. Vandenabeele, L. Moens, G. J. Puppels, *Anal. Chem.* **2004**, *76*, 6274.
[50] E. D. Weinberg, *Appl. Microbiol.* **1964**, *12*, 436.
[51] J. Charney, W. P. Fisher, C. P. Hegarty, *J. Bacteriol.* **1951**, *62*, 145.
[52] T. J. Leighton, R. H. Doi, *J. Biol. Chem.* **1971**, *246*, 3189.
[53] H. U. Kim, J. M. Goepfert, *J. Appl. Bacteriol.* **1974**, *37*, 265.
[54] P. L. Worsham, M. R. Sowers, *Can. J. Microbiol.* **1999**, *45*, 1.
[55] G. Strahs, R. E. Dickerson, *Acta Crystallogr., Sect. B, Struct. Crystallogr. Cryst. Chem.* **1968**, *24*, 571.
[56] J. J. Windle, L. E. Sacks, *Biochim. Biophys. Acta* **1963**, *66*, 173.
[57] P. Carmona, *Spectrochim. Acta, Part A, Mol. Biomol. Spectrosc.* **1980**, *36A*, 705.
[58] A. C. Gonzalez-Baro, R. Pis-Diez, O. E. Piro, B. S. Parajon-Costa, *Polyhedron* **2008**, *27*, 502.
[59] M. Kalinowska, M. Borawska, R. Swislocka, J. Piekut, W. Lewandowski, *J. Mol. Struct.* **2007**, *834–836*, 419.
[60] G. Swiderski, M. Kalinowska, S. Wojtulewski, W. Lewandowski, *Spectrochim. Acta, Part A, Mol. Biomol. Spectrosc.* **2006**, *64A*, 24.
[61] C. R. Choudhury, A. Datta, V. Gramlich, G. M. Golzar Hossain, K. M. Abdul Malik, S. Mitra, *Inorg. Chem. Commun.* **2003**, *6*, 790.
[62] L. Stecchini Mara, M. Del Torre, E. Venir, A. Morettin, P. Furlan, E. Maltini, *Int. J. Food Microbiol.* **2006**, *106*, 286.

2.1.2 Raman Spectroscopy-Compatible Inactivation Method for Pathogenic Endospores

Applied and Environmental Microbiology **2010**, 76, 2895-2907

Stephan Stöckel:	Kultivierung und Aufarbeitung von Mikroorganismen, Raman-Messungen, Datenauswertung, Manuskripterstellung
Wilm Schumacher:	Datenauswertung, Beiträge zum Manuskript
Susann Meisel:	Kultivierung und Aufarbeitung von Mikroorganismen, Beiträge zum Manuskript
Mandy Elschner:	Bereitstellung von Mikroorganismen und Messproben, Konzept- und Ergebnisdiskussion, Revision und Überarbeitung des Manuskripts
Petra Rösch:	Konzept- und Ergebnisdiskussion, Revision und Überarbeitung des Manuskripts
Jürgen Popp:	Projektleitung, Konzept- und Ergebnisdiskussion, Revision und Überarbeitung des Manuskripts

APPLIED AND ENVIRONMENTAL MICROBIOLOGY, May 2010, p. 2895–2907 Vol. 76, No. 9
0099-2240/10/$12.00 doi:10.1128/AEM.02481-09

Raman Spectroscopy-Compatible Inactivation Method for Pathogenic Endospores[▽]

S. Stöckel,[1] W. Schumacher,[1] S. Meisel,[1] M. Elschner,[2] P. Rösch,[1]* and J. Popp[1,3]

Institute of Physical Chemistry, Friedrich Schiller University Jena, Helmholtzweg 4,[1] and Friedrich Loeffler Institute, Federal Research Institute for Animal Health, Institute of Bacterial Infections and Zoonoses, Naumburger Straße 96a,[2] D-07743 Jena, and Institute of Photonic Technology, Albert-Einstein-Straße 9, D-07745 Jena,[3] Germany

Received 13 October 2009/Accepted 22 February 2010

Micro-Raman spectroscopy is a fast and sensitive tool for the detection, classification, and identification of biological organisms. The vibrational spectrum inherently serves as a fingerprint of the biochemical composition of each bacterium and thus makes identification at the species level, or even the subspecies level, possible. Therefore, microorganisms in areas susceptible to bacterial contamination, e.g., clinical environments or food-processing technology, can be sensed. Within the scope of point-of-care-testing also, detection of intentionally released biosafety level 3 (BSL-3) agents, such as *Bacillus anthracis* endospores, or their products is attainable. However, no Raman spectroscopy-compatible inactivation method for the notoriously resistant *Bacillus* endospores has been elaborated so far. In this work we present an inactivation protocol for endospores that permits, on the one hand, sufficient microbial inactivation and, on the other hand, the recording of Raman spectroscopic signatures of single endospores, making species-specific identification by means of highly sophisticated chemometrical methods possible. Several physical and chemical inactivation methods were assessed, and eventually treatment with 20% formaldehyde proved to be superior to the other methods in terms of sporicidal capacity and information conservation in the Raman spectra. The latter fact has been verified by successfully using self-learning machines (such as support vector machines or artificial neural networks) to identify inactivated *B. anthracis*-related endospores with adequate accuracies within the range of the limited model database employed.

The detection of biological warfare agents requires methods for detecting and rapidly identifying bacterial endospores—such as *Bacillus anthracis*, the etiological agent of the acute fatal zoonosis anthrax in mammals—that are released in buildings or distributed in the environment. A great number of different technologies and combinations, such as DNA detection by PCR or DNA sequencing (42), are applied for genetic analysis. In addition, different microscopic approaches, such as atomic force microscopy (64) or fluorescence microscopy (26, 27), mass spectroscopy, and infrared (23, 34, 50) and Raman spectroscopy (15), have been used. With these optical detection methods, preparation and analysis time can be considerably shortened relative to that required for currently established methods based on, e.g., microbiology, immunoassays, and genetic and molecularly based approaches for identification.

The feasibility of a variety of approaches for pathogen detection relying on Raman spectroscopy, including nonresonant Raman spectroscopy (10, 54), UV resonance Raman spectroscopy (11, 35), surface-enhanced Raman spectroscopy (SERS) (12, 62), nonlinear Raman spectroscopy (39, 40), and Raman imaging (18, 22, 46), has already been verified. In some of these studies, the possibility of performing detection and identification on a single-organism level via a micro-Raman setup was exploited.

Because Raman spectra provide a snapshot of the total molecular composition of single cells, they inherently contain all the information needed to accurately identify microorganisms to the subspecies level. Although many Raman marker bands for single biosubstances or classes of biosubstances are known, an overall understanding of the spectral fingerprint in the spectra of bacteria is usually neither attainable nor necessary, if the typing strategy is based on a pattern-matching algorithm with a comprehensive database of single-cell Raman reference spectra. The recognition algorithms applied rely mainly on unsupervised and supervised multivariate chemometrical methods (6, 13, 45, 47).

Some advantages over classical microbiological and other typing methods are apparent. First, time-consuming cultivation steps prior to the actual measurements are redundant, since detectability at the single-organism level is ensured through the use of high-numerical-aperture illumination and light-gathering optics. Second, sample preparation is limited to a minimum and generally consists only in the isolation of the microorganisms from their native surroundings. Third, there is no reliance on costly taxospecific consumables with limited shelf lives. Furthermore, the complete sequence of operations—starting with isolation, proceeding through the acquisition of Raman spectra, and ending with chemotaxonomic identification—can be performed automatically. Thus, with a micro-Raman-based sensor, rapid detection of highly pathogenic microorganisms at the very place of contamination is possible.

If biosafety level-3 (BSL-3) endospores, such as those of *B. anthracis*, are the pathogens to be identified, an appropriate inactivation procedure is essential. Unfortunately, dormant spores exhibit incredible hardiness against germicidal agents. Several parameters contributing to the spores' intrinsic resistance are discussed in the literature. The complex shell-like structure of endospores plays a key role in their resistance: the

* Corresponding author. Mailing address: Institut für Physikalische Chemie, Friedrich-Schiller-Universität Jena, Helmholtzweg 4, D-07743 Jena, Germany. Phone: (49-3641) 948381. Fax: (49-3641) 948302. E-mail: petra.roesch@uni-jena.de.

▽ Published ahead of print on 5 March 2010.

central core, which is the analogue of the protoplast or germ cell of a growing cell, is surrounded by several protective barriers containing the inner membrane, germ cell wall, cortex outer membrane, and coats. In some species a thin exosporium may also be present. Some exosporia contribute to spore resistance by their mere impermeability to exogenous chemicals or by their ability to react with or detoxify chemical agents. The other characteristics contributing to resistance can be found in the spore core: the low water content (25 to 50% of wet weight), the saturation of spore DNA with a group of unique proteins called α/β-SASP (small acid-soluble spore proteins), or the high mineral content in the form of divalent cations, in particular Ca^{2+}. Most of these cations seem to be chelated by dipicolinic acid (DPA), since calcium dipicolinate (CaDPA), the calcium chelate of dipicolinic acid (2,6-pyridinedicarboxylic acid), accounts for 5 to 15% of the spores' molecular weight (52).

Actually, several inactivation techniques are available, and their efficiencies have been studied intensively. Reliable disintegration of endospores has been achieved by means of heat inactivation (boiling, moist heat, dry heat), radiation (microwave [57], UV [63], gamma, electron beam [16]), desiccation, high pressure (31), and the application of various liquid or gaseous antiseptics and disinfectants (1, 51). Classically, inactivation of endospores is quantified by measuring the (logarithmic) reduction factors in CFU. Less time-consuming are viability assays based on the detection of DPA via luminescence microscopy, where the germination of endospores is triggered and subsequently the released DPA is detected by means of terbium dipicolinate luminescence under UV excitation. The terbium dipicolinate fluorescence method has been described as the most sensitive technique, allowing the determination of nanomolar concentrations of DPA (8).

Unfortunately, none of the methods mentioned above have been tested for their applicability with micro-Raman spectroscopy so far. That fact is the motivation for this work, where we systematically assess a number of well-established methods for the inactivation of pathogenic endospores with regard to sufficient microbial inactivation and appropriate identification on a single-endospore level via micro-Raman spectroscopy.

MATERIALS AND METHODS

***Bacillus* strains.** The following strains were examined in this study: *B. anthracis* 4463, *B. anthracis* 13/38, *Bacillus subtilis* ATCC 6633, *Bacillus mycoides* DSM 299, *Bacillus sphaericus* DSM 1867, *Bacillus thuringiensis* ATCC 10792, and *B. thuringiensis* DSM 350. All but the *B. anthracis* strains, which were provided by the Federal Research Institute for Animal Health (FLI, Jena, Germany), were purchased from the German Collection of Microorganisms and Cell Cultures (DSMZ, Braunschweig, Germany). For the selection of the most suitable inactivation method, spores of the two *Bacillus thuringiensis* strains (DSM 350 and ATCC 10792) and the two *Bacillus anthracis* strains (13/38 and 4463) were used.

Sample preparation. Bacterial cultures were prepared on blood agar plates. From each strain a spore suspension (10^7 spores per ml) was prepared. Briefly, one loop of bacterial mass was inoculated into tryptone glucose broth (TGB), consisting of 2.5 g yeast extract, 5.0 g tryptone, and 1.0 g glucose per 1,000 ml double-distilled water (pH 7.2 ± 0.2; autoclaved at 121°C for 20 min). After incubation at 37°C for 3 days, 1 ml of the inoculated TGB was inoculated onto yeast extract agar consisting of 10.00 g peptone, 2.0 g yeast extract, 0.04 g $MnSO_4$ H_2O, and 15 g agar per 1,000 ml double-distilled water (pH 7.0 ± 0.2; autoclaved at 121°C for 20 min). After cultivation at 37°C for 8 to 10 days, the spores were harvested by washing with 5 ml double-distilled water and centrifugation at 2,500 × *g* for 10 min. The sediment was washed four times using double-distilled water before the suspension was heated at 75°C for 10 min. The spore suspensions were stored at 4°C.

Inactivation. For inactivation of spore suspensions, formaldehyde (F) solutions (Sigma-Aldrich Chemie GmbH, Taufkirchen, Germany) at final concentrations of 10% and 20%, a 0.5% Wofasteril–Alcapur (CH_3COOOH, H_2O_2, CH_3COOH) mixture (Kesla, Bitterfeld-Wolfen, Germany), peracetic acid (PAA) at 1% and 2%, and the household hygiene detergent Danchlorix (NaOCl; Colgate-Palmolive GmbH, Hamburg, Germany), undiluted and at 5%, were tested. As a control, the procedure was conducted using double-distilled water. Furthermore, autoclaving was carried out at 134°C for 1 h.

The inactivation efficacy of each suspension was tested after treatment for 15 min, 30 min, 1 h, 2 h, and 4 h. For the inactivation experiment, 1 ml of the spore suspension was mixed with 9 ml of disinfectant in a 10-ml tube also containing 10 glass beads to achieve the respective final concentration. During the treatment time, the tubes were shaken continuously at 200 rpm in a laboratory shaker (Gerhardt Shaker RO 15). The treatment was stopped by centrifugation at 2,500 × *g* for 10 min. After three additional washing steps, including centrifugation, the sediment was resuspended in 1 ml double-distilled water. For the inactivation control, 100 μl of the suspension was inoculated into TGB, and after 24 h of incubation at 37°C, 100 μl of this broth was inoculated onto blood agar plates. These plates were incubated for 2 days at 37°C to determine if the inactivation of spores was successful.

Spectroscopic instrumentation. The Raman spectroscopic measurements were carried out with two different micro-Raman setups. The Raman spectra for the explorative studies were measured with a micro-Raman spectrometer (LabRam HR system with inverse microscope; Horiba Jobin Yvon). A Compass frequency-doubled Nd:YAG laser (Coherent Inc.) provides the excitation light with a wavelength at 532 nm and a power of 1.5 mW incident on the sample. The integration time for single-endospore Raman spectra was 30 s. A Leica PL Fluotar 100× objective focuses the laser light onto the sample within a focus of less than 1 μm in diameter. The spectrometer has an entrance slit of 100 μm and a focal length of 800 mm and is equipped with a 300-line/mm grating. A charge-coupled device (CCD) camera operating at 220 K is utilized over a range of 298 to 3,373 cm^{-1}. The resolution of the spectra is approximately 10 cm^{-1}.

In order to establish a database of Raman spectra, a second micro-Raman device was employed (Bio Particle Explorer; rap.ID Particle Systems GmbH, Berlin, Germany), that allowed automated measurements of single-cell Raman spectra with an excitation light of 532 nm from a solid-state frequency-doubled Nd:YAG module (LCM-S-111-NNP25; Laser-export Co. Ltd.). An Olympus MPLFLN-BD 100× objective focuses the Raman excitation light onto the sample with a spot size of <1 μm laterally, so that approximately 3.5 mW hits the sample. The integration time per Raman spectrum (276 cm^{-1} to 3,204 cm^{-1}) was 5 s. After removal of the Rayleigh scattering, the 180° back-scattered Raman light is diffracted with a single-stage monochromator (HE 532; Horiba Jobin Yvon) with a 300-line/mm grating and is collected with a thermoelectrically cooled CCD camera (DV401-BV; Andor Technology) with a spectral resolution of ca. 7 cm^{-1}. All of the Raman spectra were collected under ambient conditions.

Electron microscopy. Micrographs of differently treated endospores were obtained with a scanning electron microscope (JSM-6700F; JEOL) operated at 15.0 keV.

Multivariate analysis. For the hierarchical cluster analysis (HCA), the Opus Ident software package, version 6.5 (Bruker Optik GmbH, Ettlingen, Germany), was utilized exclusively. The preprocessing of the spectra comprised the first derivative and vector normalization. The spectral regions between 684 and 1,775 cm^{-1}, as well as those between 2,763 cm^{-1} and 3,194 cm^{-1}, were used for cluster analysis using the squared Euclidian distance and Ward algorithm.

For more-complex calculations, such as self-learning machines, GNU R (41) was used.

The main structure of the chemometric procedure is explained below. Basically, there are three steps: preprocessing, training of the self-learning machines, and validation.

The preprocessing of every data set was always the same. First the cosmic spikes and the backgrounds of the spectra were removed. The latter is necessary because the spectral background differs for different measurements of one particular substance, so it would disturb the training process of the self-learning machines. For this purpose, the SNIP algorithm was adopted (48). Afterwards, vector normalization took place to make the spectra comparable. Here, the spectrum was divided by its 2-norm. With principal-component analysis (PCA) (37), the dimensionality of the problem was reduced and, in addition, white noise was removed by cutting off the scores after a particular channel in the new spectral space. The exact number of scores used depends on the size of the data set. A good choice for the number of scores is to use 2 to 5% of the number of data points. The reduction of the dimensionality of the problem is necessary to avoid overfitting (58).

If a new set of spectra had to be labeled, the preprocessing of this new data set

TABLE 1. Results of inactivation experiments on spores of two *Bacillus thuringiensis* strains and two *Bacillus anthracis* strains[a]

Disinfectant	Growth of spores[b] inactivated at the following time:																			
	15 min				30 min				1 h				2 h				4 h			
	A	B	C	D	A	B	C	D	A	B	C	D	A	B	C	D	A	B	C	D
Formaldehyde																				
10%	+	−	+	+	+	−	+	+	+	−	−	−	−	−	−	−	+	−	−	−
20%	−	−	−	−	−	−	−	−	−	−	−	−	−	−	−	−	−	−	−	−
Danchlorix																				
Undiluted	−	−	−	−	−	−	−	−	−	−	−	−	−	−	−	−	−	−	−	−
5%	+	+	+	+	+	+	+	+	+	+	+	+	+	+	+	+	−	−	−	−
0.5% Wofasteril–Alcapur mixture	+	+	+	+	+	+	−	−	+	+	−	−	+	+	−	−	+	+	−	−
Peracetic acid																				
1%	−	−	−	−	+	−	−	−	+	−	−	−	−	−	−	−	−	−	−	−
2%	−	−	−	−	−	−	−	−	−	−	−	−	−	−	−	−	−	−	−	−
Autoclaving at 134°C	NT	NT	NT	NT	NT	NT	NT	NT	−	−	−	−	NT	NT	NT	NT	NT	NT	NT	NT
Distilled water (control)	+	+	+	+	+	+	+	+	+	+	+	+	+	+	+	+	+	+	+	+

[a] Capital letters represent strains as follows: A, *B. thuringiensis* DSM 350; B, *B. thuringiensis* ATCC 10792; C, *B. anthracis* strain 13/38; D, *B. anthracis* strain 4463.
[b] −, no growth observed after inactivation; +, visible growth observed after inactivation; NT, not tested. The initial spore concentration was 1×10^7 spores per ml.

was the same before PCA. To convert both sets in the same spectral space, we did not perform PCA with the combined data set but rotated the new set by the loadings of the PCA of the first data set into the spectral space of the first data set.

After the preprocessing was done, the classifiers were trained. The binary classifiers investigated are (i) artificial neural networks (ANN) with a feed-forward topology (44), (ii) a support vector machine (SVM) with a radial basis kernel (3), and linear discriminant analysis (LDA) (9).

These binary classifiers are not capable of distinguishing between more than two classes. There are several methods for combining the classifiers so that they can be used as multiclass classifiers. Here the "one-against-the-rest" (OATR) schema is adopted (55). The idea is that every class is separated from the rest by one binary classifier. Afterwards there are n binary classifiers for n classes. If a new spectrum now has to be labeled, it is designated by the respective classifier. If all classifiers put this new spectrum into the "rest" class, this spectrum is labeled as "unknown." The same happens if more than one classifier labels this spectrum as its associated class. An ambiguity results in labeling as "unknown."

If there is more than one classifier, it is possible to combine them by a majority-voting scheme (24), where the basic rule from Kittler (24) is adapted to the novelty detection scheme. If the majority votes for one class, it is labeled with this class; if not, it is labeled as "unknown". This procedure might enhance accuracy, but in some cases it delivers the same or even worse accuracy. This combined classifier is investigated for the purpose of identifying bacterial endospores: the three classifiers (ANN, SVM, and LDA) are combined by this method.

Finally, validation of the chosen classifiers is needed. There are several methods for estimating the quality of a classifier, e.g., hold-out, cross-validation, and bootstrapping (25).

To obtain the best classifier, cross-validation was used, and this accuracy was taken as the accuracy of the classifier. To estimate the generalization error, the hold-out technique was applied. One set of bacteria from each of the *Bacillus* species analyzed is used for training, and another, completely independent batch of the particular strain, which has been cultured separately under exactly the same conditions, is used as the validation set. The hold-out method provides a way to estimate the accuracy of the procedure with the connected database for a real application.

RESULTS

Inactivation results. It is not surprising that the analysis and handling of intentionally released BSL-3 level agents, or their products, require either BSL-3 facilities or complete inactivation if samples from contaminated areas are prepared for dispatch to standard laboratories. Within the scope of the work presented here, we have tested a number of inactivation methods: heat inactivation (autoclaving) and inactivation by formaldehyde (F), peracetic acid (PAA), or sodium hypochlorite. The disinfectants evaluated were chosen according to a selection of valid lists and guidelines with approved disinfectants for spores. For surface disinfection in laboratories and hospitals in Germany, no approved sporicidal disinfectant is available (43, 59). However, the WHO *Guidelines for the Surveillance and Control of Anthrax in Humans and Animals* recommend, for example, the use of formaldehyde and peracetic acid (56). The disadvantages of peracetic acid include its corrosive properties and pungent odor. By the combination of peracetic acid with aluminum hydroxide, e.g., Wofasteril-Alcapur (Kesla, Bitterfeld-Wolfen, Germany), the disinfectant becomes odorless. Because other authors have also shown the sporicidal potency of commercial household products containing sodium hypochlorite bleach against anthrax spores (2), we tested the product Danchlorix (NaOCl; Colgate-Palmolive GmbH, Hamburg, Germany). The most reliable disinfection procedure for spores so far has been autoclaving at 134°C.

The results of the inactivation experiments with spores of *Bacillus thuringiensis* and *Bacillus anthracis* strains are summarized in Table 1. Each entry in the table represents one independent inactivation experiment. It can be seen that the 20% formaldehyde solution, undiluted Danchlorix, and 2% peracetic acid were the most reliable and fastest spore-inactivating substances. Even after the shortest application time of 15 min, all four strains tested exhibited no viability after inactivation with these agents. In some cases, single strains showed higher resistance to the treatment; e.g., only *B. thuringiensis* strain DSM 350 survived parts of the 1% PA treatment. On the other hand, some disinfectants, such as the 10% formaldehyde or 5% Danchlorix treatment, showed time dependency.

Analysis of endospore morphology via electron microscopy. To assess spore morphology and integrity after inactivation via formaldehyde, peracetic acid, or autoclaving, scanning electron microscopic (SEM) images of single *B. thuringiensis* DSM 350

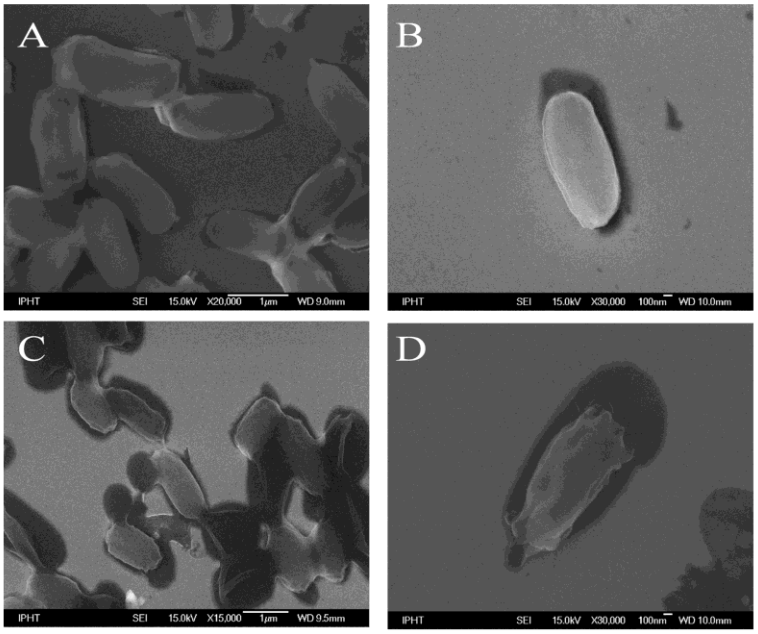

FIG. 1. Electron micrographs of differently treated endospores of *B. thuringiensis* DSM 350. (A) Viable spores not subjected to inactivation treatment; (B) spores inactivated by 20% formaldehyde for 15 min; (C) spores inactivated by 1% peracetic acid for 15 min; (D) spores inactivated by autoclaving at 134°C for 15 min.

endospores were prepared. In Fig. 1A to D, representative images of spores treated by these methods (20% formaldehyde for 15 min [Fig. 1B], 2% peracetic acid for 15 min [Fig. 1C], or 134°C autoclaving for 15 min [Fig. 1D]) are shown in comparison to an image of untreated, viable endospores (Fig. 1A).

Aiming to minimize the ratio of the outer surface to the cell volume, the untreated spores (Fig. 1A) have a roundish shape and a smooth surface.

The most obvious physical changes occurred for the spores when they were exposed to moist heat and pressure through the autoclaving process. They exhibit a wrinkled shape and have obviously lost internal volume, as evidenced by their decreased outer form and the presence of a corona of undifferentiated solids around the spore perimeter. These morphological changes seem to arise from a swelling and splitting of the cells, followed by a subsequent collapsing into a wrinkled form—a behavior well known in the literature (38). During this process, intracellular material might be released, which explains the surrounding undefined material.

The formaldehyde (Fig. 1B)- and PAA (Fig. 1C)-treated cells exhibit greater similarity to native spores. But for the latter (Fig. 1C) it is noteworthy that next to the brighter cells with apparently good structural integrity, some endospores are in contact with dark, roundish, closely attached pools, which seem to originate from outflows from the spores, since the cell wall seems to be cracked open. Nothing like this can be seen in the images of the viable endospores (Fig. 1A). Nevertheless, the absence/presence of an exosporium cannot be verified by these pictures.

Analysis of single-endospore Raman spectra. Apart from characterizing single cells according to their outward morphology by means of SEM, molecular assessment of cells on a single-endospore level can be achieved by means of micro-Raman spectroscopy. Here, the overall composition of the endospores is probed, and by the observation of a few Raman spectra, a first evaluation can easily be made. Furthermore, a more-sophisticated but fast analysis via unsupervised hierarchical cluster analysis (HCA), which pools the spectra by spectral similarity, is performed. A maximum of correspondence between the Raman profiles of inactivated spores and those of viable endospores is desirable. Furthermore, the slight spectral differences, on which the subsequent phenotypic identification is based, should still remain after the treatment with disinfectants.

Since single Raman spectra of viable cells serve as a standard, spectra of native *Bacillus* sp. endospores are shown in Fig. 2. Independently of the species, all spore spectra are dominated by signals that can be assigned to CaDPA: the C—COO^- stretching vibration at 817 cm^{-1}, the symmetric and asymmetric COO^- stretching vibrations at 1,394 cm^{-1} and 1,579 cm^{-1}, three pyridine ring vibrations at 660 cm^{-1}, 1,016 cm^{-1}, and 1,445 cm^{-1}, and the aromatic C—H stretching mode at 3,089 cm^{-1}. Small alterations in the CaDPA band intensities within these species may arise from differences in

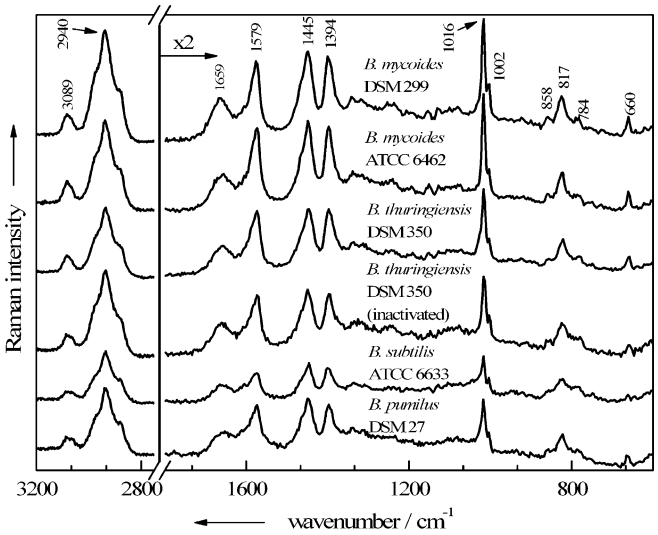

FIG. 2. Single-endospore Raman spectra of untreated viable spores of five different *Bacillus* strains plus one spectrum of a formaldehyde-inactivated *B. thuringiensis* endospore.

the spore composition of the particular culture, emerging, e.g., from fluctuating CaDPA contents in single spores among a population (19). The band positions, on the other hand, remain stable among the spectra; this is not necessarily the case, since the use of divalent manganese as a sporulation accelerator can cause some minor CaDPA band shifts (53).

Except for the $CH_{2/3}$-stretching vibrations at 2,940 cm^{-1}, all bands from the other major biological constituents of the cells exhibit lower intensities but are still clearly recognizable. Some contributions arise exclusively due to proteins (1,002 cm^{-1}, ring breath vibration of phenylalanine; 1,659 cm^{-1}, amide I vibration; 858 cm^{-1}, one of the ring breathing modes of tyrosine) or DNA/RNA moieties (784 cm^{-1}, O—P—O stretching of cytosine/uracil). In addition, some bands of those biomolecules overlap with CaDPA signals, e.g., the second ring breathing mode of tyrosine at 824 cm^{-1} with the carboxylate stretching mode and the deformation mode of $CH_{2/3}$, as well as the ring vibrations of guanine and adenine, which are expected at around 1,450 cm^{-1} and at 1,570 cm^{-1} with the pyridine ring vibrations of the DPA.

All endospores that have been sterilized by autoclaving exhibit the same changes in their Raman spectra. As examples, two mean spectra of *Bacillus mycoides* DSM 299 are shown in Fig. 3: the top spectrum was calculated from 20 single viable endospore spectra, and the middle spectrum from the spectra of 20 single endospores inactivated by autoclaving. The third spectrum represents the subtraction of the inactivated-cell spectrum from the spectrum of one of the viable spores. It can be seen clearly that the spectra of autoclaved endospores are basically devoid of any CaDPA bands, which normally dominate endospore spectra. However, bands from the other major biological constituents of the cells still appear in the spectra of autoclaved cells. Only the amide I vibration at 1,660 cm^{-1} is shifted significantly, to 1,670 cm^{-1}, after autoclaving. This Raman band is highly sensitive to changes in the secondary structures of proteins (60), which most likely occurred during the denaturation and subsequent aggregation due to autoclaving. UV-resonance Raman spectroscopy correlated with X-ray data revealed that the amide I band shows the highest wave numbers in proteins with unordered secondary structures, followed by those with β-sheets and α-helices, respectively (4).

In the bright-field image in the Fig. 4 inset, a small grouping of *B. thuringiensis* endospores, inactivated with 1% peracetic acid for 15 min, is shown. The micro-Raman spectra of the four labeled particles, which exhibit rather similar morphologies, were recorded and are shown in Fig. 4. Raman spectrum A in Fig. 4 represents a typical endospore spectrum, displaying the CaDPA bands mentioned above at 1,016, 1,400, 1,448, and 1,576 cm^{-1}, as well as signals typical of vegetative cells, e.g., the amide I band at 1,661 cm^{-1} and a sharp signal due to the ring vibration of phenylalanine at 1,002 cm^{-1}. To a lesser extent this is also true for spectrum B in Fig. 4, where again the DPA bands occur, but compared to the signals of the other bacterial components, their intensities are considerably decreased. The Raman spectrum of particle C (Fig. 4) shows almost no CaDPA bands any more, suggesting that a leakage of intracellular components, including CaDPA, took place. Although particle D is not phenotypically different from the others, its Raman spectrum does not resemble the other Raman spectra: none of the CaDPA or protein marker bands mentioned above for either vegetative cells or endospores appears. Instead, the Raman spectrum is representative of poly(3-hydroxybutyrate) (PHB), a biodegradable polymer that can be produced by certain bacteria in large amounts in re-

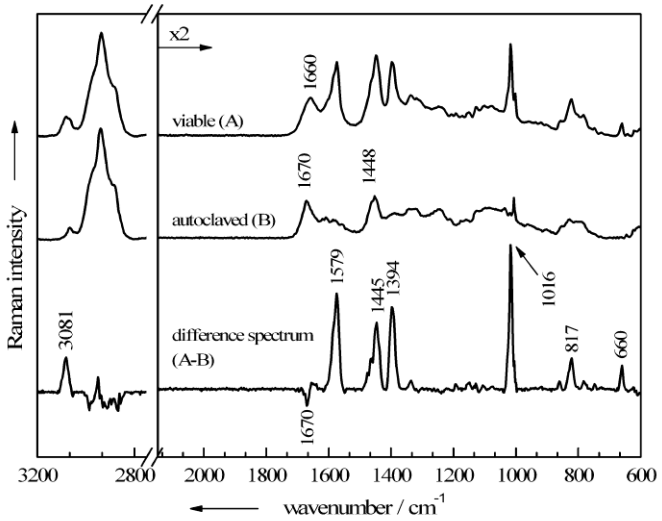

FIG. 3. Baseline-corrected mean Raman spectra, each calculated from 20 single-endospore spectra of *B. mycoides* DSM 299. Shown are spectra for viable, untreated spores (A) and spores inactivated via autoclaving (B), as well as a difference spectrum (A-B).

sponse to physiological stress (21). Recent work dealing with the analysis of microbial PHB by Raman spectroscopy has been published (7, 18) and allows for a rather complete band assignment. The bands at 3,000, 2,969, 2,932, and 2,876 cm^{-1} all arise from different $CH_{2/3}$-streching vibrations of the polymer; the 1,724-cm^{-1} band is assignable to the C═O stretching vibration of both crystalline and amorphous PHB. In the lower-wave-number region, the most intense signals, at 1,056 and 838 cm^{-1}, are also important hallmarks for this polyester and can be assigned to the C—O and the C—COO stretching vibrations, respectively.

This effect of finding PHB particles beside intact spores is

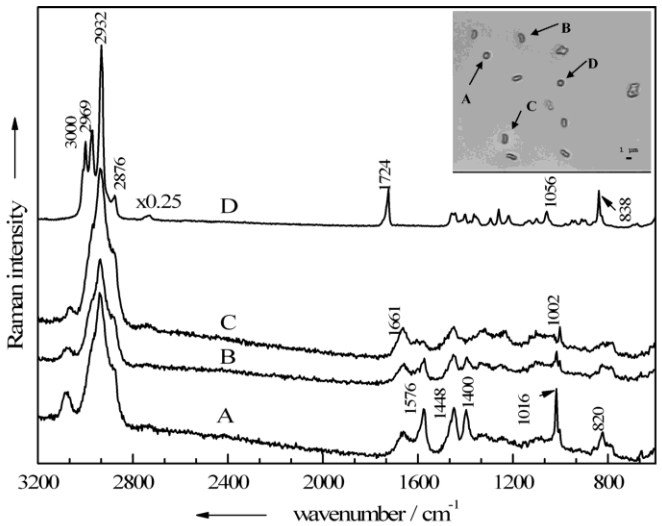

FIG. 4. Single-particle Raman spectra of four particles present in a *B. thuringiensis* DSM 350 endospore suspension treated with 1% peracetic acid for 15 min. (Inset) Corresponding bright-field image of the analyzed particles A to D.

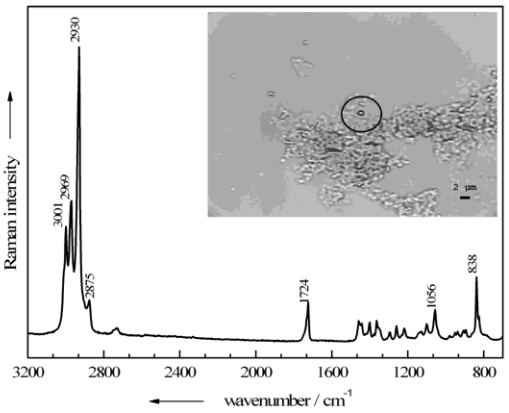

FIG. 5. Raman spectrum of a single particle found in a *B. thuringiensis* DSM 350 endospore suspension treated with 1:20-diluted Danchlorix. (Inset) Bright-field image with the corresponding particle circled.

also observed when the spores are treated with a higher concentration of PAA for longer periods. This has been verified by analyzing two *B. thuringiensis* and *B. anthracis* endospore suspensions after treatment with 1% or 2% PAA for 15, 30, 60, 120, or 240 min. For each sample, 30 single cells were measured, and roughly 20% were free of CaDPA after the suspensions had been treated for 15 or 30 min. After a 1-h exposure to PAA, nearly half of the cells seemed to be depleted of the DPA salt, and after 2 and 4 h, not a single intact endospore could be detected, and all cells gave spectra like spectrum C in Fig. 4. There is no difference between suspensions exposed to different concentrations of PAA (1% or 2%); even after treatment for 2 h with 1% PAA, all cells were depleted of the DPA salt. Therefore, this biocide not only affects the cells unevenly but also differs strongly in its effect according to the treatment time.

The sodium hypochlorite-containing bleaching agent Danchlorix presents a more uniform but also undesirable effect on the endospores. Even when Danchlorix was diluted 1:20, and after a short exposure time, not a single cell was left for Raman measurements according to the bright-field image. As shown in the Fig. 5 inset, only broad patterns of unidentifiable material could be found next to just a few single particulate entities, which turned out, again, to be PHB accumulations. The Raman spectrum of one of these deposits (circled) is shown in Fig. 5.

In contrast to the results with these two biocides, the interaction of formaldehyde with the endospores yields inactivated cells whose Raman spectra correspond well with those of native endospores without exception—no matter how long (15 to 240 min) the treatment and how high the concentration of formaldehyde (10% or 20%). In Fig. 2, a Raman spectrum of a single formaldehyde-inactivated *B. thuringiensis* endospore is shown in order to demonstrate its striking similarity with the spectra of untreated cells. It shows no remarkable changes, such as relative intensity variations or even the appearance of new signals, in the spectral profile.

Evaluation of the inactivation methods. The Raman spectra were analyzed more thoroughly by performing HCA on an ensemble of differently treated endospores of *B. thuringiensis* DSM 350. This ensemble included cells inactivated by autoclaving or by treatment with 2% PAA or 20% formaldehyde. These inactivated species were chosen because, as Table 1 shows, only 2% PAA and 20% formaldehyde treatments guaranteed consistent inactivation of *B. thuringiensis* DSM 350 endospores after a 30-min exposure. Additionally, some spectra of viable endospores were added in order to determine which—if any—of the inactivation methods results in endospores whose Raman spectra are most similar to those of viable endospores. The resultant dendrogram is shown in Fig. 6. For most of the samples, all 40 Raman spectra of the same sample are grouped in the same cluster. The five outliers (asterisked) all belong to formaldehyde-treated spectra, which are wrongly classified into the cluster of untreated endospores. All in all, of 160 spectra, 155 (96.7%) are correctly classified.

Two major groups, subdivided into three and two subclusters, respectively, can be identified in the dendrogram. One main cluster comprises spectra of formaldehyde- or PAA-treated endospores or viable endospores. The second main cluster is composed of spectra of endospores inactivated by means of autoclaving or PAA. Each of the five distinguishable subclusters can be explained according to the mean spectra shown in Fig. 6. All spectra devoid of CaDPA signals are assigned to the same main cluster. This is true for all of the autoclaved samples and a fraction of the PAA-treated samples. Interestingly, the remaining spectral information for these obviously severely altered endospores is prominent enough to produce a clear partition according to the inactivation procedure.

In the other main cluster, the second partition of the PAA-treated endospores can be located next to the joint cluster of the formaldehyde-inactivated and native endospores, suggesting that among the biocide treatments examined, inactivation with formaldehyde causes the fewest spectral changes from the spectra of viable endospores. Thus, the occurrence in the dendrogram of the five formaldehyde-inactivated endospores falsely classified as native endospores is tolerable and emphasizes the high similarity of the spectra of the two kinds of samples.

Although the mean spectrum of the PAA-treated endospores that still contain CaDPA in Fig. 6 shows high similarity to the spectra of viable cells, slight distinctions that appear reproducibly among all spectra of the sample seem to be more pronounced than those for formaldehyde-treated cells. Additionally, roughly one-third of the PAA-treated cells were sorted out into the other main cluster together with the autoclaved cells. According to the cluster spectrum that is second from the bottom in Fig. 6, these Raman spectra emerge from CaDPA-depleted endospores; thus, due to their weak resemblance to the spectra of viable endospores, they are not suitable for identification purposes and have to be discarded.

Single-cell identification. To assess whether the use of formaldehyde on endospores has a great impact on the possibility of distinguishing and identifying *Bacillus* endospores to the species level, the following data set was created: from each of four

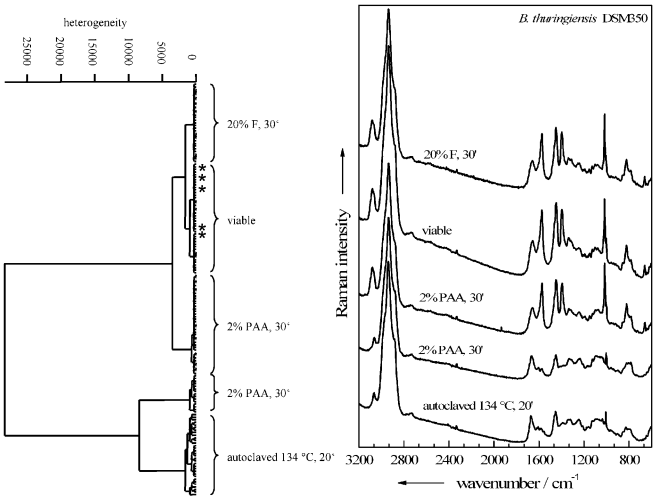

FIG. 6. Dendrogram obtained from a hierarchical cluster analysis performed on Raman spectra of differently treated single endospores of *B. thuringiensis* DSM 350. Shown are the Raman spectra (right) and dendrogram (left) for viable, untreated cells and for endospores inactivated either by 20% formaldehyde for 30 min (20% F, 30′), by 2% peracetic acid for 30 min (2% PAA, 30′), or by autoclaving at 134°C for 20 min (134°C, 20′). Asterisks mark wrongly classified spectra.

Bacillus strains (*Bacillus mycoides* DSM 299, *Bacillus subtilis* ATCC 6633, *Bacillus sphaericus* DSM 1867, and *Bacillus thuringiensis* DSM 350), four independent batches were prepared under the same conditions. Afterwards, two of the four batches per strain were inactivated with 20% formaldehyde for 2 h, while the other two remained viable. With one batch of viable endospores per strain, a reference or training database for viable spores was established by measuring approximately 100 single-endospore Raman spectra per strain. The same was done with four batches of inactivated endospores, one per strain. Thus, each of the databases, one for the viable and one for the inactivated spores, comprised roughly 400 Raman spectra. Based on these, the other four batches of viable spores and the four samples with the inactivated endospores were identified according to their taxa. Therefore, nearly 30 endospore Raman spectra were recorded for each sample, and each of them was identified to the species level by comparing the spectra to the appropriate database: if they had been inactivated, they were compared to the training database of inactivated spores, and if they had not been treated, the database of viable spores was used.

Tables 2 to 5 summarize the results obtained by using different classifiers for untreated native endospores versus formaldehyde-inactivated endospores. For the untreated-spore data set the first 9 scores were used, and for the inactivated-spore data set the first 10 scores were used, whereas the data set was not centered or scaled by channel before the PCA.

The results of the cross-validation with the associated confusion table for the viable endospores are listed in Table 2. The rows of the tables show the species identifications predicted by each classifier investigated, and the columns show the actual species identified. As can be seen, all three classifiers achieved accuracies in comparable dimensions, around 99%, for viable endospores. Table 3 shows analogous data for endospores in-

TABLE 2. Confusion table showing the accuracy each classifier[a] after the classification of four untreated native *Bacillus* species in the training data set[b]

Identification predicted by classifier	No. of spectra actually classified as indicated, grouped by classifier											
	ANN				SVM				LDA			
	B. mycoides	*B. sphaericus*	*B. subtilis*	*B. thuringiensis*	*B. mycoides*	*B. sphaericus*	*B. subtilis*	*B. thuringiensis*	*B. mycoides*	*B. sphaericus*	*B. subtilis*	*B. thuringiensis*
Unknown	0	0	1	2	0	0	0	2	0	0	1	3
B. mycoides	137	0	0	0	139	0	0	1	138	0	0	0
B. sphaericus	0	87	0	0	0	86	0	0	0	86	0	0
B. subtilis	0	0	70	0	0	0	72	0	0	0	71	0
B. thuringiensis	2	0	0	121	0	0	0	120	0	0	0	121

[a] The accuracy of each classifier for viable endospores was 99%.
[b] The species used were *B. mycoides* DSM 299, *B. sphaericus* DSM 1867, *B. subtilis* ATCC 6633, and *B. thuringiensis* DSM 350.

TABLE 3. Confusion table showing the accuracy of each classifier after the classification of four 20% formaldehyde-inactivated *Bacillus* species in the training data set

Identification predicted by classifier	No. of spectra actually classified as indicated, grouped by classifier (% accuracy)											
	ANN (83)				SVM (89)				LDA (84)			
	B. mycoides	*B. sphaericus*	*B. subtilis*	*B. thuringiensis*	*B. mycoides*	*B. sphaericus*	*B. subtilis*	*B. thuringiensis*	*B. mycoides*	*B. sphaericus*	*B. subtilis*	*B. thuringiensis*
Unknown	16	2	0	21	11	2	1	11	17	2	2	21
B. mycoides	153	0	1	21	166	0	0	16	157	0	0	25
B. sphaericus	2	111	0	1	0	110	0	0	1	110	0	0
B. subtilis	2	0	97	1	0	0	96	0	0	0	92	0
B. thuringiensis	13	0	0	39	9	1	0	57	12	1	1	39

activated by 20% formaldehyde. Although the accuracies of the classifiers are decreased to 81 to 89%, none of the classifiers is superior to the other two with respect to the classification rate. Most of the false species identifications were mix-ups between the *B. mycoides* and *B. thuringiensis* spectra, especially for the ANN results. However, spectra classified as unknown are not necessarily false-positive results.

After the classifiers were trained with the training data set, the spectra of the second batch were labeled. The accuracy of identification and the associated confusion table for untreated endospores are presented in Table 4, and the analogous data for formaldehyde-inactivated endospores are shown in Table 5. The last columns list the combined results of all three classifiers. Here, the majority voting scheme, discussed above, was employed: in case of a majority vote for one class, the spectrum is assigned to this class; otherwise, it is put into the "unknown" class.

It is obvious that for both native and inactivated endospores, the identification rate lies in the same range, around 81 to 83%, for all of the classifiers. The formaldehyde treatment does not seem to have a negative impact on the identification results. Nevertheless, most of the spectra that were incorrectly identified or were not identified at all were those of *B. thuringiensis*, which were frequently mixed up with *B. mycoides* spectra. It is known from the nucleotide sequences of the 150-bp 3′-end 16S rRNA genes, as well as from those of the 70-bp 5′ 16S–23S internal transcribed spacer (ITS) region, that the two species are phylogenetically very similar (61). Indeed, their phenotypic and genotypic similarities recently led to a proposal to regroup them, together with *B. anthracis* and *Bacillus cereus*, into a single species (17).

DISCUSSION

Fast and reliable inactivation of bacterial endospores can be achieved with a great variety of different antiseptics and disinfectants. Most of the sporicidal agents provoke lysis and leakage of intracellular constituents by degrading most of the permeability barriers, which play different roles in the endospore's resistance. The various layers of proteinaceous spore coats, which surround the spore cortex, protect the spore from attacks by a large number of chemicals, particularly oxidizing agents such as hydrogen peroxide, sodium hypochlorite, chlorine dioxide, or ozone (52). Smaller hydrophobic and hydrophilic molecules are hindered on their way to the core by the extremely low permeability of the spore's inner membrane (36).

Most of the oxidizing agents, strong acids, and ethanol kill spores by causing some type of damage to the spore's permeability barriers, such that when the treated spores germinate, these damaged membranes rupture, resulting in spore death (36, 51). For some of the oxidizing agents, the location of damage could be pinpointed to the endospore's inner membrane (5); for others, only a general disruption of spore permeability barriers is reported. Interestingly, Cortezzo et al. found out that spore inactivation via a variety of oxidizing agents is not accompanied by loss of DPA (5), whereas acid-inactivated spores extrude DPA and other fibrillar material, including DNA (51). In addition, pretreatment with oxidizing agents makes the surviving spores more sensitive to inactivation by normally nonlethal heat and osmotic stresses in the presence of high salt concentrations in plating media.

These findings are in good agreement with the results we obtained by using PAA as a disinfectant. Among other peroxides, peracetic acid is frequently used in common disinfection procedures and is considered to be a more potent biocide than hydrogen peroxide. As with hydrogen peroxide, the hydroxyl radical appears to be of prime importance, and its inactivation mechanism is based not on DNA damage but rather on a weakening of the endospore's inner membrane by disrupting sulfhydryl (—SH) and sulfur (S—S) bonds of proteins (32, 33). As shown in Fig. 4 and in the dendrogram in Fig. 6, this internal damage only partially forces the spores to extrude core material, since most of the endospores remained intact and retained intracellular DPA after a short treatment (15 min) with highly diluted PAA (1%). The leakage is more pronounced at higher PAA concentrations (2%) and with longer exposure times (>1 h). Furthermore, the probability of measuring not only intact or harmed endospores but also metabolites of the vegetative cells increased with the inactivation time and PAA concentration, as shown in Fig. 4. According to these results, not a microbial cell but a residue of formerly intracellular granules of PHB has been measured. When PHB-producing cells die, PHB is released into the environment, where it is transformed into a denatured semicrystalline state (21).

In case of the chlorine-releasing product Danchlorix, the complete spore lysis we observed was also achieved in other studies with sodium hypochlorite (28). In those studies, loss of refractivity, separation of the spore coats from the cortex,

TABLE 4. Confusion table showing the accuracy of each classifier and of the combination of all classifiers after the identification of four untreated native *Bacillus* species in the hold-out data set

Identification predicted by classifier	No. of spectra actually identified as indicated, grouped by classifier (% accuracy)																	
	ANN (82)				SVM (81)				LDA (81)				All classifiers combined (83)					
	B. mycoides	*B. sphaericus*	*B. subtilis*	*B. thuringiensis*	*B. mycoides*	*B. sphaericus*	*B. subtilis*	*B. thuringiensis*	*B. mycoides*	*B. sphaericus*	*B. subtilis*	*B. thuringiensis*	*B. mycoides*	*B. sphaericus*	*B. subtilis*	*B. thuringiensis*
Unknown	8	2	3	9	9	0	0	1	16	0	2	10	13	0	3	7
B. mycoides	48	0	0	7	43	0	0	6	39	0	0	1	43	0	0	4
B. sphaericus	0	73	0	0	0	75	1	0	1	75	1	0	0	75	1	0
B. subtilis	0	0	35	0	1	0	27	0	0	0	35	0	0	0	34	0
B. thuringiensis	7	0	0	10	10	0	10	19	7	0	0	15	7	0	0	15

extensive discharge of Ca^{2+}, dipicolinic acid, and DNA/RNA, and finally lysis occurred.

Inactivation of endospores by wet heat had the same depleting effect. Here again, not the DNA but proteins are assumed to be the target (36), explaining the shift of the amide III band in the observed Raman spectra of Fig. 3. This is confirmed by previous work (38), where alterations of amide I and amide II bands due to autoclaving could be monitored by means of Fourier transform infrared spectroscopy (FT-IR), and where the absorption band at 1,570 cm^{-1}, a diagnostic band for DPA, was lost, as shown in Fig. 3. Since the major part of this salt is deposited in the core of endospores, these ruptures due to autoclaving-induced cleavage of endospores seem to reach into the inner part of the cell, where most spore enzymes, as well as DNA, ribosomes, and tRNA, are located. Thus, not only denaturation of macromolecules and subcellular structures, including proteins, cytoplasmic membranes, and nucleic acids, occurs during autoclaving, but also a major loss of those biomolecules, as well as the ubiquitous DPA salt, takes place.

This method of extracting soluble microbial proteins can be beneficial for some analysis methods that rely on those proteins as biomarkers, e.g., for the matrix-assisted laser desorption–time-of-flight (MALDI-TOF)/intact-cell mass spectrometry (ICMS) methodology (29). But unlike these approaches, Raman spectroscopy does not analyze bulk samples or fractions thereof but intact single cells.

That is why all the types of chemical agents discussed above are inappropriate for the purpose of identifying bacterial spores by means of Raman spectroscopy, since retaining the structural integrity and most of the biochemical composition of single cells is a necessity for micro-Raman-based identification of inactivated pathogenic endospores. The considerable alterations of spore integrity by PAA, Danchlorix, and autoclaving obviously have a nonnegligible impact on the Raman spectra of the endospores, which coincide with a loss of information in the Raman spectra and thus with decreased identification accuracy. Additionally, the homogeneity of the inactivation treatment has to be guaranteed. The achievement of a maximum of uniformity among the sterilized cells is another important objective, since chemotaxonomic classification relies mainly on constantly recurring spectral patterns among an ensemble of single-cell spectra. If the inactivation treatment alters cells of the same species differently and thus decreases the uniformity of the respective spectra, these Raman data are less useful for building up a database for supervised identification routines. Alternatively, the database might comprise all the inactivation-induced spectral variances, but then it would probably gain a dimension of enormous extent.

Formaldehyde is also employed for a variety of decontamination processes, since it is sporicidal (49). Loshon et al. achieved a 99% killing rate for *B. subtilis* endospores in 40 min at 30°C with 25 g/liter formaldehyde (30). Endospores are inactivated by formaldehyde due to some unique features of this molecule. This small molecule can pass through all the protective layers to advance directly into the core of the endospore. There the genotoxic properties of formaldehyde take effect, causing spore inactivation at least in part by DNA damage; protein-DNA cross-linking is proposed to be one mutagenic mechanism of formaldehyde (30). However, the precise nature of the DNA damage is as yet unknown. The major

resistance mechanisms of spores against formaldehyde are the saturation of spore DNA with α/β-SASPs and the *recA*-encoded repair pathway, which can repair at least some of the formaldehyde-induced lesions in DNA (36). The interaction of formaldehyde with proteins might also give rise to degradation of the spore integuments, but apparently not to such an extent that spore core material is released.

For the purposes of Raman spectroscopy, the use of formaldehyde to inactivate endospores is superior to any of the other treatments analyzed in this work. The inactivation experiments suggest the usage of this agent as a sporicide, since reliable, strain-independent, and fast inactivation of the *Bacillus* strains analyzed was achieved. It was shown by Raman spectroscopy that the formaldehyde inactivation technique is suitable for obtaining reproducible Raman spectra.

Possible reasons for competing intraspecies varieties in the Raman spectra are manifold, e.g., the preparation/inactivation process might induce spectral variances on the single-cell level, as can be seen in the case of PAA-inactivated endospores; cultivation parameters, such as growth time, temperature, and nutritional conditions, which have an impact on whole batches, are also factors to be reckoned with (14, 20). According to our results shown in Tables 4 and 5, at least the formaldehyde-induced inhomogeneities can be neglected, since all four different *Bacillus* strains were chemotaxonomically identified with the help of other, independently cultivated batches of the same strains grown under the same cultivation conditions. The interspecies distinctions are obviously still high enough to obtain satisfactory identification rates for different *Bacillus* species, which serve as *B. anthracis* models. This is noteworthy insofar as only a very limited model database was used, comprising just four different *Bacillus* species. The comparison between the accuracies of the cross-validation and the hold-out techniques for the bacterial database shows that the main problem of our current evaluation method is overfitting. Accuracy decreases if a trained classifier is adopted to an independent data set. This can be avoided by building a database up out of more than one batch and more data. But even with a larger and more diverse database, preprocessing and, most importantly, dimension reduction is necessary.

For anthrax detection, evaluation of as many different *B. anthracis* strains as possible, as well as genetic near neighbors, is mandatory. Currently, we are elaborating a micro-Raman-based procedure for the identification of *B. anthracis* strains inactivated with 20% formaldehyde according to the procedure described here.

Taken together, the results of this study showed that detection of the anthrax agent, isolated from real-world samples, via micro-Raman spectroscopy can be a reliable alternative for fast point-of-care testing. On-site diagnosis is ensured by inactivating the samples with the formaldehyde treatment described in this study, which is compatible with the micro-Raman identification approach. Further investigations should aim at analyzing possible interference due to, e.g., the influence of the native surrounding matrices or the isolation procedure. Additionally, efforts should be focused on the question of whether the inactivation efficacy of formaldehyde is reduced due to matrix effects.

TABLE 5. Confusion table showing the accuracy of each classifier and of the combination of all classifiers after the identification of four 20% formaldehyde-inactivated *Bacillus* species in the hold-out data set

Identification predicted by classifier	No. of spectra actually identified as indicated, grouped by classifier (% accuracy)																	
	ANN (83)				SVM (80)				LDA (80)				All classifiers combined (82%)					
	B. mycoides	*B. sphaericus*	*B. subtilis*	*B. thuringiensis*	*B. mycoides*	*B. sphaericus*	*B. subtilis*	*B. thuringiensis*	*B. mycoides*	*B. sphaericus*	*B. subtilis*	*B. thuringiensis*	*B. mycoides*	*B. sphaericus*	*B. subtilis*	*B. thuringiensis*		
Unknown	4	1	5	3	5	0	1	5	6	0	7	6	5	1	4	7		
B. mycoides	53	0	0	15	47	2	1	10	52	0	0	13	52	0	0	11		
B. sphaericus	0	74	1	0	2	73	4	1	1	75	3	0	1	74	3	0		
B. subtilis	0	0	32	0	0	0	32	1	0	0	28	0	0	0	31	0		
B. thuringiensis	6	0	0	8	9	0	0	9	4	0	0	7	5	0	0	8		

ACKNOWLEDGMENTS

Funding of the research projects "Pathosafe" FKZ 13N9547 and FKZ 13N9549 from the Federal Ministry of Education and Research, Germany (BMBF), is gratefully acknowledged.

We also thank Franka Jahn (Institute of Photonic Technology, Germany) for performing the EM experiment and Katja Fischer (Friedrich Loeffler Institute, Germany) for doing the inactivation experiments.

REFERENCES

1. **Baron, P. A., C. F. Estill, J. K. Beard, M. J. Hein, and L. Larsen.** 2007. Bacterial endospore inactivation caused by outgassing of vaporous hydrogen peroxide from polymethyl methacrylate (Plexiglas). Lett. Appl. Microbiol. **45:**485–490.
2. **Black, D. G., T. M. Taylor, H. J. Kerr, S. Padhi, T. J. Montville, and P. M. Davidson.** 2008. Decontamination of fluid milk containing Bacillus spores using commercial household products. J. Food Prot. **71:**473–478.
3. **Burges, C. J. C.** 1998. A tutorial on support vector machines for pattern recognition. Data Mining Knowledge Discov. **2:**121–167.
4. **Chi, Z., X. G. Chen, J. S. W. Holtz, and S. A. Asher.** 1998. UV resonance Raman-selective amide vibrational enhancement: quantitative methodology for determining protein secondary structure. Biochemistry **37:**2854–2864.
5. **Cortezzo, D. E., K. Koziol-Dube, B. Setlow, and P. Setlow.** 2004. Treatment with oxidizing agents damages the inner membrane of spores of Bacillus subtilis and sensitizes spores to subsequent stress. J. Appl. Microbiol. **97:** 838–852.
6. **De Gelder, J., P. Scheldeman, K. Leus, M. Heyndrickx, P. Vandenabeele, L. Moens, and P. De Vos.** 2007. Raman spectroscopic study of bacterial endospores. Anal. Bioanal. Chem. **389:**2143–2151.
7. **De Gelder, J., D. Willemse-Erix, M. J. Scholtes, J. I. Sanchez, K. Maquelin, P. Vandenabeele, P. De Boever, G. J. Puppels, L. Moens, and P. De Vos.** 2008. Monitoring poly(3-hydroxybutyrate) production in Cupriavidus necator DSM 428 (H16) with Raman spectroscopy. Anal. Chem. (Washington, DC) **80:**2155–2160.
8. **Fichtel, J., J. Koester, J. Rullkoetter, and H. Sass.** 2007. Spore dipicolinic acid contents used for estimating the number of endospores in sediments. FEMS Microbiol. Ecol. **61:**522–532.
9. **Fisher, R.** 1936. The use of multiple measurements in taxonomic problems. Ann. Eugenics **7:**179–188.
10. **Gaus, K., P. Rösch, R. Petry, K.-D. Peschke, O. Ronneberger, H. Burkhardt, K. Baumann, and J. Popp.** 2006. Classification of lactic acid bacteria with UV-resonance Raman spectroscopy. Biopolymers **82:**286–290.
11. **Ghiamati, E., R. Manoharan, W. H. Nelson, and J. F. Sperry.** 1992. UV resonance Raman spectra of Bacillus spores. Appl. Spectrosc. **46:**357–364.
12. **Guicheteau, J., L. Argue, D. Emge, A. Hyre, M. Jacobson, and S. Christesen.** 2008. Bacillus spore classification via surface-enhanced Raman spectroscopy and principal component analysis. Appl. Spectrosc. **62:**267–272.
13. **Harz, M., M. Kiehntopf, S. Stöckel, P. Rösch, E. Straube, T. Deufel, and J. Popp.** 2009. Direct analysis of clinical relevant single bacterial cells from cerebrospinal fluid during bacterial meningitis by means of micro-Raman spectroscopy. J. Biophotonics **2:**70–80.
14. **Harz, M., P. Rösch, K. D. Peschke, O. Ronneberger, H. Burkhardt, and J. Popp.** 2005. Micro-Raman spectroscopic identification of bacterial cells of the genus Staphylococcus and dependence on their cultivation conditions. Analyst **130:**1543–1550.
15. **Harz, M., P. Rösch, and J. Popp.** 2009. Vibrational spectroscopy—a powerful tool for the rapid identification of microbial cells at the single-cell level. Cytometry A **75:**104–113.
16. **Helfinstine, S. L., C. Vargas-Aburto, R. M. Uribe, and C. J. Woolverton.** 2005. Inactivation of bacillus endospores in envelopes by electron beam irradiation. Appl. Environ. Microbiol. **71:**7029–7032.
17. **Helgason, E., O. A. Okstad, D. A. Caugant, H. A. Johansen, A. Fouet, M. Mock, I. Hegna, and A.-B. Kolsto.** 2000. Bacillus anthracis, Bacillus cereus, and Bacillus thuringiensis—one species on the basis of genetic evidence. Appl. Environ. Microbiol. **66:**2627–2630.
18. **Hermelink, A., A. Brauer, P. Lasch, and D. Naumann.** 2009. Phenotypic heterogeneity within microbial populations at the single-cell level investigated by confocal Raman microspectroscopy. Analyst **134:**1149–1153.
19. **Huang, S.-S., D. Chen, P. L. Pelczar, V. R. Vepachedu, P. Setlow, and Y.-Q. Li.** 2007. Levels of Ca2+-dipicolinic acid in individual Bacillus spores determined using microfluidic Raman tweezers. J. Bacteriol. **189:**4681–4687.
20. **Hutsebaut, D., K. Maquelin, P. De Vos, P. Vandenabeele, L. Moens, and G. J. Puppels.** 2004. Effect of culture conditions on the achievable taxonomic resolution of Raman spectroscopy disclosed by three Bacillus species. Anal. Chem. **76:**6274–6281.
21. **Jendrossek, D., and R. Handrick.** 2002. Microbial degradation of polyhydroxyalkanoates. Annu. Rev. Microbiol. **56:**403–432.
22. **Kalasinsky, K. S., T. Hadfield, A. A. Shea, V. F. Kalasinsky, M. P. Nelson, J. Neiss, A. J. Drauch, G. S. Vanni, and P. J. Treado.** 2007. Raman chemical imaging spectroscopy reagentless detection and identification of pathogens: signature development and evaluation. Anal. Chem. **79:**2658–2673.
23. **Kirschner, C., K. Maquelin, P. Pina, N. A. N. Thi, L. P. Choo-Smith, G. D. Sockalingum, C. Sandt, D. Ami, F. Orsini, S. M. Doglia, P. Allouch, M. Mainfait, G. J. Puppels, and D. Naumann.** 2001. Classification and identification of enterococci: a comparative phenotypic, genotypic, and vibrational spectroscopic study. J. Clin. Microbiol. **39:**1763–1770.
24. **Kittler, J.** 1998. Combining classifiers: a theoretical framework. Pattern Anal. Appl. **1:**18–27.
25. **Kohavi, R.** 1995. A study of cross-validation and bootstrap for accuracy estimation and model selection, p. 1137–1143. *In* Proceedings of the 14th International Joint Conference on Artificial Intelligence, vol. 2. Morgan Kaufmann Publishers Inc., San Francisco, CA.
26. **Krause, M., B. Radt, P. Rösch, and J. Popp.** 2007. The investigation of single bacteria by means of fluorescence staining and Raman spectroscopy. J. Raman Spectrosc. **38:**369–372.
27. **Krause, M., P. Rösch, B. Radt, and J. Popp.** 2008. Localizing and identifying living bacteria in an abiotic environment by a combination of Raman and fluorescence microscopy. Anal. Chem. **80:**8568–8575.
28. **Kulikovsky, A., H. S. Pankratz, and H. L. Sadoff.** 1975. Ultrastructural and chemical changes in spores of Bacillus cereus after action of disinfectants. J. Appl. Bacteriol. **38:**39–46.
29. **Lasch, P., H. Nattermann, M. Erhard, M. Staemmler, R. Grunow, N. Bannert, B. Appel, and D. Naumann.** 2008. MALDI-TOF mass spectrometry compatible inactivation method for highly pathogenic microbial cells and spores. Anal. Chem. **80:**2026–2034.
30. **Loshon, C. A., P. C. Genest, B. Setlow, and P. Setlow.** 1999. Formaldehyde kills spores of Bacillus subtilis by DNA damage and small, acid-soluble spore proteins of the alpha/beta-type protect spores against this DNA damage. J. Appl. Microbiol. **87:**8–14.
31. **Margosch, D., M. G. Gaenzle, M. A. Ehrmann, and R. F. Vogel.** 2004. Pressure inactivation of Bacillus endospores. Appl. Environ. Microbiol. **70:** 7321–7328.
32. **Marquis, R. E., G. C. Rutherford, M. M. Faraci, and S. Y. Shin.** 1995. Sporicidal action of peracetic acid and protective effects of transition metal ions. J. Ind. Microbiol. **15:**486–492.
33. **McDonnell, G., and A. D. Russell.** 1999. Antiseptics and disinfectants: activity, action, and resistance. Clin. Microbiol. Rev. **12:**147–179.
34. **Naumann, D.** 2000. Infrared spectroscopy in microbiology, p. 102–131. *In* R. A. Meyers (ed.), Encyclopedia of analytical chemistry. John Wiley & Sons, Chichester, United Kingdom.
35. **Nelson, W. H., R. Dasari, M. Feld, and J. F. Sperry.** 2004. Intensities of calcium dipicolinate and Bacillus subtilis spore Raman spectra excited with 244 nm light. Appl. Spectrosc. **58:**1408–1412.
36. **Nicholson, W. L., N. Munakata, G. Horneck, H. J. Melosh, and P. Setlow.** 2000. Resistance of Bacillus endospores to extreme terrestrial and extraterrestrial environments. Microbiol. Mol. Biol. Rev. **64:**548–572.
37. **Pearson, K.** 1901. On lines and planes of closest fit to systems of points in space. Philos. Mag. **2:**559–572.
38. **Perkins, D. L., C. R. Lovell, B. V. Bronk, B. Setlow, P. Setlow, and M. L. Myrick.** 2004. Effects of autoclaving on bacterial endospores studied by Fourier transform infrared microspectroscopy. Appl. Spectrosc. **58:**749–753.
39. **Pestov, D., X. Wang, G. O. Ariunbold, R. K. Murawski, V. A. Sautenkov, A. Dogariu, A. Sokolov, and M. O. Scully.** 2008. Single-shot detection of bacterial endospores via coherent Raman spectroscopy. Proc. Natl. Acad. Sci. U. S. A. **105:**422–427.
40. **Petrov, G. I., R. Arora, V. V. Yakovlev, X. Wang, A. V. Sokolov, and M. O. Scully.** 2007. Comparison of coherent and spontaneous Raman microspectroscopies for noninvasive detection of single bacteria endospores. Proc. Natl. Acad. Sci. U. S. A. **104:**7776–7779.
41. **R Development Core Team.** 2008. R: a language and environment for statistical computing. R Foundation for Statistical Computing, Vienna, Austria.
42. **Read, T. D., S. L. Salzberg, M. Pop, M. Shumway, L. Umayam, L. Jiang, E. Holtzapple, J. D. Busch, K. L. Smith, J. M. Schupp, D. Solomon, P. Keim, and C. M. Fraser.** 2002. Comparative genome sequencing for discovery of novel polymorphisms in Bacillus anthracis. Science **296:**2028–2033.
43. **Robert Koch-Institut.** 2007. Liste der vom Robert Koch-Institut geprüften und anerkannten Desinfektionsmittel und -verfahren Stand vom 31.5.2007 (15. Ausgabe). Bundesgesundheitsblatt Gesundheitsforschung Gesundheitsschutz **50:**1335–1356.
44. **Rojas, R.** 1996. Neural networks: a systematic introduction. Springer, Berlin, Germany.
45. **Rösch, P., M. Harz, K.-D. Peschke, O. Ronneberger, H. Burkhardt, and J. Popp.** 2006. Identification of single eukaryotic cells with micro-Raman spectroscopy. Biopolymers **82:**312–316.
46. **Rösch, P., M. Harz, K.-D. Peschke, O. Ronneberger, H. Burkhardt, A. Schuele, G. Schmauz, M. Lankers, S. Hofer, H. Thiele, H.-W. Motzkus, and J. Popp.** 2006. On-line monitoring and identification of bioaerosols. Anal. Chem. **78:**2163–2170.
47. **Rösch, P., M. Harz, M. Schmitt, K.-D. Peschke, O. Ronneberger, H. Burkhardt, H.-W. Motzkus, M. Lankers, S. Hofer, H. Thiele, and J. Popp.** 2005. Chemotaxonomic identification of single bacteria by micro-Raman spectroscopy: application to clean-room-relevant biological contaminations. Appl. Environ. Microbiol. **71:**1626–1637.

48. **Ryan, C. G., E. Clayton, W. L. Griffin, S. H. Sie, and D. R. Cousens.** 1988. SNIP, a statistics-sensitive background treatment for the quantitative analysis of PIXE spectra in geoscience applications. Nucl. Instrum. Methods Phys. Res. B **34:**396–402.
49. **Sagripanti, J. L., and A. Bonifacino.** 1996. Comparative sporicidal effects of liquid chemical agents. Appl. Environ. Microbiol. **62:**545–551.
50. **Samuels, A. C., A. P. Snyder, D. K. Emge, D. St. Amant, J. Minter, M. Campbell, and A. Tripathi.** 2009. Classification of select category A and B bacteria by Fourier transform infrared spectroscopy. Appl. Spectrosc. **63:**14–24.
51. **Setlow, B., C. A. Loshon, P. C. Genest, A. E. Cowan, C. Setlow, and P. Setlow.** 2002. Mechanisms of killing spores of Bacillus subtilis by acid, alkali and ethanol. J. Appl. Microbiol. **92:**362–375.
52. **Setlow, P.** 2006. Spores of Bacillus subtilis: their resistance to and killing by radiation, heat and chemicals. J. Appl. Microbiol. **101:**514–525.
53. **Stöckel, S., S. Meisel, R. Böhme, M. Elschner, P. Rösch, and J. Popp.** 2009. Effect of supplementary manganese on the sporulation of Bacillus endospores analysed by Raman spectroscopy. J. Raman Spectrosc. **40:**1469–1477.
54. **Tarcea, N., M. Harz, P. Rösch, T. Frosch, M. Schmitt, H. Thiele, R. Hochleitner, and J. Popp.** 2007. UV Raman spectroscopy—a technique for biological and mineralogical in situ planetary studies. Spectrochim. Acta A **68:** 1029–1035.
55. **Tax, D. M. J., and R. P. W. Duin.** 2002. Using two-class classifiers for multiclass classification, p. 124–127. *In* R. Kasturi et al. (ed.), 16th International Conference on Pattern Recognition: Proceedings, vol. 2. IEEE Computer Society Press, Los Alamitos, CA.
56. **Turnbull, P. C. B.** 2008. Guidelines for the surveillance and control of anthrax in humans and animals. WHO/EMC/ZDI/98/6. World Health Organization, Geneva, Switzerland.
57. **Vaid, A., and A. H. Bishop.** 1998. The destruction by microwave radiation of bacterial endospores and amplification of the released DNA. J. Appl. Microbiol. **85:**115–122.
58. **Vapnik, V. N.** 2000. The nature of statistical learning theory. Springer. New York, NY.
59. **Verbund für Angewandte Hygiene.** 31 July 2006, accession date. Desinfektionsmittel-Liste. Flächendesinfektion. Desinfektionsmittel-Kommission im Verbund für Angewandte Hygiene (VAH) e.V., Bonn, Germany.
60. **Williams, R. W.** 1983. Estimation of protein secondary structure from the laser Raman amide I spectrum. J. Mol. Biol. **166:**581–603.
61. **Xu, D., and J.-C. Cote.** 2003. Phylogenetic relationships between Bacillus species and related genera inferred from comparison of 3′ end 16S rDNA and 5′ end 16S–23S ITS nucleotide sequences. Int. J. Syst. Evol. Microbiol. **53:**695–704.
62. **Zhang, X., M. A. Young, O. Lyandres, and R. P. Van Duyne.** 2005. Rapid detection of an anthrax biomarker by surface-enhanced Raman spectroscopy. J. Am. Chem. Soc. **127:**4484–4489.
63. **Zhao, J., V. Krishna, B. Hua, B. Moudgil, and B. Koopman.** 2009. Effect of UVA irradiance on photocatalytic and UVA inactivation of Bacillus cereus spores. J. Photochem. Photobiol. B **94:**96–100.
64. **Zolock, R. A., G. Li, C. Bleckmann, L. Burggraf, and D. C. Fuller.** 2006. Atomic force microscopy of Bacillus spore surface morphology. Micron **37:**363–369.

2.1.3 Identification of *Bacillus anthracis* via Raman spectroscopy and chemometric approaches

Analytical Chemistry, DOI: 10.1021/ac302250t

Stephan Stöckel[♣]:	Kultivierung und Aufarbeitung von Mikroorganismen, Raman-Messungen, Datenauswertung, Manuskripterstellung
Susann Meisel[♣]:	Kultivierung und Aufarbeitung von Mikroorganismen, Raman-Messungen, Datenauswertung, Beiträge zum Manuskript
Mandy Elschner:	Bereitstellung von Mikroorganismen und Messproben, Konzept- und Ergebnisdiskussion, Revision und Überarbeitung des Manuskripts
Petra Rösch:	Konzept- und Ergebnisdiskussion, Revision und Überarbeitung des Manuskripts
Jürgen Popp:	Projektleitung, Konzept- und Ergebnisdiskussion, Revision und Überarbeitung des Manuskripts

♣ Koautoren

analytical chemistry

Article

pubs.acs.org/ac

Identification of *Bacillus anthracis* via Raman Spectroscopy and Chemometric Approaches

S. Stöckel,[†,‡] S. Meisel,[†,‡] M. Elschner,[§] P. Rösch,*[,†] and J. Popp[†,∥]

[†]Institute of Physical Chemistry and Abbe School of Photonics, Friedrich Schiller University Jena, Helmholtzweg 4, 07743 Jena, Germany

[§]Friedrich Loeffler Institut, Federal Research Institute for Animal Health, Institute of Bacterial Infections and Zoonoses, Naumburger Straße 96a, 07743 Jena, Germany

[∥]Institute of Photonic Technology, Albert-Einstein-Straße 9, 07745 Jena, Germany

Supporting Information

ABSTRACT: Raman micro-spectroscopy was applied to compile a large-scale database of Raman spectra of single *Bacillus* endospores and to calculate classification functions, which were trained to discriminate between endospores of 66 strains from 13 *Bacillus* and *Bacillus*-related species including *B. anthracis*. The developed two-stage classification system comprising two support vector machines and one linear discriminant analysis classifier was then challenged by a test set of 27 samples to simulate the case of a real-world-scenario, when "unknown samples" are to be identified. In the end, all 27 test set samples including six *B. anthracis* strains were identified correctly. The samples thereby covered a diverse selection of species within the phylogenetically broad *Bacillus* genus and also included strains, which were not incorporated in the database before. All of them were correctly identified on the species level with accuracies between 88 and 100%. The sample analysis itself requires no biomass enrichment step prior to the analysis and qualifies the presented Raman spectroscopic approach to be a rapid analysis system in term of *Bacillus* endospore typing.

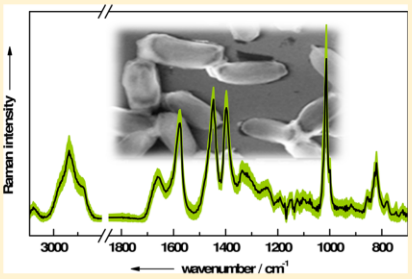

Bacillus is a large genus of aerobic endospore-forming genera and comprises bacteria of an enormous breadth in physiological and genetic diversity. Several taxa are of outstanding scientific or societal importance as for example members of the so-called *B. cereus* group (CG). Today, six validly published species collectively compose the group: *B. anthracis*, a highly pathogenic risk group 3 species as causative agent of anthrax,[1] and *B. cereus*, a risk group 2 species best known for causing symptoms of vomiting or diarrhea in food poisonings.[2] Further members are *B. thuringiensis*, *B. mycoides*, *B. pseudomycoides*, and *B. weihenstephanensis*. There are controversies concerning the taxonomy of this very group: While some authors suggest to include one more species (or subspecies),[3] others prefer to consider *B. anthracis*, *B. cereus*, and *B. thuringiensis* as one single species due to very high DNA sequence similarities.[4] The equivocal taxonomic interrelationship of these species makes a rapid discrimination difficult, although various detection methods have been developed, and many more are in the development phase. The main workhorses are still conventional microbiological methods, where a phenotypic differentiation especially of *B. cereus* group members in environmental samples is difficult.[5] Additionally, they tend to be most labor intensive and often require 1−2 days of testing. They have to be performed by well-trained and certificated personal under restrictive Biological Safety Level 3 (BSL 3) containment environments. And most of the so-called typical reactions are culture dependent and/or plasmid coded. Strains with characteristics of *B. cereus* have been isolated from animals with clinical anthrax.[6] Other studies showed that only 85% of *B. anthracis* strains were phage-sensitive, and a few nonanthrax strains underwent phage-lysis.[7]

Second in line of the *B. anthracis* detection systems are a battery of nucleic-acid based assays, which are also challenged by a number of pitfalls. Endospores have been reported as difficult to process because their nucleic acid is encased in a very resistant shell.[8] The 16S rRNA sequence analysis is of no avail for *B. cereus* group members, since their sequences are almost identical: A 100% sequence identity between *B. anthracis* and *B. cereus* was reported, and a difference of only 4−9 nucleotides from the sequences of *B. mycoides* and *B. thuringiensis* was found.[9] The strategy to detect sequences on the *B. anthracis* virulence plasmids pXO1 and pXO2 falls short in the case of *B. anthracis* strains lacking either one or both of these genome segments or non-*B. anthracis* strains that acquired those plasmids via horizontal gene transfer.[6] Most of these amplification methods therefore have to rely on both a chromosomal marker and a marker on one of the virulence plasmids.[10] Other molecular methods like amplified fragment

Received: August 6, 2012
Accepted: October 25, 2012

dx.doi.org/10.1021/ac302250t | *Anal. Chem.* XXXX, XXX, XXX−XXX

length polymorphism analysis (AFLP) or variable number tandem repeats analysis (VNTR) achieved very high levels of resolution even for strain identification of *B. anthracis*, but these methods are designed to work on isolated colonies and hence are unlikely to achieve relevant identification of *B. anthracis* on field.[11] A general drawback of PCR-based methods is the need for a clean starting sample due to the method's liability to a myriad of inhibitory substances.[12] An application for real-time biodetection of environmental samples is therefore limited, since a precultivation is still mandatory.

Antibody-based tests use conjugated monoclonal and polyclonal antibodies induced against *B. anthracis*. However, many of them have shown cross-reactivity with CG-members and their production is often difficult.[13] A further limitation is the relatively high detection limit compared to other techniques,[14] which also is not a supportive for a convenient, rapid, and real-time detection of *B. anthracis*.

Modern analytical technologies based on mass spectrometry follow a strategy after which specific biomarker signatures of bacteria, like patterns of proteins, carbohydrates, or fatty acids, are registered. This makes a microbial identification by a pattern-matching algorithm with the help of chemometrics possible. For example, extensive work has been done to elaborate discriminating spectral features between different *Bacillus* species relying on protein patterns.[15,16] However, a successful application of mass spectroscopy-based techniques still requires a cultivation phase under rigorous conditions and, apart from intact-cell mass spectroscopy (ICMS), work steps to release and derivatize biomarkers from the cells into components, which are amenable to the analysis.

The joint concept of microscopy and Raman spectroscopy (Raman micro-spectroscopy) with visible light excitation allows probing of bacteria at single-cell level and thus makes biomass enrichment steps prior to analysis redundant.[17] It is also possible to identify bacteria by matching experimental spectral Raman fingerprints of single bacteria with reference members of the same biological species in preformed spectral databases. This pattern-matching approach was applied in medical, food-processing, or military fields to sense a various number of different pathogenic micro-organisms.[18−20] Even several in-depth studies concerning the Raman-spectroscopic characterization of *Bacillus* endospores have already been performed,[21−23] including an assay to sense endospores in complex matrices like baking powder or sand.[24] Especially the latter publication exemplifies the robustness of Raman micro-spectroscopy in dealing with environmental samples, in which the sensitivity for PCR-based detection systems is deteriorated due to attenuating and inhibitory effects of matrix constituents. This is all the more important, since nucleic acid amplification-based techniques are strongly adapted to the target agents by the chosen set of primers, e.g., amplifying sequences on both of the *B. anthracis*-specific virulence plasmids pXO1 and pXO2 allows solely the detection of (virulent) *B. anthracis*. However, a Raman-spectroscopic approach represents a multiplex sensing system when combined with a comprehensively armed spectral database, i.e., containing reference Raman spectra of a wide range of *Bacillus* and *Bacillus*-related species. All species, of which end-member spectra are registered in that database, can then be simultaneously identified. Out of this reason, we compiled a large database of single-endospore Raman spectra to cover a broader fraction of the genotypic diversity among the *Bacillus* genus and related genera and employed it in combination with statistical analytical methods to identify not only samples of *B. anthracis* but also other more or less closely related *Bacillus* species, e.g., the food contaminant *B. cereus* or harmless soil saprophytes like *B. pumilus* or *B. subtilis*. To achieve this, we also developed a multistep classification scheme with two types of supervised classifiers: linear discriminant analysis (LDA) and support vector machines (SVM).

MATERIALS AND METHODS

Species and Strains Used. An overview of the *Bacillus*, *Geobacillus*, and *Paenibacillus* species and strains used throughout this study is provided in Table 1. Most of the nonpathogenic strains were obtained from the German Collection of Microorganisms and Cell Culture GmbH, Braunschweig, Germany, whereas all pathogenic and a few nonpathogenic *Bacillus* strains were provided by the Federal Research Institute for Animal Health, Jena, Germany.

Sample Preparation and Inactivation. To account for biological variability, at least two independently cultivated batches of each *Bacillus* strain were prepared. Thus, suspensions of each *Bacillus* species with concentrations around 10^7 spores per milliliter were produced via two different methods: One method was the cultivation on nutrient agar (NA) plates at 30 °C. The medium is formulated as follows: 5.0 g of peptone, 3.0 g of meat extract, 0.04 g of $MnSO_4 \cdot H_2O$, 15 g of agar, and 1000 mL of distilled water (pH 7.0 ± 0.2, autoclaved at 121 °C, 20 min). The bacteria were rinsed off the plates after seven days of cultivation and washed three times by centrifugation for 2 min at 12 100*g* (MiniSpin, Eppendorf, Hamburg) and resuspension in distilled water (pH 7.0 ± 0.2, autoclaved at 121 °C, 20 min). For the other cultivation approach, bacteria were inoculated into Trypton-Glucose-Broth (TGB) consisting of 2.5 g of yeast extract, 5.0 g of trypton, and 1.0 g of glucose per 1000 mL of distilled water (pH 7.2 ± 0.2, autoclaved at 121 °C, 20 min). After incubation at 37 °C for 3 d, 1 mL of the TGB was inoculated on yeast extract agar consisting of 10.0 g of peptone, 2.0 g of yeast extract, 0.04 g of $MnSO_4 \cdot H_2O$, and 15 g of agar per 1000 mL distilled water (pH 7.0 ± 0.2, autoclaved at 121 °C, 20 min). After incubation at 37 °C for 9 days, the spores were harvested by washing with 5 mL of distilled water and centrifugation at 2218*g* for 10 min (Heraeus Biofuge Primo R, Thermo Fisher Scientific Inc., USA). The sediment was washed four times using distilled water before the suspension was heated at 75 °C for 10 min. Formaldehyde (1.5 mL of 20% solution, Sigma-Aldrich Chemie GmbH, Taufkirchen, Germany) was applied to the endospore pellets, which were acquired after centrifugation of the prepared suspensions to inactivate the potentially pathogenic endospores.[25] The samples were rotated continuously (VWR tube rotator, VWR, Leuven, Belgium) during the time of treatment of one hour until the process was stopped by centrifugation with 12 100*g* (MiniSpin, Eppendorf, Hamburg, Germany) for one minute. The final suspensions were stored at 4 °C until further processing.

Spectroscopic Instrumentation. All of the Raman spectra were collected under ambient conditions. The Raman spectroscopic measurements were carried out with a micro-Raman device (BioParticleExplorer, rap.ID Particle Systems GmbH, Berlin, Germany) that allows automated measurements of single-cell Raman spectra with an excitation light of 532 nm from a solid-state frequency-doubled Nd:YAG module (LCM-S-111-NNP25, Laser-export Co. Ltd.). An Olympus MPLFLN 100×BD objective focused the Raman excitation light onto the sample with a spot size of <1 μm laterally so that approximately 7 mW hit the sample. The integration time per Raman

dx.doi.org/10.1021/ac302250t | Anal. Chem. XXXX, XXX, XXX−XXX

Table 1. *Bacillus* Strains, Abbreviations, Number of Raman Spectra in the Database, and Standard Deviation of the Means (SDM) per Species

species	abbr	strains[a]	no. spectra	SDM
B. anthracis[a] (18)	Bant	13/38, 19/37, 19/39, 19/57, 25/20, 53/59, 527, 4463, 5261, B11/38, B22/39, UD III-7[b]; A58, Ames A93, Vollum[c,f], 03–1640, 03–1641[d], Sterne[e]	2227	0.14
B. atrophaeus (3)	Batr	DSM 675, DSM 2277, DSM 5551	817	0.19
B. cereus (6)	Bcer	DSM 31[f], DSM 345, DSM 487, DSM 626, DSM 4490, DSM 6791	796	0.17
B. licheniformis	Blic	DSM 13	201	0.15
B. megaterium (2)	Bmeg	DSM 32, DSM 90	315	0.19
B. mycoides (3)	Bmyc	DSM 299, DSM 307, DSM 2048	691	0.15
B. pumilus (7)	Bpum	DSM 354, DSM 361, DSM 492, DSM 766, DSM 1794[f], DSM 2893, DSM 13835	832	0.18
B. sphaericus (4)	Bsph	DSM 28, DSM 488, DSM 1867, DSM 2899[f]	407	0.21
B. subtilis (8)	Bsub	DSM 10, DSM 347, DSM 618, DSM 704, DSM 1091[f], DSM 2109, DSM 6399, DSM 6405	1010	0.20
B. thuringiensis (6)	Bthu	DSM 350, DSM 2046, DSM 5725, DSM 5815, DSM 6070, DSM 6890[f]	1023	0.17
B. weihenstephanensis (9)	Bwei	WSBC 10067, WSBC 10206, WSBC 10208, WSBC 10379, WSBC 10389, WSBC 10396, WSBC 10415, WSBC 10550, WSBC 10690[f]	1326	0.13
G. kaustophilus	Geob	DSM 7263	206	0.14
G. stearothermophilus (2)	Geob	DSM 22, DSM 297	412	
P. polymyxa (3)	Ppol	DSM 36, DSM 256, DSM 740	496	0.14

[a]*B. anthracis* strain collection of Friedrich Loeffler Institut, Jena – originating in detail from the following; [b]Federal Institute for Risk Assessment, Berlin, Germany. [c]University Hohenheim, Stuttgart, Germany. [d]Robert Koch-Institut, Wernigerode, Germany. [e]EQADeBa-Repository, Robert Koch-Institut, Berlin, Germany. [f]All marked strains were not included in the database but taken as validation samples to be identified by the classifiers. DSM, Deutsche Sammlung von Mikroorganismen, Braunschweig, Germany; WSBC, Weihenstephan *Bacillus* collection, Institute of Mikrobiology, Technische Universität München, Freising-Weihenstephan, Germany.

spectrum (−113 to 3186 cm^{-1}) was five seconds after a photobleaching period of one second to mitigate spectral contributions because of fluorescence, though it was already of minor extent in most of the endospore spectra. After removal of the Rayleigh scattering via two edge filters, the 180° backscattered Raman light was diffracted with a single-stage monochromator (HE 532, Horiba Jobin Yvon) with a 920 lines/mm grating and collected with a thermoelectrically cooled charge-coupled device camera (DV401-BV, Andor Technology) with a spectral resolution of ca. 7 cm^{-1}. For single-cell measurements, one spectrum of each cell was recorded after 2.5 s and one after 5 s. These two were afterward compared for spike removal.

Multivariate Analysis. Gnu R was used for the statistical analyses.[26] The procedure mainly consisted of three steps: preprocessing, training of the self-learning machines to build a model, and validation. The preprocessing of every data set was always the same. First, the background of the spectra and cosmic spikes were removed. The background was stripped off by employing a statistics-sensitive nonlinear iterative peak-clipping algorithm (SNIP), which is in principle a composite of a low statistics filter and a peak-clipping algorithm.[27] A fourth-order-algorithm was applied with a clipping window of seven to generate an individual background for each spectrum, which then is subtracted from the corresponding original spectrum. Because of their origin, the cosmic spikes are neither correlated in time nor in space and could therefore be localized by recording two Raman spectra of the same endospore. Intensity differences for each channel and their standard deviation were calculated and spikes located in channels, where the intensity difference exceeded twice the standard deviation. The spectra afterward underwent a wavenumber calibration with acetaminophen as standard[28] before a cut off took place: For the calculation the wavenumber regions 639–1802 cm^{-1} and 2783–3186 cm^{-1} were used. A further preprocessing step was normalization: A spectrum was divided by its area, which was calculated as the Euclidean distance of the spectrum to the zero spectrum. Optionally, a principal component analysis (PCA) was performed to reduce the dimensionality of the problem and to remove white noise.[29] After a particular channel the scores were cut off in the new spectral space. The number of chosen scores correlates with the size of the data set, but a good choice is to use not more than 5% of the number of spectra to avoid overfitting.[30] New sets of spectra were always preprocessed the same way. To convert two sets in the same spectral space we did not perform a PCA with the combined data set but rather rotated the new set by the loadings of the PCA of the first data set into the spectral space of the first data set. For the unsupervised hierarchical cluster analysis (squared Euclidian distance and Ward algorithm), only the first 5 scores of the PCA were considered. We chose a LDA and SVM as supervised classifiers to evaluate the spectral data sets.[31,32] For the LDA, only the first 21 scores of a PCA went into the calculation, whereas no PCA was performed in advance of a SVM. 10-fold cross-validation was used to validate the classifiers and determine the optimal kernel parameters of the employed radial basis kernel in case of the SVM via grid search. The resulting accuracy was taken as accuracy of the classification model. An estimation of the generalization error was done by means of a hold-out technique: Sets of endospores from all the analyzed *Bacillus* species were used for training, other completely independent batches of the same strains, which were separately cultured, were used as identification set

dx.doi.org/10.1021/ac302250t | *Anal. Chem.* XXXX, XXX, XXX–XXX

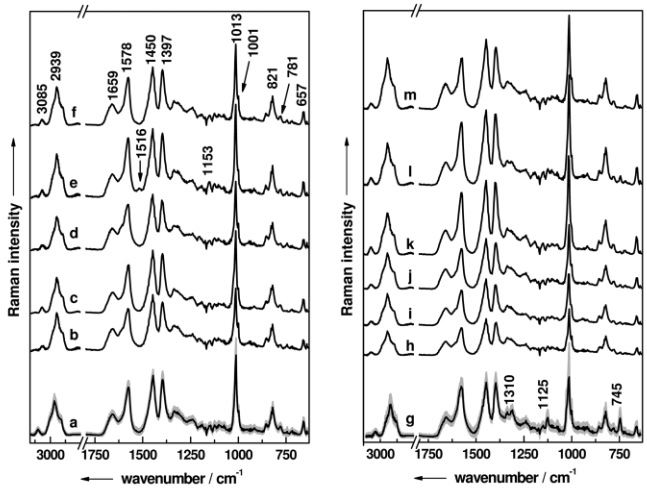

Figure 1. Mean Raman spectra of each of the analyzed *Bacillus* species: (a) *B. anthracis* (calculated from 2227 single endospore Raman spectra, double standard deviation depicted as gray corona), (b) *B. atrophaeus* (817 spectra), (c) *B. cereus* (796 spectra), (d) *B. licheniformis* (201 spectra), (e) *B. megaterium* (315 spectra), (f) *B. mycoides* (691 spectra), (g) *B. sphaericus* (407 spectra, double standard deviation depicted as gray corona), (h) *B. pumilus* (832 spectra), (i) *B. subtilis* (1010 spectra), (j) *B. thuringiensis* (1023 spectra), (k) *B. weihenstephanensis* (1326 spectra), (l) *Geobacillus* spp. (618 spectra), (m) *P. polymyxa* (496 spectra).

(validation set). In doing so, an application of the procedure under realistic conditions was simulated and its accuracy assessed.

■ RESULTS AND DISCUSSION

Mean Raman spectra from analyzed *Bacillus* and *Bacillus*-related species are displayed in Figure 1. They were obtained by averaging preprocessed single-cell Raman spectra and are presented to give a species-wise overview of the typical signal patterns in endospore Raman spectra. The most dominant Raman signals in all of the spectra are attributable to the calcium chelate of pyridine-2,6-dicarboxylic acid (calcium dipicolinate, CaDPA). This endospore-specific substance is largely deposited in the endospore's core (ca. 5−15% of the spore dry weight) and is responsible for the low water content in the core giving the endospores their remarkable heat resistance.[33] The observed bands can basically be divided in two groups according to their origin: Skeletal vibrations of the pyridine ring (657, 1013, 1450, and 3085 cm^{-1}) and vibrational modes due to the carboxylate group (821, 1397, and 1578 cm^{-1}).[34] Band positions and relative intensities of these signals vary only slightly between the spectra in Figure 1, and since CaDPA is ubiquitously present in all *Bacillus* endospores, these bands taken alone are not diagnostic beyond indicating the general presence of endospores. Thus, also signals of other biopolymers in the bacteria need to be taken into account, such as the ring vibrations of cytosine/uracil at 781 cm^{-1}, the 1001-cm^{-1} band of the ring breathing vibration of phenylalanine, or the 1659-cm^{-1} biomarker for the amid I mode.[21] Not all bands arise exclusively due to one single class of molecules but are rather superpositions of several types of biomolecules. This can be seen, e.g., at the aforementioned band at 821 cm^{-1}, where the tyrosine ring breathing mode overlaps with a COO^- signal of CaDPA. Another example is the CH_2/CH_3 deformation mode of proteins and lipids at 1450 cm^{-1} supplemented by the CaDPA pyridine ring vibration. Also 1578 cm^{-1} is made up by ring vibrations of guanine and adenine combined with the asymmetric carboxylate vibration. Finally, the prominent C−H band in the high-wavenumber region at 2939 cm^{-1} is a generic marker for almost all types of biopolymers in bacteria bearing carbon and hydrogen. Upon closer inspection, some signals unique for certain *Bacillus* species can be located. The inconspicuous bands at 1153 and 1516 cm^{-1} are exclusive features of the *B. megaterium* spectrum (Figure 1e) and are normally typical hallmarks of carotenoids. Indeed, strains of *B. megaterium* were found to express several pigments, most probably as safeguard mechanisms against UV radiation.[35] Another, in this case *B. sphaericus*-specific, signal pattern (Figure 1g) is clearly evident in form of the band triplet at 745, 1125, and 1310 cm^{-1}, which presumably originates from heme-bearing proteins such as cytochromes.[36] It is obvious that the mean spectra of different species share a tremendous similarity with each other, and no unique features strike out as possible marker bands for a certain species. Bare-eyed discrimination of the average spectra (and the single-cell Raman spectra behind them as well) in Figure 1 is therefore a futile endeavor. A more promising way to dig out the miniscule interspecies differences is by interpreting the whole spectrum in a multivariate way as spectral fingerprint. An in-depth and exhaustive knowledge of each of the signals in the Raman signatures is not mandatory in these pattern-matching approaches, nonetheless the whole information is considered in the data evaluation. However, an important premise to do so is a sufficient reproducibility of the spectra within the species, although the spectra of one species stem from different strains and batches from two different laboratories and were measured on different days by different operators. After preprocessing, the treated spectra have to be analyzed for inherent variations due to the fact that single cells are measured: Unavoidable

dx.doi.org/10.1021/ac302250t | *Anal. Chem.* XXXX, XXX, XXX−XXX

fluctuations in the biochemical makeup from cell to cell in one batch cause spectral variations.[37] To compare the species among each other, a normalized standard deviation is calculated for each species. The mean of the standard deviation per channel is normalized to the standard deviation of the channel means resulting in a standard deviation of the means (SDM).[38] Thus, the standard deviation per channel is put into relation of a mean spectrum's statistical property. The SDM values for each species are given in the rightmost column of Table 1, where low SDM numbers represent low channel-wise variabilities and thus high reproducibility and reliability of the data set. High numbers in the range of nearly 1 would stand for high volatilities per channel and would cast doubt on the data's reliability. All calculated SDMs are significantly lower than 1 in a tight interval between 0.14 to 0.21. *B. anthracis* spectra (SDM 0.14) sticks out by a very high homogeneity only topped by B. *weihenstephanensis* (SDM 0.13), whereas *B. sphaericus* has the highest SDM of 0.21. To identify the underlying spectral variations, the distribution of all individual class spectra is depicted in Figure 1 by visualizing the double standard deviation per wavenumber for *B. anthracis* (a) and *B. sphaericus* (g) in the form of gray coronas surrounding the mean spectra: Spectral features remain widely constant in both cases in terms of signal locations and band intensities. Especially the ensemble of single *B. anthracis* spectra exhibits a remarkably high reproducibility with almost constant standard deviations for all wavenumbers. The situation however is slightly different for *B. sphaericus*, as specifically the bands of CaDPA bear a relatively high variance compared to other signals, which is readily identifiable at the 1016 cm^{-1} peak. This is a reasonable outcome, as Huang et al. have already ascertained significant variations of CaDPA levels among single endospores of one species hypothesizing a size effect of single endospores between and in-between single strains.[22] We therefore built a database with more than 10 000 Raman signatures of single endospores (Table 1) to mirror the naturally occurring variations of CaDPA in individual cells as good as possible, so that any detrimental effects on the data mining operations described below are minimized.

The database consisted of single endospore Raman spectra from 13 species and 66 strains. In an attempt to structure this massive amount of data, a HCA was performed to organize the spectra according to interspectral similarities. Since this is a nonhypothesis technique, no particular attention to the underlying class structure was paid, and all 66 (*Geo-*, *Paeni-*) *Bacillus* strain average spectra were fed into the algorithm in an unbiased way. The resulting outcomes can help to structure and devise strategies for more sophisticated data evaluation approaches as outlined below, which also consider a priori class information. The dendrogram in Figure S1 of the Supporting Information depicts partitions that mirror well-expected relations known from taxonomic considerations: While block A almost exclusively contains the spectra of *B. anthracis*, *B. cereus*, *B. mycoides*, *B. thuringiensis*, and *B. weihenstephanensis* strains, block B pools together the spectra of all the other *Bacillus* species plus the two non-*Bacillus* species with the exception of two *B. thuringiensis* strains and one *B. cereus* strain, which are boldfaced in the dendrogram. The whole data set is apparently divided by the HCA into a *B. cereus* group (BC group) cluster A and non-*B. cereus* (NBC group) cluster B. This principle breakdown suggests an evident harmony between Raman spectroscopic fueled relationships and phylogenetic or taxonomic ones.

In the upcoming calculations we were trying to derive a benefit from this basic information by structuring the classification systems in two steps. The idea is to condition computer algorithms, which learn by example, to assign labels (*Bacillus* species) to objects (single-endospore Raman spectra) by modeling probabilities of class membership. The training ground for the classifier is a comprehensive compilation of bacterial reference Raman spectra, which ideally comprises end member spectra of all species that are to be identified. Thus, 10759 Raman spectra of single *Bacillus*, *Geobacillus*, and *Paenibacillus* endospores, broken down in species and strains in Table 1, represented the input or training data. Scheme 1

Scheme 1. Structure and Parameters of the Classification Tree and the Underlying Database

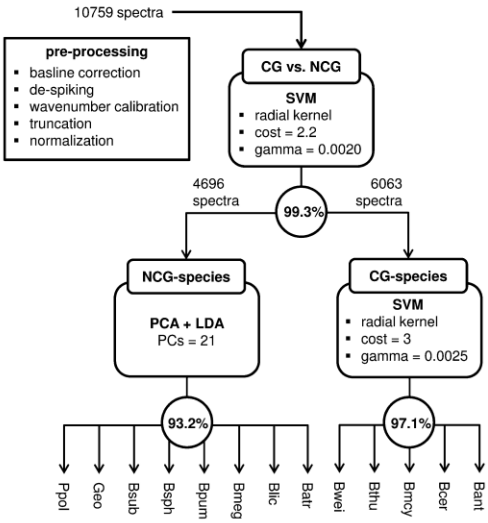

portrays the overall work flow for the data analysis. It shows not only the hierarchy in the training data set, but also the succession of decision steps of the classification and identification process. This decision tree was orientated on a spectral hierarchy in the data, as was worked out under the preceding paragraph. At the top level, a decision between species of the *B. cereus* group (CG) and non-*B. cereus* group (NCG) is done before at the second hierarchical level a subdivision into the respective species is carried out. We chose two elementary binary classifiers to perform the task at hand: LDA in combination with a PCA and SVM. Both were recently applied to discriminate bacteria and particles of inorganic origin according their Raman spectra and demonstrated different suitability and application potentials.[39,40] Thus, a toolbox of not only differently operating classification algorithms but also of parameters thereof stand to the disposal to optimally design and fine-tune a classification system. All crucial parameters (type of kernel, kernel parameters cost and gamma, number of scores) were determined by optimizing each knot toward a maximum of predictive ability, determined via cross-validation and reduced reliability to overfitting. The final values for each knot are delivered in Scheme 1. Attempts to calculate a classifier, which was trained to discriminated all 13 species in

Table 2. Results of the Three Classifiers after Processing 27 Test Samples[a]

			top level			species level			
sample	class	strain	CG	NCG	assigned to	TP/all	sensitivity	classes of FP	assigned to
1	Bant	03−1641	70	0	**CG**	68/70	97.1%	Bthu (2)	**Bant**
2	Bant	19−57	73	0	**CG**	72/73	98.6%	Bcer (1)	**Bant**
3	Bant	5261	81	0	**CG**	81/81	100%		**Bant**
4	Bant	A58	72	0	**CG**	70/72	97.2%	Bcer (2)	**Bant**
5	Bant	Sterne	93	0	**CG**	90/93	96.8%	Bthu (2)	**Bant**
								Bwei (1)	
6*	Bant	Vollum	81	1	**CG**	80/82	97.6%	Bthu (2)	**Bant**
7	Batr	DSM 5551	0	145	**NCG**	145/145	100%		**Batr**
8	Bcer	DSM 487	89	0	**CG**	82/89	92.1%	Bant (7)	**Bcer**
9*	Bcer	DSM 31	77	1	**CG**	76/78	97.4%	Bant (2)	**Bcer**
10	Blic	DSM 13	0	119	**NCG**	116/119	97.5%	Batr (1)	**Blic**
								Bpum (1)	
								Bsub (1)	
11	Bmeg	DSM 90	13	83	**NCG**	95/96	99.0%	Bpol (1)	**Bmeg**
12	Bmyc	DSM 299	108	0	**CG**	103/108	95.4%	Bthu (4)	**Bmyc**
								Bcer (1)	
13	Bpum	DSM 354	0	71	**NCG**	70/71	98.6%	Batr (1)	**Bpum**
14	Bpum	DSM 361	1	66	**NCG**	67/67	100%		**Bpum**
15*	Bpum	DSM 1794	0	118	**NCG**	115/118	97.5%	Batr (3)	**Bpum**
16	Bsph	DSM 488	0	87	**NCG**	81/87	93.1%	Geo (6)	**Bsph**
17*	Bsph	DSM 2899	0	151	**NCG**	151/151	100%		**Bsph**
18	Bsub	DSM 6399	0	95	**NCG**	95/95	100%		**Bsub**
19*	Bsub	DSM 1091	1	188	**NCG**	184/189	97.4%	Batr (4)	**Bsub**
								Ppol (1)	
20	Bthu	DSM 2046	86	0	**CG**	76/86	88.4%	Bmyc (5)	**Bthu**
								Bwei (3)	
								Bant (2)	
21	Bthu	DSM 6070	75	0	**CG**	75/75	100%		**Bthu**
22*	Bthu	DSM 6890	201	0	**CG**	200/201	99.5%	Bwei (1)	**Bthu**
23	Bwei	WSBC 10389	96	0	**CG**	95/96	99.0%	Bmyc (1)	**Bwei**
24	Bwei	WSBC 10415	95	0	**CG**	93/95	97.9%	Bant (1)	**Bwei**
								Bmyc (1)	
25*	Bwei	WSBC 10690	168	0	**CG**	163/168	97.0%	Bant (3)	**Bwei**
								Bthu (2)	
26	Geo	DSM 22	0	131	**NCG**	130/131	99.2%	Bsub (1)	**Geo**
27	Ppol	DSM 740	1	117	**NCG**	118/118	100%		**Ppol**

[a]CG = *B. cereus* group, NCG = non-*B. cereus* group, TP = true positives, FP = false positives.

one step, were to no avail, as only an unsatisfactory generalization ability was obtained, although the cross-validation worked well (data not shown). Especially a discrimination of the BC members proved to be difficult.

The top-level classifier was a SVM, which was fed with all 10759 Raman spectra of the training set to learn to tell the difference between Raman spectra of CG and NCG species. The internal cross-validation determined the accuracy of this classifier to be 99.3%, i.e., 10 680 of 10 759 of the training set spectra were correctly assigned according their CG or NCG affiliation. On the lower tier, a second SVM classifier made full use of all 6063 true CG spectra to be capable of discriminating between the five CG species *B. anthracis*, *B. cereus*, *B. mycoides*, *B. thuringiensis*, and *B. weihenstephanensis*. The classifier's performance was determined by cross-validation to 97.1%. The other second-layer classifier was an LDA optimized by training with 4696 Raman spectra of the eight NCG species *B. atrophaeus*, *B. licheniformis*, *B. megaterium*, *B. pumilus*, *B. sphaericus*, *B. subtilis*, *Geobacillus* spp., and *P. polymyxa*. This time, the accuracy amounted for 93.2% (4377 of 4696 spectra were correctly classified).

Having the classification system at hand, it is now possible to ask the system about the class-membership of 27 "unknown" samples (1−27 as given in Table 2). These samples were prepared anew and completely independent from the samples produced for the model built-up but were processed and analyzed as all the samples before. By challenging the model with the Raman spectra of the 27 test samples, its generalization ability (or insusceptibility to overfitting) was assessed. Thereby, not only the predictive accuracy was measured but also the case simulated, when real-world samples are to be analyzed. To complicate the matter even more, we included in the test sets Raman spectra of strains (samples marked with asterisk), which had not been included in the model before. This was done for all the species with more than three different strains in the database: *B. anthracis* (test sample 6*), *B. cereus* (9*), *B. pumilus* (15*), *B. sphaericus* (17*), *B. subtilis* (19*), *B. thuringiensis* (22*), and *B. weihenstephanensis* (25*). This gives an important estimation of the robustness of the system, as it is highly possible to encounter nondatabase strains of a specific species in real-world samples. Each spectrum of the 27 test samples was interrogated twice during the identification

dx.doi.org/10.1021/ac302250t | *Anal. Chem.* XXXX, XXX, XXX−XXX

process: First, it is determined whether the spectrum is from a CG or NCG endospore, thereafter to which species it belongs to. Both decisions are done sample wise, i.e., the class to which the majority of spectra is assigned to determines the class of the whole sample. The outcomes of the classifiers are presented in a somewhat condensed form in Table 2 and more detailed in the confusion tables of Tables S1 and S2 of the Supporting Information. The results of the top-level classifier can be found under the column "top-level" in Table 2, where all samples 1−27 were labeled as either CG or NCG. Correct diagnoses can be stated for all the 27 samples giving rise to an average accuracy of 99.4%. In 6 of 27 samples false negatives occurred, notably in sample 11 (*B. megaterium*) with 13 of 96 wrongly labeled spectra. The distribution of the samples in the end corresponds perfectly with the true sample-classes: Samples 1−6*, 8, 9*, 12, and 20−25* were categorized as CG samples, while samples 7, 10, 11, 13−19*, 26, and 27 were categorized to contain NCG endospores.

After the 27 validation samples passed the top-level classifier, they were evaluated by the respective species-determining classifiers. A sufficient discrimination of CG-endospores was only achieved by a SVM, which was explicitly trained to perform this very task (97.1% classification accuracy). The columns under "species-level" in Table 2 outline the outcomes: In the case of the 15 putative CG samples, a flawless performance was achieved, as all samples were identified correctly with accuracies in the range of 88.4% (sample 20, *B. thuringiensis*) to 100% (samples 3, *B. anthracis*, and 21, *B. thuringiensis*). Especially the diagnostic certainty for the six *B. anthracis* samples is comparatively high with only 10 false negatives among all 471 Raman spectra of this species plus 15 false positives coming from five different samples. Six of the *B. anthracis* spectra were misidentified as being *B. thuringiensis*, a tendency, which is to be expected, as it is advised to use this species as nonpathogenic surrogate for *B. anthracis*.[41] Even sample 6* was identified correctly as *B. anthracis*, although it contained endospores of the Vollum strain, of which no reference spectra were incorporated in the database before; the same is true for the non-*B. anthracis* strains 9* (*B. cereus*), 22* (*B. thuringiensis*), and 25* (*B. weihenstephanensis*). To summarize, the overall identification rate of this classifier can be calculated to 97.1% (1424 of 1467 spectra correctly labeled). The other second-layer NCG classifier—this time a less computational-intensive PCA/LDA approach—also perfectly assigned each of the 12 putative NCG-samples to the correct species. The identification accuracies per sample were in all but one case (16 *B. sphaericus* with 93.1% sensitivity) above 97% and 1367 of all 1387 Raman spectra that passed this classifier were put into the right class (98.6% sensitivity). The samples with strains new to the model (15*, 17*, and 19*) were all assigned to the correct class, too, with sensitivities in the range of the other samples.

Inspired by these results, we challenged the 2-step classification system even further by testing Raman spectra of endospores, which were isolated out of spiked household powders.[24] Spectra of eight samples (P1−P8) of *B. anthracis* Sterne (isolated from common salt), *B. megaterium* DSM 90 (bird sand), *B. subtilis* DSM 10 (milk powder), and *B. thuringiensis* DSM 350 (baking powder) were labeled as Table S3 of the Supporting Information presents: The top-level classifier (97.8% accuracy) as well as both species classifiers (CG, 92.1%; NCG, 97.2%) performed sufficiently so that all eight samples were in the end identified correctly. A slight tendency toward intermixing spectra of *B. anthracis* and *B. thuringiensis* is given again. All in all, the accuracy levels of the cross-validation were retained—or even slightly better in case of the NCG-LDA classifier—for all validation samples and a tendency toward overfitting was also not detectable. Therefore, all "unknown" samples were correctly identified without exception. This holds true even for *Bacillus* endospores extracted from real-world samples. Finally, the database strains obviously provide a generalization potential high enough to identify even strains new to the model.

■ CONCLUSION

Within this work, we strived to show that Raman spectroscopy as a diagnostic tool for *Bacillus* endospores can complement already established techniques by compensating some of their weak spots. Above all, the independency of time-extensive biomass enrichment steps peaks out. Only 50−100 intact bacterial cells are required to deduce a diagnostic result for one sample—a number of micro-organisms that can be quickly extracted out of various kinds of environmental samples, when an appropriate isolation protocol is at hand. This is all the more true because inhibiting effects of the matrix, from which the endospores have to be extracted, play, if any, only a minor role. Another plus is the fact that the whole organism is probed, not only specific biomarkers like plasmidic gene. Consequently, the identification of *B. anthracis* with differing plasmid loadings posed not a problem in our study: Virulent strains with a full virulence plasmid setup like 03−1641 and 19−57 (samples 1 and 2) as well as nonvirulent pXO1-depleted (*B. anthracis* 5261, sample 3), pXO2-depleted (sample 5 Sterne) strains and also strains lacking both plasmids (*B. anthracis* A58) were correctly determined as being *B. anthracis*. A further merit of the herein described Raman spectroscopic approach is its general applicability in terms of discrimination of endospores throughout the whole *Bacillus* genus and related genera. No matter, whether pathogenic (for example *B. anthracis* or *B. cereus*), environmental (among them *B. pumilus* or *B. subtilis*), or industrially used endospores (e.g., *B. licheniformis*) are target organisms, an identification via Raman spectroscopy is always possible as long as reference-spectra of the respective taxon are incorporated in the database and considered by the classifier. We could also show that even *Bacillus* strains absent in the database can safely be identified on species level. Thus, also newly discovered strains from novel, often exotic, environments can be taken into account in the future. In the end, this allows an identification of multiple targets, which is beneficial in eliminating false-negative and false-positive results, especially in case of environmental samples with possible bacterial mixtures.

■ ASSOCIATED CONTENT

Supporting Information

Additional information as noted in text. This material is available free of charge via the Internet at http://pubs.acs.org.

■ AUTHOR INFORMATION

Corresponding Author

*Phone: +49-3641-948381. Fax: +49-3641-948302. E-mail: petra.roesch@uni-jena.de.

Author Contributions

‡These authors contributed equally.

Notes

The authors declare no competing financial interest.

■ ACKNOWLEDGMENTS

Funding of the research projects "Pathosafe" (FKZ 13N9547 and FKZ 13N9549) and "RamaDek" (FKZ 13N11168) from the Federal Ministry of Education and Research, Germany (BMBF), "MikroPlex" (PE113-1) from the Thüringische Exzellenzinitiative (TMBWK), as well as funding of "EQADeBa" by the EU, EAHC Agreement No. 2007 204 is gratefully acknowledged. We also thank Matthias Frank and Katja Fischer (Friedrich Loeffler Institute, Germany) for doing the sample preparation and inactivation experiments.

■ REFERENCES

(1) Mock, M.; Fouet, A. *Annu. Rev. Microbiol.* **2001**, *55*, 647−671.
(2) Bottone, E. J. *Clin. Microbiol. Rev.* **2010**, *23*, 382−398.
(3) Jackson, P. J.; Hill, K. K.; Laker, M. T.; Ticknor, L. O.; Keim, P. *J. Appl. Microbiol.* **1999**, *87*, 263−269.
(4) Helgason, E.; Okstad, O. A.; Caugant, D. A.; Johansen, H. A.; Fouet, A.; Mock, M.; Hegna, I.; Kolsto, A.-B. *Appl. Environ. Microbiol.* **2000**, *66*, 2627−2630.
(5) Klee, S. R.; Nattermann, H.; Becker, S.; Urban-Schriefer, M.; Franz, T.; Jacob, D.; Appel, B. *J. Appl. Microbiol.* **2006**, *100*, 673−681.
(6) Klee, S. R.; Oezel, M.; Appel, B.; Boesch, C.; Ellerbrok, H.; Jacob, D.; Holland, G.; Leendertz, F. H.; Pauli, G.; Grunow, R.; Nattermann, H. *J. Bacteriol.* **2006**, *188*, 5333−5344.
(7) Schuch, R.; Nelson, D.; Fischetti, V. A. *Nature* **2002**, *418*, 884−889.
(8) Belgrader, P.; Okuzumi, M.; Pourahmadi, F.; Borkholder, D. A.; Northrup, M. A. *Biosens. Bioelectron.* **2000**, *14*, 849−852.
(9) Ash, C.; Farrow, J. A. E.; Dorsch, M.; Stackebrandt, E.; Collins, M. D. *Int. J. Syst. Bacteriol.* **1991**, *41*, 343−346.
(10) Hoffmaster, A. R.; Meyer, R. F.; Bowen, M. P.; Marston, C. K.; Weyant, R. S.; Barnett, G. A.; Sejvar, J. J.; Jernigan, J. A.; Perkins, B. A.; Popovic, T. *Emerg. Infect. Dis.* **2002**, *8*, 1178−1182.
(11) Keim, P.; Pearson, T.; Okinaka, R. *Anal. Chem.* **2008**, *80*, 4791−4799.
(12) Wilson, I. G. *Appl. Environ. Microbiol.* **1997**, *63*, 3741−3751.
(13) Tamborrini, M.; Oberli, M. A.; Werz, D. B.; Schurch, N.; Frey, J.; Seeberger, P. H.; Pluschke, G. *J. Appl. Microbiol.* **2009**, *106*, 1618−1628.
(14) Rao, S. S.; Mohan, K. V. K.; Atreya, C. D. *J. Microbiol. Methods* **2010**, *82*, 1−10.
(15) Lasch, P.; Beyer, W.; Nattermann, H.; Stammler, M.; Siegbrecht, E.; Grunow, R.; Naumann, D. *Appl. Environ. Microbiol.* **2009**, *75*, 7229−7242.
(16) Callahan, C.; Fox, K.; Fox, A. *Mol. Cell. Probes* **2009**, *23*, 291−297.
(17) Harz, M.; Rösch, P.; Popp, J. *Cytometry, Part A* **2009**, *75A*, 104−113.
(18) Wulf, M. W. H.; Willemse-Erix, D.; Verduin, C. M.; Puppels, G.; van Belkum, A.; Maquelin, K. *Clin. Microbiol. Infect.* **2012**, *18*, 147−152.
(19) Meisel, S.; Stöckel, S.; Elschner, M.; Melzer, F.; Rösch, P.; Popp, J. *Appl. Environ. Microbiol.* **2012**, *78*, 5575−5583.
(20) Tripathi, A.; Jabbour, R. E.; Treado, P. J.; Neiss, J. H.; Nelson, M. P.; Jensen, J. L.; Snyder, A. P. *Appl. Spectrosc.* **2008**, *62*, 1−9.
(21) De Gelder, J.; Scheldeman, P.; Leus, K.; Heyndrickx, M.; Vandenabeele, P.; Moens, L.; De Vos, P. *Anal. Bioanal. Chem.* **2007**, *389*, 2143−2151.
(22) Huang, S. S.; Chen, D.; Pelczar, P. L.; Vepachedu, V. R.; Setlow, P.; Li, Y. Q. *J. Bacteriol.* **2007**, *189*, 4681−4687.
(23) Zhang, P.; Kong, L.; Wang, G.; Scotland, M.; Ghosh, S.; Setlow, B.; Setlow, P.; Li, Y. Q. *J. Appl. Microbiol.* **2012**, *112*, 526−536.
(24) Stöckel, S.; Meisel, S.; Elschner, M.; Rösch, P.; Popp, J. *Angew. Chem., Int. Ed.* **2012**, *51*, 5339−5342.
(25) Stöckel, S.; Schumacher, W.; Meisel, S.; Elschner, M.; Rösch, P.; Popp, J. *Appl. Environ. Microbiol.* **2010**, *76*, 2895−2907.
(26) R. Development Core Team. R Foundation for Statistical Computing: Vienna, Austria, 2008.
(27) Morhác, M. *Nucl. Instrum. Methods A* **2009**, *600*, 478−487.
(28) Carrabba, M. M. In *Handbook of Vibrational Spectroscopy*; John Wiley & Sons, Ltd., 2006; Vol. *1*.
(29) Pearson, K. *Philos. Mag.* **1901**, *2*, 559−572.
(30) Vapnik, V. N. *The Nature of Statistical Learning Theory*, 2nd ed.; Springer: New York, 2000.
(31) Fisher, R. *Ann. Eugenic.* **1936**, *7*, 179−188.
(32) Burges, C. J. C. *Data Min. Knowl. Discovery* **1998**, *2*, 121−167.
(33) Setlow, P. *J. Appl. Microbiol.* **2006**, *101*, 514−525.
(34) Carmona, P. *Spectrochim. Acta, Part A* **1980**, *36A*, 705−12.
(35) Mitchell, C.; Iyer, S.; Skomurski, J. F.; Vary, J. C. *Appl. Environ. Microbiol.* **1986**, *52*, 64−67.
(36) Desbois, A. *Biochimie* **1994**, *76*, 693−707.
(37) Hermelink, A.; Brauer, A.; Lasch, P.; Naumann, D. *Analyst* **2009**, *134*, 1149−1153.
(38) Walter, A.; März, A.; Schumacher, W.; Rösch, P.; Popp, J. *Lab Chip* **2011**, *11*, 1013−1021.
(39) Schumacher, W.; Kühnert, M.; Rösch, P.; Popp, J. *J. Raman Spectrosc.* **2011**, *42*, 383−392.
(40) Meisel, S.; Stöckel, S.; Elschner, M.; Rösch, P.; Popp, J. *Analyst* **2011**, *136*, 4997−5005.
(41) Greenberg, D. L.; Busch, J. D.; Keim, P.; Wagner, D. M. *Invest. Genet.* **2010**, *1*, 4.

Supporting Information

Identification of *Bacillus anthracis* via Raman spectroscopy and chemometric approaches

S. Stöckel,[1] S. Meisel,[1] M. Elschner,[2] P. Rösch,[1] and J. Popp[1,3]

[1] Institute of Physical Chemistry and Abbe School of Photonics, Friedrich Schiller University Jena, Helmholtzweg 4, 07743 Jena, Germany.

[2] Friedrich Loeffler Institut, Federal Research Institute for Animal Health, Institute of Bacterial Infections and Zoonoses, Naumburger Straße 96a, 07743 Jena, Germany.

[3] Institute of Photonic Technology, Albert-Einstein-Straße 9, 07745 Jena, Germany.

table of content

Table S-1. Results of the CG-Classifier After Processing the 15 Test Samples, Which Had Been Categorized to be CG-Endospores by the Top-Level Classifier Before S-2

Table S-2. Results of the NCG-Classifier After Processing the 12 Test Samples, Which Had Been Categorized to be NCG-Endospores by the Top-Level Classifier Before S-3

Table S-3. Results of the Three Classifiers After Processing 8 Test Samples of Endospores Isolated out of 4 Types of Household Powders[a] S-4

Figure S-1. Hierarchical Cluster Analysis of 66 *Bacillus*, *Geobacillus*, and *Paenibacillus* Strain Mean Raman Spectra. A Euclidian Metric and Ward's Algorithm as Clustering Method were used. The Misclassified Spectra are Boldfaced S-5

Table S-1. Results of the CG-Classifier After Processing the 15 Test Samples, Which Had Been Categorized to be CG-Endospores by the Top-Level Classifier Before

sample	class	Bant	Bcer	Bmyc	Bthu	Bwei	sensitivity	assigned to
1	Bant	**68**	0	0	2	0	97.1%	**Bant**
2	Bant	**72**	1	0	0	0	98.6%	**Bant**
3	Bant	**81**	0	0	0	0	100%	**Bant**
4	Bant	**70**	2	0	0	0	97.2%	**Bant**
5	Bant	**90**	0	0	2	1	96.8%	**Bant**
6*	Bant	**80**	0	0	2	0	97.6%	**Bant**
8	Bcer	7	**82**	0	0	0	92.1%	**Bcer**
9*	Bcer	2	**76**	0	0	0	97.4%	**Bcer**
12	Bmyc	0	1	**103**	4	0	95.4%	**Bmyc**
20	Bthu	2	0	5	**76**	3	88.4%	**Bthu**
21	Bthu	0	0	0	**75**	0	100%	**Bthu**
22*	Bthu	0	0	0	**200**	1	99.5%	**Bthu**
23	Bwei	0	0	1	0	**95**	99.0%	**Bwei**
24	Bwei	1	0	1	0	**93**	97.9%	**Bwei**
25*	Bwei	3	0	0	2	**163**	97.0%	**Bwei**

The actual class and the labeling of all spectra per sample are given line-wise along with the respective sensitivities (true-positive rate) and the final class assignments. The overall identification accuracy was 97.1% (1424 of 1467 Raman-spectra correctly identified on species level). Samples marked with asterisks were strains with no reference-spectrum in the database.

Table S-2. Results of the NCG-Classifier After Processing the 12 Test Samples, Which Had Been Categorized to be NCG-Endospores by the Top-Level Classifier Before

sample	class	Batr	Blic	Bmeg	Bpum	Bsph	Bsub	Geo	Ppol	sensitivity	assigned to
7	Batr	**145**	0	0	0	0	0	0	0	100%	**Batr**
10	Blic	1	**116**	0	1	0	1	0	0	97.5%	**Blic**
11	Bmeg	0	0	**95**	0	0	0	0	1	99.0%	**Bmeg**
13	Bpum	1	0	0	**70**	0	0	0	0	98.6%	**Bpum**
14	Bpum	0	0	0	**67**	0	0	0	0	100%	**Bpum**
15*	Bpum	3	0	0	**115**	0	0	0	0	97.5%	**Bpum**
16	Bsph	0	0	0	0	**81**	0	6	0	93.1%	**Bsph**
17*	Bsph	0	0	0	0	**151**	0	0	0	100%	**Bsph**
18	Bsub	0	0	0	0	0	**95**	0	0	100%	**Bsub**
19*	Bsub	4	0	0	0	0	**184**	0	1	97.4%	**Bsub**
26	Geo	0	0	0	0	0	1	**130**	0	99.2%	**Geo**
27	Ppol	0	0	0	0	0	0	0	**118**	100%	**Ppol**

The actual class and the labeling of all spectra per sample are given line-wise along with the respective sensitivities (true-positive rate) and the final assignments. The overall identification accuracy was 98.6% (1367 of 1387 Raman-spectra correctly identified on species-level). Samples marked with asterisks were strains with no reference-spectrum in the database.

Table S-3. Results of the Three Classifiers After Processing 8 Test Samples of Endospores Isolated out of 4 Types of Household Powders[a]

sample	class	matrix	top-level			species-level			
			CG	NCG	assigned to	TP/all	sensitivity	classes of FP	assigned to
P1	Bant	C	108	1	**CG**	97/109	89.0%	Bthu (8) Bwei (3) Bmyc (1)	**Bant**
P2	Bant	C	82	0	**CG**	68/82	82.9%	Bthu (12) Bwei (2)	**Bant**
P3	Bmeg	S	6	53	**NCG**	52/59	88.1%	Ppol (5) Bpum (2)	**Bmeg**
P4	Bmeg	S	7	58	**NCG**	64/65	98.5%	Ppol (1)	**Bmeg**
P5	Bsub	MP	0	100	**NCG**	99/100	99.0%	Batr (1)	**Bsub**
P6	Bsub	MP	0	100	**NCG**	100/100	100%	-	**Bsub**
P7	Bthu	BP	100	1	**CG**	98/101	97.0%	Bmyc (2) Bwei (1)	**Bthu**
P8	Bthu	BP	76	0	**CG**	76/76	100%	-	**Bthu**

[a] C = common salt, S = bird sand, MP = milk powder, BP = baking powder;
CG = B. cereus group, NCG = non-B. cereus group, TP = true-positives, FP = false-positives

The actual class and the labeling of all spectra per sample are given line-wise along with the respective sensitivities (true-positive rate) for the species-level classifiers and the final assignments. The overall identification accuracies were 97.8% (top-level classifier), 92.1% (CG), and 97.2% (NCG).

Figure S-1. Hierarchical Cluster Analysis of 66 *Bacillus*, *Geobacillus*, and *Paenibacillus* Strain Mean Raman Spectra. A Euclidian Metric and Ward's Algorithm as Clustering Method were used. The Misclassified Spectra are Boldfaced.

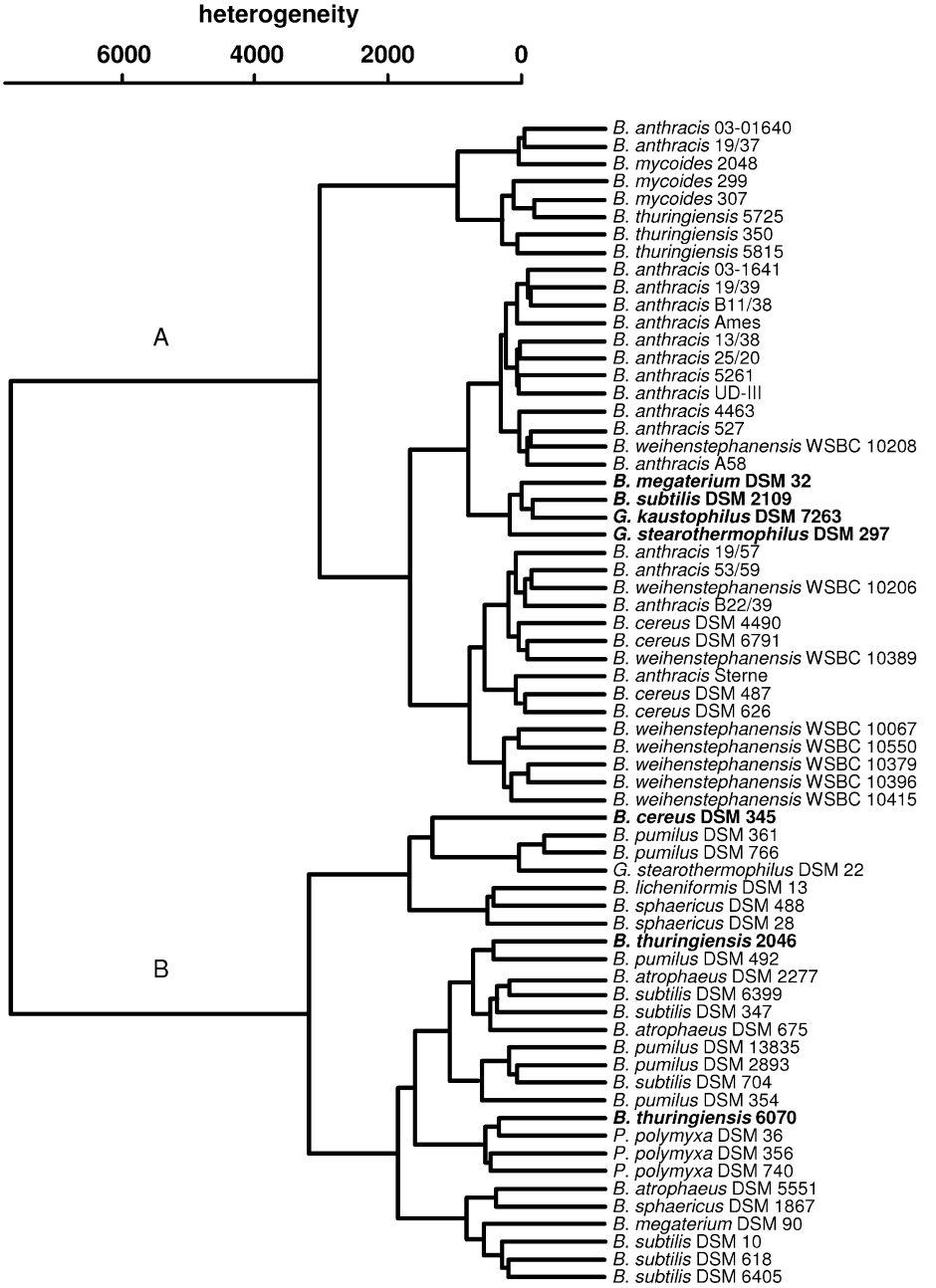

S-5

2.1.4 Raman Spectroscopic Detection of Anthrax Endospores in Powder Samples

Angewandte Chemie, International Edition **2012**, 51, 5339-5342

Stephan Stöckel:	Kultivierung und Aufarbeitung von Mikroorganismen, Raman-Messungen, Datenauswertung, Manuskripterstellung
Susann Meisel:	Kultivierung und Aufarbeitung von Mikroorganismen, Revision und Überarbeitung des Manuskripts
Mandy Elschner:	Bereitstellung von Mikroorganismen und Messproben, Konzept- und Ergebnisdiskussion, Revision und Überarbeitung des Manuskripts
Petra Rösch:	Konzept- und Ergebnisdiskussion, Revision und Überarbeitung des Manuskripts
Jürgen Popp:	Projektleitung, Konzept- und Ergebnisdiskussion, Revision und Überarbeitung des Manuskripts

Angewandte International Edition Chemie

Spectroscopic Analysis

DOI: 10.1002/anie.201201266

Raman Spectroscopic Detection of Anthrax Endospores in Powder Samples**

*S. Stöckel, S. Meisel, M. Elschner, P. Rösch, and J. Popp**

Polymerase chain reaction (PCR) is becoming the method of choice for detecting microorganisms concealed in complex matrices or "hoax materials" like household dry powders, food, and soil.[1] However, adding samples directly to a PCR reaction is in most cases not possible because of the presence of PCR inhibitors in the sample.[2] Thus, in order to reliably use PCR, one must either enrich the culture prior to the analysis, which is time-consuming for fastidious organisms, or extract the total DNA directly from the sample, which requires an extraction technique capable of processing different sample types. However, since most DNA extraction methods are often not generic in that sense, they lead to unreliable DNA recovery yields.[2,3]

By combining microscopy and Raman spectroscopy with visible-light excitation, it is possible to probe bacteria at the single-cell level making biomass-enrichment steps prior to analysis unnecessary.[4] The whole organism is characterized by its Raman spectrum comprising information about the intracellular, membrane, and surface material of the cells. The Raman spectral fingerprints of the bacteria can be compared to reference spectra of the same or related species such that bacteria can be identified in various possible civilian and military scenarios, for example, *Bacillus anthracis*, the etiological agent of the acute disease anthrax.[5] Several publications have dealt with testing for *Bacillus* endospores embedded in hoax materials and mail letters, but these relied solely on detecting the endospore-specific substance calcium dipicolinate (CaDPA).[6] This strategy is limited, however, since nonpathogenic bacilli other than *B. anthracis* may deliver false alarms.

We report here the first application of Raman spectroscopy to detect and identify anthrax endospores in environmental samples, even in the presence of other *Bacillus* species. Our suggested process provides results within 3 h after sample removal with minimal investment of material and time: First, the contaminated samples (roughly 100 mg) must be inactivated for 1 h with formaldehyde solution to kill possible pathogens.[7] The subsequent endospore extraction based on density-gradient centrifugation takes up to 30 min, before a microliter of the final suspension is dried on fused-silica plates and probed with a micro-Raman setup (6 s per endospore, 532 nm excitation).[8] Finally the obtained endospore Raman spectra are compared by means of chemometric analysis and a spectral database.

We focused particularly on powders, because they are among the most common nonclinical types of samples to be tested for *B. anthracis*.[9] To cover a broad range of sample types we selected seven household powders (baking powder, gypsum, milk powder, baking soda, analgesic tablet, bird sand, washing detergent) and spiked them with endospores of two strains of *B. anthracis* plus four other *Bacillus* species. The genetically closely related *B. anthracis*, *B. mycoides*, and *B. thuringiensis* belong to the *Bacillus cereus* clade, which often provoke cross-reactions with each other in PCR assays.[10] More distant species are the soil saprophytes *B. megaterium* and *B. subtilis*.

Studies performed on cynomolgus monkeys led to the assumption that the LD_{50} value for humans is in the range of around 8000 to 50000 colony forming units (cfu) for aerosolized anthrax spores, which is equivalent to roughly 8–50 ng.[11] We inoculated defined spore loads into baking powder and bird sand samples to test whether the chosen isolation procedure is sensitive enough. Both matrices were spiked with viable *B. thuringiensis* endospores in concentrations of 10^8, 10^6, 10^4, and 10^3 cfu per gram of matrix. The recovered endospores were enumerated by viable cell counting (Table S1 in the Supporting Information): 1% to 12% of the initial cells were isolated, which is sufficient, since 100 endospores per sample are enough to give reasonable results in the following Raman measurements. A 1 µL portion of each of the prepared samples was analyzed by Raman spectroscopy on the single-particle level as illustrated in Figure 1 for a processed baking powder sample spiked with *B. anthracis* Sterne. A dark-field image is transformed into a binary image to assess particles according to morphological features. The five labeled particles in Figure 1b were then measured; their unprocessed Raman spectra are shown in Figure 1c (i–iv: endospores, v: poly(3-hydroxybutyrate),

[*] S. Stöckel, S. Meisel, Dr. P. Rösch, Prof. Dr. J. Popp
Institut für Physikalische Chemie
Friedrich-Schiller-Universität Jena
Helmholtzweg 4, 07743 Jena (Germany)
E-mail: juergen.popp@uni-jena.de
Prof. Dr. J. Popp
Institut für Photonische Technologien
Albert-Einstein-Strasse 9, 07745 Jena (Germany)
Dr. M. Elschner
Friedrich Loeffler Institut, Bundesforschungsinstitut für Tiergesundheit, Institut für bakterielle Infektionen und Zoonosen
Naumburger Strasse 96a, 07743 Jena (Germany)

[**] Funding of the research projects "Pathosafe" (FKZ 13N9547 and FKZ 13N9549) and "RamaDek" (FKZ 13N11168) by the Federal Ministry of Education and Research (Germany) (BMBF) and "MikroPlex" (PE113-1) by the Thüringische Exzellenzinitiative (TMBWK) as well as funding by the EU, EAHC Agreement (No. 2007 204) is gratefully acknowledged.

Supporting information for this article is available on the WWW under http://dx.doi.org/10.1002/anie.201201266.

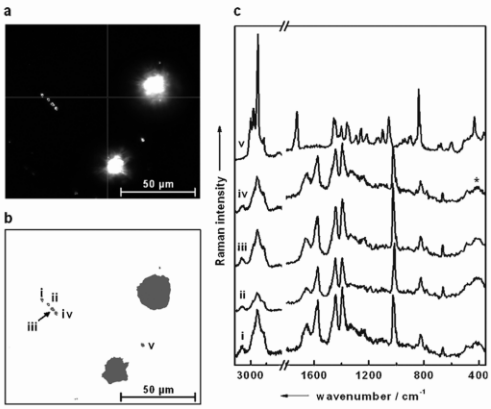

Figure 1. Particle analysis applied on a baking powder sample spiked with *B. anthracis* Sterne endospores. a) Dark-field-illuminated field of view. b) Five particles (i–v) match the morphological criteria for bacterial cells in the binary image. c) Unprocessed Raman spectra of the particles i–v. The asterisk denotes a band from the fused-silica substrate.

a common bacterial metabolite). In this way, roughly 50 particles per sample were measured with an integration time of 5 s plus 1 s preburning time to mitigate the spectral contributions of fluorescence, though this was already a minor factor in most of the endospore spectra.

Figure 2a displays mean Raman spectra of each of the analyzed *Bacillus* species. Dominating features in the spectra

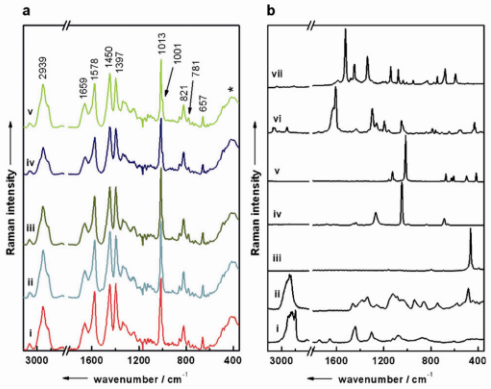

Figure 2. Raman spectra of *Bacillus* endospores and various matrix particles. a) Background-corrected mean Raman spectra of *B. anthracis* (i, calculated from 997 single-endospore Raman spectra), *B. megaterium* (ii, 1420 spectra), *B. mycoides* (iii, 1142 spectra), *B. subtilis* (iv, 1217 spectra), and *B. thuringiensis* (v, 947 spectra). The asterisk denotes a band from the fused-silica substrate. b) Raman spectra of particles of powdered milk (i, milk fat), baking powder (ii, starch), bird sand (iii, quartz), baking soda (iv, sodium bicarbonate), gypsum (v, calcium sulfate dihydrate), analgesic tablet (vi, acetylsalicylic acid), and washing powder (vii, copper phthalocyanine). The spectra are scaled and offset vertically for clarity.

are mainly bands arising from the endospore-specific salt CaDPA at 657, 1013, and 1397 cm^{-1}. Other spectral contributions arise exclusively from proteins, for example bands at 1001 cm^{-1} (ring-breathing vibration of phenylalanine) and 1659 cm^{-1} (amide I), and are complemented by signals from nucleic acids like the band at 781 cm^{-1} (ring vibration of cytosine/uracil). Some bands can be assigned to superpositions of signals from different biomolecules with CaDPA, for example the bands at 821 cm^{-1} (superposition of the ring-breathing mode of tyrosine with the CaDPA carboxylate stretching mode), at 1450 cm^{-1} (the CH_2/CH_3 deformation mode of proteins and lipids), and at 1578 cm^{-1} (ring vibration of guanine and adenine with pyridine ring vibrations of CaDPA). The intense signal in the high-wavenumber region at 2939 cm^{-1} is due to symmetric and asymmetric CH stretching vibrations of mainly proteins and lipids.[12]

In samples with low bacterial load, not only endospores but also biotic and abiotic matrix particles with endospore-like appearance might be probed in this way. Spectra of these clutter materials may disturb the subsequent statistical evaluation, since the spectral libraries cannot contain spectra of all possible matrix material. Figure 2b displays a collection of Raman spectra of matrix particles encountered during the measurements. An array of strongly distinctive Raman spectra is visible and stands in stark contrast to the Raman spectra of endospores (Figure 2a). It is therefore not a problem if matrix particles are measured, since their spectra can easily be recognized and sorted out.

A proper data evaluation step is the third mainstay for our concept. We selected a linear discriminant analysis (LDA) as the algorithm of choice. This classifier was recently applied to discriminate bacteria and particles of inorganic origin according to their Raman spectra.[13] To perform the classification problem at hand the algorithm was trained to distinguish between Raman spectra of the five different species. Thus, a collection of Raman spectra of known origin was fed into the algorithm to define discriminant functions for the best discrimination between the groups. Endospores from at least ten independently cultivated batches for each nonpathogenic *Bacillus* species were either taken directly from the culture medium or were inoculated into the powder matrices for at least 24 h, inactivated, isolated, and analyzed by Raman spectroscopy. This was done twice for every endospore–matrix combination (for *B. anthracis* only baking powder and bird sand) leading to a model database with a total of 5723 Raman spectra (Table S2a in the Supporting Information). The considerable partitioning of the data due to three of four discriminant functions is shown in Figure S1 in the Supporting Information. After the discrimination functions were parameterized a cross-validation was performed: 5427 Raman spectra were labeled correctly (94.8%, Table S3 in the Supporting Information). Most of the false negatives occurred between *B. mycoides* and *B. thuringiensis*; most of the wrongly labeled *B. anthracis* spectra could also be found in these two classes. Apparently the spectra of the *Bacillus cereus* class are more similar than those of the other classes.

To simulate the analysis of unknown real-world samples, samples spiked with new batches of the five *Bacillus* species were prepared. In this way we could also estimate the model's

propensity to overfit the data. If the model is too specific to the samples in the training data set, the model generalization potential would be drastically lowered. This new set of 1650 spectra with "unknown identities" (Table S2 b in the Supporting Information) was tested against the aforementioned LDA model. In Figure 3 a the data have been rearranged after the spectra had been projected on two of the LD axes. The clustering of the data is pronounced; that is, data for each single class are pooled together in coherent point clouds, which are mainly located within the classification model's confidence intervals (double standard deviation, depicted as ellipses) of the respective class. The confusion table (Table 1) reflects the identification accuracies for each species, giving an overall accuracy of 96.8%. The highest and lowest rates are reported for *B. subtilis* (100%) and *B. thuringiensis* (91.2%), respectively; specifically for *B. anthracis* a sensitivity of 99.6% was achieved. Falsely labeled spectra occurring for *B. anthracis*, *B. mycoides*, and *B. thuringiensis* were assigned to one of these three classes. All in all, the recognition rates for the new set of spectra are in the range of those achieved by cross-validation by using model inherent spectra. This can be said for all the different sample types, since no matrix type included in the model obviously corrupted the endospore spectra.

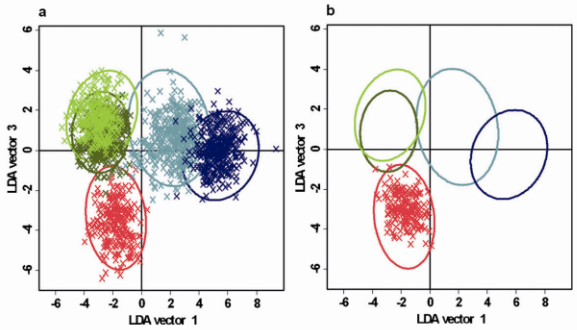

Figure 3. LDA score plots of the validation data. The ellipsoids display the model confidence intervals (double standard deviation) for each class. a) *B. anthracis* (red), *B. megaterium* (cyan), *B. mycoides* (olive-green), *B. subtilis* (blue), and *B. thuringiensis* (light green). b) The red crosses represent 191 spectra of *B. anthracis* 367 endospores, which were isolated from a matrix (table salt) unknown to the LDA model.

To test whether a sample type yet unknown to the model can be handled, we spiked common table salt with *B. anthracis* and processed it in the described way. 191 Raman spectra of isolated spores were measured and labeled by using the model. In Figure 3 b most of them (183/191 spectra, 95.8%, Table 1) were put into the area populated by the *B. anthracis* data of the model and misclassified spectra were solely labeled to be members of the *B. mycoides* class. However, it is apparent that satisfactory identification rates can be achieved even when the endospores originated from sample types not integrated in the database in the first place.

This low susceptibility of the method's efficiency to matrix influences stands in marked contrast to nucleic acid based detection techniques like PCR, which require a very clean starting sample. For cultured organisms PCR works well but has had little success in real-time biodetection of environmental samples owing to inhibition by a myriad of possible interferents. We think that the vibrational spectroscopic approach presented here perfectly compensates for these deficits of PCR methodologies. It displays high robustness concerning matrix interferences, and since reliable results can be obtained within 3 h, point-of-care detection of *B. anthracis* is possible in "real-world samples".

Table 1: Results of the validation experiment with an independent dataset.[a]

Identified as[b]	Bant	Bmeg	Bmyc	Bsub	Bthu	Bant [C]
Bant	**241**	4	3	0	0	**183**
Bmeg	0	**374**	0	0	0	0
Bmyc	0	0	**382**	0	26	8
Bsub	0	0	0	**331**	0	0
Bthu	1	2	17	0	**269**	0
Sens. [%]	99.6	98.4	95.0	100	91.2	95.8

[a] The species-wise sensitivities (sens.) are given. The overall rate was 96.8%. The last column reflects the labeling of endospores isolated from table salt [C]. [b] Bant = *B. anthracis*, Bmeg = *B. megaterium*, Bmyc = *B. mycoides*, Bsub = *B. subtilis*, Bthu = *B. thuringiensis*.

Experimental Section

Details of the methods can be found in the Supporting Information. Inactivation of endospores was achieved by exposure to 20% formaldehyde solution for one hour. A solution of polyvinylpyrrolidone-covered silica colloidal particles diluted in 0.15 M sodium chloride solution was employed as a density gradient medium for the isolation. Endospore enumeration after the isolation step was performed by microbial plating. The Raman spectra were collected with a Raman microspectrometer under ambient conditions on fused-silica substrates with 532 nm excitation. The samples were irradiated with 7 mW with a laser spot of ca. 1 μm during an integration time per endospore of 5 s plus 1 s of preburning. All chemometrical calculations were conducted with Gnu R.

Received: February 15, 2012
Published online: April 13, 2012

Keywords: analytical methods · anthrax · endospores · Raman spectroscopy

[1] L. Settanni, A. Corsetti, *J. Microbiol. Methods* **2007**, *69*, 1–22.
[2] H. L. Rose, C. A. Dewey, M. S. Ely, S. L. Willoughby, T. M. Parsons, V. Cox, P. M. Spencer, S. A. Weller, *PLoS One* **2011**, *6*, 8.
[3] P. R. Wielinga, L. de Heer, A. de Groot, R. A. Hamidjaja, G. Bruggeman, K. Jordan, B. J. van Rotterdam, *Int. J. Food Microbiol.* **2011**, *150*, 122–127.
[4] M. Harz, P. Rösch, J. Popp, *Cytometry Part A* **2009**, *75A*, 104–113.

[5] K. S. Kalasinsky, T. Hadfield, A. A. Shea, V. F. Kalasinsky, M. P. Nelson, J. Neiss, A. J. Drauch, G. S. Vanni, P. J. Treado, *Anal. Chem.* **2007**, *79*, 2658 – 2673.
[6] S. Farquharson, G. Lawrence, K. Victor, S. Wayne, F. S. Jay, F. Gerard, *J. Raman Spectrosc.* **2004**, *35*, 82 – 86.
[7] S. Stöckel, W. Schumacher, S. Meisel, M. Elschner, P. Rösch, J. Popp, *Appl. Environ. Microbiol.* **2010**, *76*, 2895 – 2907.
[8] S. Meisel, S. Stöckel, M. Elschner, P. Rösch, J. Popp, *Analyst* **2011**, *136*, 4997 – 5005.
[9] A. Luna Vicki, D. King, C. Davis, T. Rycerz, M. Ewert, A. Cannons, P. Amuso, J. Cattani, *J. Clin. Microbiol.* **2003**, *41*, 1252 – 1255.
[10] E. Helgason, O. A. Okstad, D. A. Caugant, H. A. Johansen, A. Fouet, M. Mock, I. Hegna, A.-B. Kolsto, *Appl. Environ. Microbiol.* **2000**, *66*, 2627 – 2630.
[11] C. J. Peters, D. M. Hartley, *Lancet* **2002**, *359*, 710 – 711.
[12] a) J. De Gelder, P. Scheldeman, K. Leus, M. Heyndrickx, P. Vandenabeele, L. Moens, P. De Vos, *Anal. Bioanal. Chem.* **2007**, *389*, 2143 – 2151; b) K. Maquelin, C. Kirschner, L. P. Choo-Smith, N. van den Braak, H. P. Endtz, D. Naumann, G. J. Puppels, *J. Microbiol. Methods* **2002**, *51*, 255 – 271.
[13] a) W. Schumacher, M. Kühnert, P. Rösch, J. Popp, *J. Raman Spectrosc.* **2011**, *42*, 383 – 392; b) R. Fisher, *Ann. Eugenic.* **1936**, *7*, 179 – 188.

Angewandte Chemie
Eine Zeitschrift der Gesellschaft Deutscher Chemiker

Supporting Information

69451 Weinheim, Germany

Raman Spectroscopic Detection of Anthrax Endospores in Powder Samples**

*S. Stöckel, S. Meisel, M. Elschner, P. Rösch, and J. Popp**

anie_201201266_sm_miscellaneous_information.pdf

table of content

Material and Methods 2
Bacillus strains 2
Sample preparation 2
Inactivation and isolation procedures 2
Spectroscopic instrumentation 3
Multivariate analysis 3
Isolation yield determination. 4
Figures 5
Tables 6
References 8

1

Material and Methods

Bacillus strains

The following strains were examined in this publication: *B. anthracis* 5261 (Federal Research Institute for Animal Health, Jena, Germany), *B. anthracis* Sterne (EQADEBA-Repository, Robert-Koch-Institute, Berlin, Germany), *B. megaterium* DSM 90, *B. mycoides* DSM 299, *B. subtilis* DSM 10, and *B. thuringiensis* DSM 350. All but the *B. anthracis* strains were purchased from the German Collection of Microorganisms and Cell Cultures (DSMZ, Braunschweig, Germany).

Sample preparation

Endospore suspensions with concentrations around 10^7 spores per ml were prepared *via* two different methods: One method was the cultivation on nutrient agar (NA) plates at 30 °C. The medium is formulated as follows: 5.0 g peptone, 3.0 g meat extract, 0.04 g $MnSO_4$ H_2O, 15 g agar and 1000 ml distilled water (pH 7.0 ± 0.2, autoclaved at 121 °C, 20 minutes). The bacteria were rinsed off the plates after seven days of cultivation and washed three times by centrifugation and re-suspension in distilled water. The other cultivation approach at 37 °C relied on yeast extract agar consisting of 10.0 g peptone, 2.0 g yeast extract, 0.04 g $MnSO_4$ H_2O, 15 g agar per 1000 ml aqua bidest (pH 7.0 ± 0.2, autoclaved at 121 °C, 20 min) and was described previously in Stöckel *et al.*[1] Batches of *B. megaterium* DSM 90, *B. mycoides* DSM 299, *B. subtilis* DSM 10, and *B. thuringiensis* DSM 350 were prepared with both procedures, whereas the *B. anthracis* strains were cultivated solely following the second method.
The studied powder matrices were acquired in local common stores. In detail the powders were as follows: baking powder (Back-Gold Backpulver, Meier Pudding, Trittau, Germany), table salt (MarkenSalz, Bad Reichenhaller, Südsalz GmbH, Heilbronn, Germany), gypsum (Sycofix Bau- und Hobby-Gips, Sieder GmbH, Plaue, Germany), baking soda (HausNatron, Lucullus Backen & Genießen GmbH & Co. KG, Darmstadt, Germany), milk powder (Sucofin Magermilchpulver, TSI GmbH & Co. KG, Zeven, Germany), analgesic tablets (Thomapyrin® intensiv, Boehringer Ingelheim Pharma GmbH & Co. KG, Ingelheim am Rhein, Germany), bird sand (Vitakraft Vogelsand, Vitakraft-Werke Wührmann & Sohn GmbH & Co. KG, Bremen, Germany), washing powder (Weißer Riese KraftPulver, Henkel AG & Co. KGaA, Düsseldorf, Germany).
Endospores, coming from at least ten independently cultivated batches for each *Bacillus* species to account for biological variability, were inoculated to the powdery matrices for at least 24 h.

Inactivation and isolation procedures

1.5 ml of 20% formaldehyde solution (Sigma-Aldrich Chemie GmbH, Taufkirchen, Germany) were applied to 100 mg spiked powder to inactivate the potentially pathogenic endospores. The samples were rotated continuously (VWR tube rotator, VWR, Leuven, Belgium) during the time of treatment of one

hour until the process was stopped by centrifugation with 12100g (MiniSpin, Eppendorf, Hamburg, Germany) for one minute.
After three additional washing steps the sediments were suspended into 0.2 ml distilled water. After homogenization via shaking the suspension was carefully layered on top of two density gradient volumes of 0.5 ml (densities of 1.050 g/ml and 1.123 g/ml) in a 1.5 ml micro-tube. The density gradient medium Percoll (Biochrom AG, Easycoll Separating Solution, Berlin, Germany) consisted of PVP (polyvinylpyrrolidone) covered sodium-stabilized silica colloidal particles diluted in 0.15 M sodium chloride solution.[2] The samples were afterwards centrifuged for five minutes at 12100g to form stable density gradient in the vessel. If necessary, like in case of milk powder, light weighted matrix components swam on top of the liquids and were removed. The upper liquid volume was recovered together with the boundary layer to gather most of the less dense endospores. The matrix residue including the denser endospores was afterwards thoroughly mixed again with the remaining supernatant Percoll solution plus 1 ml of added distilled water and was allowed to stand undisturbed for a maximum of five minutes. Most of the present matrix material was soon sedimented so that the supernatant appeared quite clear, which was then abstracted and joined with the first aliquot containing the less denser spores in a 2.0 ml micro-tube. The suspension was finally washed three times with distilled water to get rid of the Percoll residues and stored at 4 °C until further processing.

Spectroscopic instrumentation

All of the Raman spectra were collected under ambient conditions. The Raman spectroscopic measurements were carried out with a micro-Raman device (BioParticleExplorer, rap.ID Particle Systems GmbH, Berlin, Germany) that allows automated measurements of single-cell Raman spectra with an excitation light of 532 nm from a solid-state frequency-doubled Nd:YAG module (LCM-S-111-NNP25, Laser-export Co. Ltd.). An Olympus MPLFLN 100xBD objective focused the Raman excitation light onto the sample with a spot size of <1 µm laterally, so that approximately 7 mW hit the sample. The integration time per Raman spectrum (-113 cm^{-1} – 3186 cm^{-1}) was five seconds after a pre-burning period of one second to mitigate spectral contributions because of fluorescence, though it was already of minor extent in most of the endospore spectra. After removal of the Rayleigh scattering via two edge filters, the 180° back-scattered Raman light was diffracted with a single-stage monochromator (HE 532, Horiba Jobin Yvon) with a 920 lines/mm grating and collected with a thermoelectrically cooled CCD camera (DV401-BV, Andor Technology) with a spectral resolution of ca. 7 cm^{-1}. For single cell measurements, one spectrum of each cell was recorded after 2.5 seconds and one after 5 seconds. These two were afterwards compared for spike removal.

Multivariate analysis

Gnu R was used for the statistical analyses.[3] The procedure mainly consisted of three steps: pre-processing, training of the self-learning machine to build a model and validation. The pre-processing of every dataset was always the same. First the spectra underwent a wavenumber calibration with acetaminophen as standard.[4] Then the background of the spectra and cosmic spikes were removed. The background was stripped off by employing a statistics sensitive nonlinear iterative peak-clipping

algorithm (SNIP), which is in principle a composite of a low statistics filter and a peak clipping algorithm.[5] A forth-order-algorithm was applied with a clipping window of seven. Because of their origin the cosmic spikes are neither correlated in time nor in space and could therefore be localized by recording two Raman spectra of the same endospore. Intensity differences for each channel and their standard deviation were calculated and spikes located in channels, where the intensity difference exceeded twice the standard deviation. After the removal of cosmic spikes a cut off of the fingerprint regions of the spectra took place. For the calculation the wavenumber regions 639 to 1802 cm^{-1} and 2783 to 3186 cm^{-1} were used. A further pre-processing step was normalization: A spectrum was divided by its area, which was calculated as the Euclidean distance of the spectrum to the zero spectrum (2-norm).
To reduce the dimensionality of the problem and to remove white noise a principal component analysis (PCA) was performed.[6] The data were neither scaled by channel nor centered before the PCA. After a particular channel the scores were cut off in the new spectral space. The number of chosen scores correlates with the size of the data set, but a good choice is to use not more than 2-5% of the number of spectra to avoid overfitting.[7] If a new set of spectra had to be labeled the pre-processing of this new dataset was the same as before PCA. To convert both sets in the same spectral space we did not perform a PCA with the combined dataset, but rather rotated the new set by the loadings of the PCA of the first dataset into the spectral space of the first dataset.
We chose a linear discriminant analysis (LDA) as supervised classifier to evaluate the spectral datasets.[8] Cross-validation was used to validate the classifier and this accuracy was taken as accuracy of the classification model. An estimation of the generalization error was done by means of a hold-out technique: Sets of endospores from all the analyzed *Bacillus* species were used for training, other completely independent batches of the same strains, which were separately cultured under exact the same conditions, were used as validation set. In doing so an application of the procedure under realistic conditions was simulated and its accuracy assessed.

Isolation yield determination.

Endospore enumeration after an isolation step was performed by standard microbial plating technique using NA agar plates to assess the recovery performance of the isolation method. Samples of autoclaved baking powder and sand with known inoculation numbers of viable *B. thuringiensis* endospores were prepared trice for each starting concentration, which amounted to 10^8, 10^6, 10^4, and 10^3 cfu/g matrix. All 24 samples were left to stand for 24 h and underwent the isolation procedure afterwards. The resulting suspensions were serially diluted to achieve solutions of appropriate cell concentrations, of which two times 100 µl were put onto NA agar plates. After 24 h of incubation at 30 °C the visible colonies on the plates were enumerated. The two lowest concentrations are obviously too low to pose a threat in, e. g., standard letters but have been considered to approach towards the possible limit of detection. Three replicates of each inoculation concentration and matrix were prepared and subjected to the isolation procedure. Hereby 100 mg of the respected matrix were spiked.

Figures

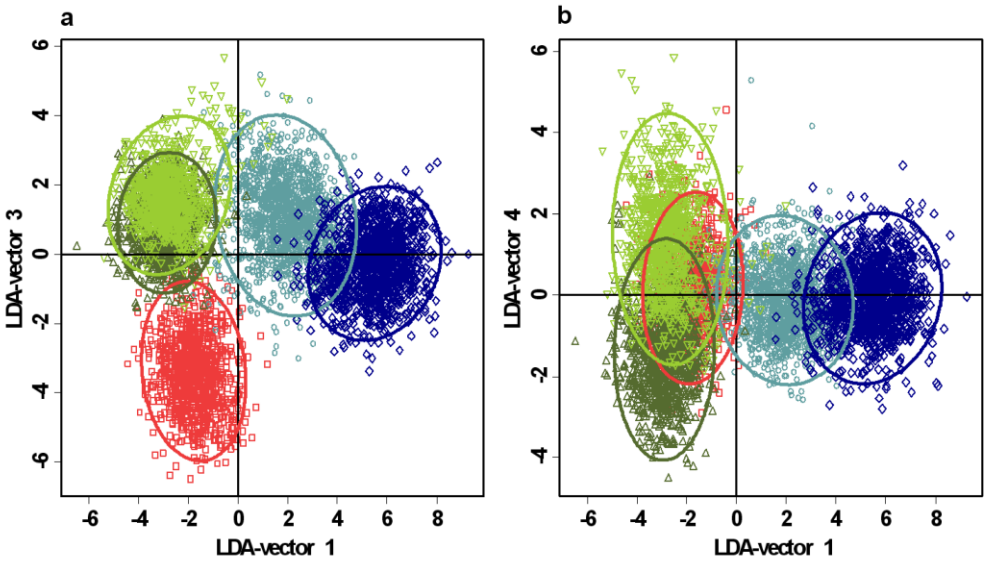

Figure S1. Score plots of the LDA model. a) The spectra are arranged according to their scores of the linear discriminant functions 1 and 3: *B. anthracis* (□), *B. megaterium* (○), *B. mycoides* (△), *B. subtilis* (◊), and *B. thuringiensis* (▽). The *B. anthracis* spectra bear negative scores on LD1 and LD3 and therefore cluster in quadrant III. Ellipsoids depict the distribution of the group members via double standard deviation. b) The spectra are arranged according to their scores of the linear discriminant functions 1 and 4: Coding vide supra. Different scores on LD4 of *B. mycoides* and *B. thuringiensis* explain the discrimination between these two classes.

Tables

Table S1. Recovery results for the performed viable cell counting of *B. thuringiensis* endospores. Three baking powder and sand samples á 100 mg were spiked with defined loads of viable *B. thuringiensis* endospores in concentrations from $3.5x10^2$ to $3.5x10^7$ cfu. The recovered endospores after the isolation were determined twice for each trial via viable cell counting and the average yield per trial is given.

c_0 [cfu/100 mg]	cfu isolated from baking powder			cfu isolated from sand		
	trial 1	trial 2	trial 3	trial 1	trial 2	trial 3
$3.5x10^7$	$2.0x10^5$	$0.6x10^5$	$3.3x10^5$	$3.1x10^5$	$3.5x10^5$	$1.8x10^5$
$3.5x10^5$	$4.8x10^4$	$4.8x10^4$	$6.2x10^4$	$4.5x10^4$	$3.1x10^4$	$2.1x10^4$
$3.5x10^3$	$3.7x10^2$	$5.5x10^2$	$4.0x10^2$	$2.1x10^2$	$3.2x10^2$	$2.5x10^2$
$3.5x10^2$	$1.0x10^1$	$0.5x10^1$	$4.3x10^1$	$1.5x10^1$	$2.0x10^1$	$0.7x10^1$

Table S2. Summary of the compiled data. a) The number of single endospore Raman spectra per *Bacillus* species measured to build the LDA model is given together with the sample types, from which the endospores had been isolated from (A agar plates, B baking powder, G gypsum, M milk powder, N baking soda (natron), P analgesic tablets (painkiller), S bird sand, W washing powder). Endospores with sample type A were taken directly from agar plates, underwent formaldehyde treatment and were measured without being inoculated into one of the matrices. b) The number of single endospore Raman spectra per *Bacillus* species measured from the validation samples to test the LDA model is given together with the sample types, from which the endospores have been isolated from (C common table salt and rest of abbreviations vide supra).

a)

Bacillus species	no. spectra	isolated from
B. anthracis 367 & Sterne	997	B S
B. megaterium DSM 90	1420	A B G M N P S W
B. mycoides DSM 299	1142	A B G M N P S W
B. subtilis DSM 1051	1217	A B G M N P S W
B. thuringiensis DSM 350	947	A B G M N S W

b)

Bacillus species	no. spectra	isolated from
B. anthracis 367 & Sterne	242	B S
B. megaterium DSM 90	380	A B N S
B. mycoides DSM 299	402	A B N S
B. subtilis DSM 1051	331	A B M P W
B. thuringiensis DSM 350	295	A B G M
B. anthracis 367	191	C

Table S3. Results of the cross-validation to evaluate the LDA model classification accuracy. The confusion table depicts the labeling of Raman spectra used to train the LDA classifier after leave-one-out cross-validation including the sensitivities (true positive rates, sens.) and specificities (true negative rate, spec.) per *Bacillus* species. The overall classification rate was 96.5% (5037 spectra of 5218 correctly labeled).

actual / predicted	*B. anthracis*	*B. megaterium*	*B. mycoides*	*B. subtilis*	*B. thuringiensis*	sens. [%]	spec. [%]
B. anthracis	**983**	11	1	0	3	98.6	99.7
B. megaterium	2	**1392**	1	2	3	98.0	99.8
B. mycoides	6	2	**1036**	0	140	90.7	96.7
B. subtilis	0	11	0	**1215**	0	99.8	99.7
B. thuringiensis	6	4	104	0	**801**	84.6	97.6

References

[1] S. Stöckel, W. Schumacher, S. Meisel, M. Elschner, P. Rösch, J. Popp, *Appl. Environ. Microbiol.* **2010**, *76*, 2895-2907.
[2] H. Pertoft, *J. Biochem. Biophys. Methods* **2000**, *44*, 1-30.
[3] R. Development Core Team, R Foundation for Statistical Computing, Vienna, Austria, **2008**.
[4] M. M. Carrabba, in *Handbook of Vibrational Spectroscopy, Vol. 1*, John Wiley & Sons, Ltd, **2006**.
[5] M. Morhác, *Nucl. Instrum. Meth. A* **2009**, *600*, 478-487.
[6] K. Pearson, *Philos. Mag.* **1901**, *2*, 559-572.
[7] V. N. Vapnik, *The nature of statistical learning theory*, 2 ed., Springer, New York, **2000**.
[8] R. Fisher, *Ann. Eugenic.* **1936**, *7*, 179-188.

2.1.5 Weitere Publikationen

Referierte Publikationen

Analysis of single blood cells for CSF diagnostics via a combination of fluorescence staining and micro-Raman spectroscopy, M. Harz, M. Kiehntopf, S. Stöckel, P. Rösch, T. Deufel und J. Popp, *Analyst (Cambridge, United Kingdom)* **2008**, 133, 1416-1423.

Direct analysis of clinical relevant single bacterial cells from cerebrospinal fluid during bacterial meningitis by means of micro-Raman spectroscopy, M. Harz, M. Kiehntopf, S. Stöckel, P. Rösch, E. Straube, T. Deufel und J. Popp, *Journal of Biophotonics* **2009**, 2, 70-80.

Assessment of two isolation techniques for bacteria in milk towards their compatibility with Raman spectroscopy, S. Meisel, S. Stöckel, M. Elschner, P. Rösch und J. Popp, *Analyst (Cambridge, United Kingdom)* **2011**, 136, 4997-5005.

Raman Spectroscopy as a Potential Tool for Detection of Brucella spp. in Milk, S. Meisel, S. Stöckel, M. Elschner, F. Melzer, P. Rösch und J. Popp, *Applied and Environmental Microbiology* **2012**, 78, 5575-5583.

Buchartikel

Identification and Characterization of Microorganisms by Vibrational Spectroscopy, S. Stöckel, A. Walter, A. Boßecker, S. Meisel, V. Ciobotă, W. Schumacher, P. Rösch und J. Popp, in: *Handbook of Biophotonics, Vol. 2: Photonics for Health Care* (Eds. V. V. Tuchin, A. Chiou und S. H. Heinemann), Wiley-VCH, Berlin, 105-142, 2011.

Tracing Bioagents - a Vibrational Spectroscopic Approach for a Fast and Reliable Identification of Bioagents, P. Rösch, U. Münchberg, S. Stöckel und J. Popp, in: *Infrared and Raman Spectroscopy in Forensic Science* (Eds. J. M. Chalmers, H. G. M. Edwards und M. Hargreaves), John Wiley & Sons, Ltd, Chichester (UK), 233-250, 2012.

Applications of Raman Spectroscopy to Virology and Microbial Analysis, M. Harz, S. Stöckel, V. Ciobotă, D. Cialla, P. Rösch und J. Popp, in: *Emerging Raman Applications and Techniques in Biomedical and Pharmaceutical Fields (Biological and Medical Physics, Biomedical Engineering)* (Eds. P. Matousek und M. D. Morris), Springer, Heidelberg, 439-466, 2010.

Sonstige Publikationen

Raman spectroscopic characterization of single cells, J. Popp, S. Stöckel, S. Meisel, T. Bocklitz, W. Schumacher, M. Putsche und P. Rösch, *Proceedings of SPIE* **2010**, 7560 (Biomedical Vibrational Spectroscopy IV: Advances in Research and Industry), 75600B.

A Raman spectroscopic approach for the cultivation-free identification of microbes, P. Rösch, S. Stöckel, S. Meisel, U. Münchberg, S. Kloß, D. Kusic, W. Schumacher und J. Popp, *Proceedings of SPIE* **2011**, 8311 (Optical Sensors and Biophotonics III), 83111B.

Bacterial identification in real samples by means of micro-Raman spectroscopy, P. Rösch, S. Stöckel, S. Meisel, A. Boßecker, U. Münchberg, S. Kloß, W. Schumacher und J. Popp, *Proceedings of SPIE* **2011**, 8087 (Clinical and Biomedical Spectroscopy and Imaging II), 808708.

2.2 Konferenzbeiträge

Vorträge

Tracing Single Bacteria via Raman Spectroscopy, S. Stöckel, S. Meisel, C. Ciobotă, M. Krause, M. Harz, P. Rösch und J. Popp, in: *European Network of Excellence – Photonics4Life (P4L), internal scientific meeting*, Brüssel (Belgien), 2008.

Raman Spectroscopic Identification of Anthrax, S. Stöckel, S. Meisel, W. Schumacher, P. Rösch und J. Popp, in: *Abbe School of Photonics Seminar Summer Term 2012*, Jena (Deutschland), 2012.

Raman Spectroscopic Analysis & Identification of Pathogenic Microorganisms, S. Stöckel, S. Meisel, W. Schumacher, P. Rösch und J. Popp, in: *Raman Imaging Workshop 2012*, Olmütz (Tschechische Republik), 2012.

Poster

Detection and identification of single endospores of the genus *Bacillus* by means of micro-Raman spectroscopy, S. Stöckel, M. Elschner, S. Meisel, M. Lankers, P. Rösch und J. Popp, in: *XXIst International Conference on Raman Spectroscopy (ICORS)*, London (UK), 2008.

Detection and Identification of Single Endospores of the Genus *Bacillus* by Means of Micro-Raman Spectroscopy, S. Stöckel, S. Meisel, W. Schumacher, M. Elschner, M. Lankers, P. Rösch und J. Popp, in: *ANAKON*, Berlin (Deutschland), 2009.

Micro-Raman Study and Identification of *Bacillus* Endospores Isolated from Soil-Like Matrices, S. Stöckel, S. Meisel, W. Schumacher, M. Elschner, M. Lankers, P. Rösch und J. Popp, in: *5th International Conference on Advanced Vibrational Spectroscopy (ICAVS)*, Melbourne (Australien), 2009.

Micro-Raman Study and Identification of Inactivated *Bacillus* Endospores, S. Stöckel, S. Meisel, W. Schumacher, M. Elschner, M. Lankers, P. Rösch und J. Popp, in: *Workshop des Robert Koch-Institutes "FTIR Spectroscopy in Microbiological and Medical Diagnostics"*, Berlin (Deutschland), 2009.

Micro-Raman Study and Identification of Inactivated Anthrax Endospores, S. Stöckel, S. Meisel, W. Schumacher, M. Elschner, M. Lankers, P. Rösch und J. Popp, in: *Tagung der Deutschen Veterinärmedizinischen Gesellschaft (DVG) der Fachgruppe "Bakteriologie und Mykologie"*, Jena (Deutschland), 2010.

Micro-Raman Based Identification of Anthrax Endospores Isolated from Different Matrices, S. Stöckel, S. Meisel, W. Schumacher, M. Elschner, P. Rösch und J. Popp, in: *XXIIst International Conference on Raman Spectroscopy (ICORS)*, Boston (USA), 2010.

PathoSafe: Mikro-Raman-Spektroskopie zur Detektion bioterroristisch relevanter Erreger, S. Stöckel, S. Meisel, W. Schumacher, M. Elschner, M. Lankers, P. Rösch und J. Popp, in: *Workshop "Sicherheit durch innovative Detektionstechnologien - Nachweissysteme für chemische, biologische und explosive Gefahrstoffe"*, Berlin (Deutschland), 2011.

Micro-Raman Spectroscopic Identification of *Bacillus Anthracis* Isolated from Hoax Materials, S. Stöckel, S. Meisel, W. Schumacher, B. Kampe, M. Elschner, P. Rösch und J. Popp, in: *Workshop des Robert Koch-Institutes "FTIR Spectroscopy in Microbiological and Medical Diagnostics"*, Berlin (Germany), 2011.

Curriculum Vitae

Persönliche Daten

Name	Stephan Stöckel
Geburtsdatum	25.12.1980
Geburtsort	Jena, Deutschland

Schulausbildung

09/1987 – 07/1999	Clara-Zetkin-Schule in Jena Carl-Zeiss-Gymnasium in Jena (Abschluss: Abitur)

Hochschulausbildung

09/2000 – 10/2007	Studium der Chemie (Diplom) an der Friedrich-Schiller-Universität Jena (Abschluss: Diplom-Chemiker)
seit 01/2008	Anfertigen der Dissertation im Institut für Physikalische Chemie der Friedrich-Schiller-Universität Jena

Jena, den 12. November 2012 _____

Stephan Stöckel

Selbstständigkeitserklärung

Ich erkläre, dass ich die vorliegende Arbeit selbstständig und unter Verwendung der angegebenen Hilfsmittel, persönlichen Mitteilungen und Quellen angefertigt habe.

Jena, den 12. November 2012 _____

Stephan Stöckel